uOttawa

L'Université canadienne
Canada's university

FACULTÉ DES ÉTUDES SUPÉRIEURES ET POSTOCTORALES

u Ottawa

L'Université canadienne
Canada's university

FACULTY OF GRADUATE AND POSDOCTORAL STUDIES

Enshirah Da'na

AUTEUR DE LA THÈSE / AUTHOR OF THESIS

M.A.Sc. (Chemical Engineering)

GRADE / DEGREE

Department of Chemical Engineering

FACULTÉ, ÉCOLE, DÉPARTEMENT / FACULTY, SCHOOL, DEPARTMENT

Amine-Modified Mesoporous Silica for Adsorption of Copper from Aqueous Solutions

TITRE DE LA THÈSE / TITLE OF THESIS

Dr. A. Sayari

DIRECTEUR (DIRECTRICE) DE LA THÈSE / THESIS SUPERVISOR

CO-DIRECTEUR (CO-DIRECTRICE) DE LA THÈSE / THESIS CO-SUPERVISOR

EXAMINATEURS (EXAMINATRICES) DE LA THÈSE / THESIS EXAMINERS

Dr. B. Kruczek

Dr. M. Ternan

Gary W. Slater

Le Doyen de la Faculté des études supérieures et postdoctorales / Dean of the Faculty of Graduate and Postdoctoral Studies

Amine-Modified Mesoporous Silica for Adsorption of Copper from Aqueous Solutions

By

Enshirah Da'na

A thesis submitted in partial fulfillment of the requirements for the degree of

Master of Applied Science

In the

DEPARTMENT OF CHEMICAL ENGINEERING

UNIVERSITY OF OTTAWA

Your file Votre référence
ISBN: 978-0-494-50870-1
Our file Notre référence
ISBN: 978-0-494-50870-1

Abstract

During the last few decade governments all around the world have increased concerns about water shortages and pollution. Consequently, they issued a multitude of environmental legislations and regulations, land and water-use planning measures, and other environmentally related procedures. The objective of this work was to contribute in developing efficient adsorbent for heavy metal ions from wastewater. Two different kinds of adsorbents were studied: MCM-41 (Mobil Catalytic Material number 41) mesoporous silica whose pores have been expanded by a post-synthesis hydrothermal treatment in the presence of N,N-dimethyldecylamine (DMDA), and 3-aminopropyltrimethoxysilane (AMP) grafted MCM-41 after being pore expanded and calcined.

The pore-expanded MCM-41, (PE)MCM-41, (i.e., containing DMDA) has been tested as adsorbent for Cu^{2+} cations. Regeneration ability and factors affecting the stability of this material such as pH and stirring time have been investigated. The results showed that (PE)MCM-41 is fast, sensitive, and high capacity adsorbent. However, it is not an appropriate material for environmental applications due to its poor stability in aqueous solutions.

Further studies using calcined and pore-expanded MCM-41, (CPE)MCM-41, silica as support for grafting AMP have been carried out. A systematic investigation of the amine loading as a function of the relative amount of AMP and water used during the grafting procedure was carried out. The surface characteristics, AMP loading, Cu^{2+}

adsorption capacitiy, CO_2 adsorption capacitiy, and rate of CO_2 adsorption were determined for all materials. Surface area, pore size and pore volume decreased significantly from 950 m^2/g, 11.3 nm and 2.16 mL/g for unmodified (CPE)MCM-41 to 783 m^2/g, 7.4 nm and 1.54 mL/g for the materials grafted under dry conditions in the presence of 1.0 mL AMP/g silica, and to 730 m^2/g, 6.34 nm and 0.77 mL/g for the materials grafted under wet conditions in the presence of 2.0 mL AMP/g silica and 0.4 mL water/g silica. The maximum amine loading, CO_2 adsorption capacity and Cu^{2+} adsorption capacity suggested that the optimum grafting conditions are 2 mL AMP/g silica and 0.4 mL of water/g silica, and that any excess of water or amine added to the grafting mixture has negative effect on the adsorption performance of the material.

Two approaches have been investigated to recycle the copper loaded adsorbent: treatment with acidic solution and treatment with complexing agent, ethylenediamine-tetra acetic acid tetra sodium salt (EDTA). The results showed a significant drop in the adsorption capacity after the first regeneration cycle. With further testing of the material, it was concluded that the (CPE)MCM-41 is not stable when being in contact with water and thus, even the material was still loaded with amine, structural changes of the material caused the amine to become inaccessible for Cu^{2+} or CO_2 molecules. So, further work is still required to improve the stability of this material in water or to use more robust material.

Acknowledgements

I would like to express my appreciation and acknowledgements to my thesis supervisor, Prof. Abdelhamid Sayari for his guidance and advices. I thank him also for providing me an opportunity to grow as a student and engineer in the unique research environment he created.

Special thanks and appreciation to Dr. Peter Harlick for providing me with lots of his experiences regarding the experimental work and analysis of data. His advices were really valuable and appreciated.

Great appreciation to all Sayari's group for being a great team. Our working together with a spirit of team has greatly influenced this thesis.

Great of thanks and love to my husband and my wonderful kids Majid, Mohammad, and Hashim for being patients while I'm busy and away from them. You are the candles lighting my life. Also my Parents, who provided the item of greatest worth-opportunity. Thank you for standing by me through the many trials and decisions of my educational career.

List of Tables

Table	Description	Page
1	The distribution of renewable river water across the Earth's surface.....	7
2	Dissolved trace metal concentrations in water samples collected in 2001 from 12 lakes in the Sudbury basin, Ontario, Canada	9
3	Dissolved trace metal concentrations in water samples collected in 1993-1994 from 10 lakes in the Sudbury basin, Ontario, Canada.....	10
4	Dissolved trace metal concentrations in water samples collected in 1993-1994 and in 2001 from lakes Ramsey and Kelley in the Sudbury basin, Ontario, Canada.....	10
5	Ontario Drinking Water Standards.....	13
6	Authorized Levels of Deleterious Substances Prescribed in the MMLER....	14
7	Materials characterization.....	47
8	TOC Values for different MCM-41 samples.....	49
9	Stability test as a function of pH	51
10	Effect of copper-loaded material on the pH of the solution.....	52
11	Adsorption-desorption cycles using acidic solution as a regeneration agent	52
12	Adsorption-desorption cycles using acidic solution as a regeneration agent obtained by Sayari, A. et al.(2005).....	53
13	Adsorption-desorption cycles using EDTA solution as a regeneration agent for 1 hour stirring period.....	53
14	Adsorption-desorption cycles using EDTA solution as a regeneration agent for 5 minutes stirring period.....	54

15 Summary of amine-grafted silica based adsorbent prepared under different grafting conditions and applied for heavy metal cations and anions..... 59

16 Freundlich isotherm constants..... 75

17 Freundlich isotherm constants obtained by Sayari et al. (2005) for (PE)MCM-41..... 75

18 Cu^{2+} and CO_2 Adsorption-desorption cycles of amine-grafted adsorbent using EDTA solution as a regeneration agent..... 88

List of Figures

Figure	Description	Page
1	Performance of Mines Subject to the MMLER in the Ontario region in 2001...	14
2	Formation mechanisms of FSM-16 according to Inagaki, S. et al., 1993.....	20
3	Microscopic view of MCM-41.....	22
4	Scheme of synthesis of periodic mesoporous silica.	23
5	Schematic phase diagram of surfactant in water.....	24
6	Schematic representation of post-synthesis grafting of alkoxysilane with different functionalities.....	28
7	Schematic representation of one step modification of uncalcined MCM-41.....	31
8	Scheme of materials pore expansion.....	35
9	Scheme of materials extraction.....	36
10	Scheme of materials calcination.....	37
11	Nitrogen adsorption-desorption isotherm for MCM-41 after different stages of preparation.....	46
12	Pore size distribution for MCM-41 after different stages of preparation.....	47
13	DMDA released from (PE)MCM-41 as a function of time for two cycles.....	48
14	Effect of AMP added on the structural characteristics of the dry grafted material.....	55
15	Assumed surface species obtained by dry grafting.....	56
16	Effect of AMP added on the structural characteristics of the wet grafted material in the presence of 0.3 mL water/g silica	57

	.....	
17	Effect of water added on the structural characteristics of the wet grafted material with 2 mL AMP/g silica	58
18	FT-IR spectra of (PE)MCM-41, (CPE)MCM-41 and AMP grafted MCM-41.....	61
19	^{13}C NMR spectra of (CPE)MCM-41 and AMP grafted MCM-41.....	62
20	TG profile for AMP-grafted material.....	64
21	MS response profile for AMP-grafted materials.....	65
22	Schematic representation of dehydroxylation process which takes place at high temperature	65
23	Schematic representation of the AMP grafting on the silica surface	66
24	Effect of AMP added to the dry grafting mixture on the amount of AMP grafted.....	68
25	Effect of AMP added to the wet grafting mixture (0.3 mL water/g silica) on the amount of AMP grafted.....	68
26	Effect of water added to the grafting mixture (2 mL AMP/g silica) on the amount of AMP grafted.....	69
27	Effect of AMP added to the dry grafting mixture on CO_2 adsorption capacity.....	71
28	Effect of AMP added to the wet grafting mixture (0.3 mL water/g silica) on CO_2 adsorption capacity.....	72
29	Effect of water added to the grafting mixture (2 mL AMP/g silica) on CO_2	72

adsorption capacity .....

30 Adsorption isotherm of Copper on AMP-grafted material 74

31 Adsorption isotherm of Copper on AMP-grafted material according to Freundlich model 74

32 Effect of amount of AMP added to the dry grafting mixture on the Cu^{2+} adsorption capacity..... 76

33 Effect of amount of AMP added to the wet grafting mixture (0.3 mL water/g silica) on the Cu^{2+} adsorption capacity..... 77

34 Effect of amount of water added to the grafting mixture (2 mL AMP/g silica) on the Cu^{2+} adsorption capacity..... 77

35 Effect of amount of AMP added to the dry grafting mixture on the CO_2 and Cu^{2+} adsorption efficiency 80

36 Effect of amount of AMP added to the wet grafting mixture (0.3 mL water/g silica) on the CO_2 and Cu^{2+} adsorption efficiency 80

37 Effect of amount of water added to the grafting mixture (2 mL AMP/g silica) on the CO_2 and Cu^{2+} adsorption efficiency..... 81

38 Scheme of CO_2 reaction pathways with primary amines..... 81

39 Effect of amount of AMP added to the dry grafting mixture on the CO_2 adsorption rate..... 83

40 Effect of amount of AMP added to the wet grafting mixture (0.3 mL water/g silica) on the CO_2 adsorption rate..... 83

41 Effect of amount of water added to the grafting mixture (2 mL AMP/g silica) on the CO_2 adsorption rate..... 84

42 Effect of the AMP surface density on the Cu^{2+} and CO_2 adsorption capacity for dry grafted materials 85

43 Effect of the AMP surface density on the Cu^{2+} and CO_2 adsorption capacity for wet grafted materials (0.3 mL water/g silica; 0.2-10 mL AMP/g silica)..... 84

44 Effect of the AMP surface density on the Cu^{2+} and CO_2 adsorption capacity for wet grafted materials (3 mL AMP/g silica, 0-1 mL water/g silica)..... 86

45 FT-IR spectra of AMP-grafted (CPE)MCM-41, acid-treated AMP-grafted and base- treated AMP-grafted (CPE)MCM-41MCM-41..... 88

Table of Contents

1 Introduction..... 1

2 Water..... 5

2.1 Importance of Water..... 5

2.2 Water Distribution 6

2.3 Occurrence of Heavy Metal in Water..... 8

2.4 Hazard Identification..... 11

2.5 Conventional Methods for Removal of Heavy Metals from Water..... 14

2.5-1 Precipitation Processes..... 15

2.5-2 Ion Exchange 15

2.5-3 Membrane Processes..... 16

2.6 Conventional Adsorbents for Wastewater Treatment..... 17

3 MCM-41 Silica 20

3.1 Discovery of Periodic Mesoporous Silica 20

3.2 Synthesis and Modification of MCM-41 Mesoporous Silica..... 23

4 Objectives of the Work..... 33

5 Experimental Work 34

5.1 Preparation of MCM-41..... 34

5.2 Pore Expansion of as-synthesized MCM-41..... 35

5.3 Selective Extraction of DMDA..... 36

5.4 Calcination..... 37

5.5 Surface Analysis..... 38

5.6 Copper adsorption Measurement..... 38

5.7 Stability Test of (PE)MCM-41 39
5.7-1 Total Organic Carbon (TOC) Measurements 39
5.7-2 Adsorption-Desorption Cycles 40
5.8 Amine Grafting on (CPE)MCM-41 40
5.9 Characterization of Grafted Materials 41
5.9-1 Surface Analysis 41
5.9-2 Thermogravimetric Analysis Mass Spectrometry (TGA-MS): CO_2 Adsorption and Thermal Decomposition 42
5.9-3 Copper Adsorption Capacity 42
5.9-4 FT-IR Characterization 43
6 Results and Discussion 44
6.1 Support Structural Characterization 44
6.2 (PE)MCM-41 Stability in Aqueous Solution 47
6.3 Effect of pH on the Stability of (PE) MCM-41 in Aqueous Solution 47
6.4 Regeneration of Copper Loaded (PE)MCM-41 50
6.5 Surface Characterization of Grafted Materials 54
6.6 FT-IR Characterization 60
6.7 ^{13}C NMR Characterization 61
6.8 Thermal Gravimetry- Mass Spectrometry Analysis; CO_2 Adsorption 62
6.9 Effect of Grafting Conditions 66
6.9-1 Effect of Grafting Conditions on Amount of Amine Grafted 66
6.9-2 Effect of Grafting Conditions on CO_2 Adsorption Capacity 69
6.9-3 Effect of Grafting Conditions on Adsorption of Cu^{2+} 73

6.9-4 Effect of Grafting Conditions on the Adsorption Performance for Cu^{2+} 75

6.10 Recycling of Amine-Grafted Material 86

7 Conclusions..... 89

8 References..... 91

9 Appendix 109

List of abbreviations

AAPTS	3-(2-aminoethylamino) propyltrimethoxyisilane
Ads.	Adsorbent
AMP	3-aminopropyl trimethoxy silane.
amu	Atomic mass unit
AO	Aesthetic Objective Concentration (mg/L)
(AS)MCM-41	The as-synthesized MCM-41
ATA	Alkyltrimethylammonium
ATAB	Alkyltrimethyl ammonium bromide
ATU	1-allyl-3-propylthiourea
BTU	1-benzol-3-propylthiourea
CMC	Carboxyl methylcellulose
CMC1	First critical micelle concentration
CMC2	Second critical micelle concentration
(CPE)MCM-41	Calcined pore-expanded MCM-41
CTAB	Cetylrtimethyl ammonium bromide
DDA	Dodecylamine
DTAB	Decyltrimethyl ammonium bromide
DMDA	N,N-dimethyldocylamine
EDTA	Ethylenediamine-tetra acetic acid tetra sodium
(EPE)MCM-41	Extracted pore-expanded MCM-41
FSM-16	Folded sheet material

IC	In organic carbon
ICP	Inductive coupled plasma
IMAC	Interm Maximum Acceptable Concentration (mg/L)
IUPAC	International Union of Pure and Applied Chemistry
IR	Infrared
LCT	Liquid crystal template
MAC	Maximum Acceptable Concentration (mg/L)
MCM-41	Mobil catalytic material number 41
MCM-48	Mobil catalytic material number 48
M41S	Molecular sieves number 41
MMLEG	Metal Mining Liquid Effluent Guidlines
MMLER	Metal Mining Liquid Effluent Regulations
MS	Mass spectrometry
MW	Measured weight loss
ND	Not detected
NF	Nanofiltration
OG	Operational Guidelines Concentration (mg/L)
(PE)MCM-41	The pore-expanded MCM-41
P/P^0	Relative pressure
PSDs	Pore size distribution
RO	Reverse osmosis
R_i(PE)MCM-41	(PE)MCM-41 after being recycled for i times
SBA-1	Cubic mesoporous silica (Santa Barbara-1)

SBET	Surface area determined by Brunauer-Emmett-Teller
Sol.	Solution
TC	Total carbon
TEOS	Tetraethylorthosilicate
TGA	Thermal gravimetric analysis
TMAOH	Tetramethyl ammonium hydroxide
TOC	Total organic carbon
TW	Theoretical weight loss
UF	Ultrafiltration
UHP	Ultra high purity
Wt	Weight

List of symbols

C_e	Equilibrium concentration (ppm)
C_i	Initial concentration (ppm)
k	Freundlich constant (mmol/g)
m	Mass of adsorbent (mg)
n	Freundlich constant (1/g)
q_e	Equilibrium adsorption capacity (mg/g)
V	Volume of solution (mL)

1 Introduction

Water Pollution means the addition of any foreign material (inorganic, biological or radiological) or any physical change in the natural water which may harmfully affect the living species (human, animals or plants) directly or indirectly, immediately, after some time or after a very long time. According to the report of the Environmental Pollution Panel of the U.S. President's Science Advisory Committee (1965), environmental pollution is the unfavorable changing of our surroundings, wholly or largely as a by product of man's actions, through direct or indirect effects of changes in energy patterns, radiation levels, chemical and physical constitution and abundance of organisms (Kudesia, V.P., 1990).

Nowadays the world is becoming too small place to live in because of various technological advancements. Problems like water pollution are no longer the concern of individual nations. The entire global community is responsible. The water that sustains us in different ways belongs to the world and therefore the responsibility for keeping it pollution-free must necessarily be shared by all of us.

Consequently during the last few decade governments all around the world have increased concerns about the rapid deterioration of the environment. In Canada, the protection of water is a shared responsibility between governmental and nongovernmental organizations. Governments administer a multitude of environmental legislations and regulations, land and water-use planning measures, and other environmentally oriented measures. The responsibility for the management of water and

natural resources is also shared with the Aboriginal people in land claims settlement areas. A description of the key pieces of federal, provincial, and territorial legislation related to the water is found in section 2.2 of the national report to the 2001 intergovernmental review meeting on implementation of the global program of action, November 2001 (Environment Canada, 2001).

Municipal governments, industry, nongovernmental organizations, communities, and individual Canadians are also important partners in protecting the water environment. Recognizing the value and contribution of community-based actions and stewardship programs, governments are working towards improving partnerships at the community level, building the capacity of these groups, and developing new, joint programs. Canadians are also taking it upon themselves to reduce their own impacts on the environment and share in the task of cleaning up existing problems, as is witnessed by the growing number of environmental programs, best practices, and codes of conduct being initiated by communities, industry, non-governmental organizations, and the public.

Environment Canada developed a process and plans to obtain multi-stakeholder input on regulatory issues associated with the implementation of aquatic effects of mining in Canada (AQUAMIN) recommendations in early 1997. This led to the development and subsequent publication of the proposed Metal Mining Effluent Regulations (MMER) in the Canada Gazette, part II, on June 19, 2002.

The story is the same in all large cities. Even small town municipalities are having difficulties dealing with the growing water pollution problem, which has assumed frightening dimensions. We have still to recognize that sustainable environment is the fundamental right of every citizen as it is essential for his physical, moral and social health.

Although several drastic measures have been taken during the last few years, the problem of water pollution continues to be a serious challenge to mankind and much effort is still required to develop new technologies to achieve the required environmental standards. Although there is a wide range of technologies available for such purpose (Veeken, A. et al., 2003; Feng, D. et al., 2000; Dąbrowski, A. et al., 2004; Trivunac, K. and Stevanovic, S., 2006), this work is focused on the adsorption technology as a purification technique because of its very high efficiency and relatively low cost compared to the other available technologies.

Adsorption of heavy metals is a particularly important topic in water pollution prevention and control, because a wide variety of toxic and carcinogenic chemicals are discharged into the water streams causing a quickly growing pollution problem for our oceans, lakes, and rivers due to rapid urbanization and industrialization and their consequences. In the first section of this work, the stability of pore-expanded MCM-41 silica [(PE)MCM-41] (Sayari, A. et al., 2005) as adsorbent for the removal of metallic cations from wastewater was investigated. The second part of this work dealt with surface modification of (PE)MCM-41 by introducing amine functionality to the

mesoporous silica through grafting of aminosilane. The grafting procedure was optimized and the adsorption capacity was measured. The ability of this material for recycling and reuse was also investigated.

2 Water

2.1 Importance of Water*

Our Earth seems to be unique among the other known planets. It has water, which covers 3/4 of its surface and constitutes 60-70 wt % of the living world. Water regenerates and is redistributed through evaporation, making it seem endlessly renewable. So why worry?

Actually, only 1% of the world's water is usable to humankind. About 97% is salty seawater, and 2% is frozen in glaciers and polar ice caps. Thus that 1% of the world's water supply is a precious commodity necessary for our survival. Lack of water will kill us faster than lack of food. Since the plants and animals we eat also depend on water, lack of it could cause both dehydration and starvation. The scenario gets worse. Water that looks drinkable can contain harmful elements, which could cause illness and death if ingested.

Water is a fundamental part of our lives. It is easy to forget how completely we depend on it. Human survival is dependent on water, which was ranked by experts as second only to oxygen as essential for life. The average adult body is 55 % water. A human embryo is more than 80% water. A newborn baby is 74% water. Since such a large percentage of our bodies is water, water must obviously affect heavily in how our bodies function. We need lots of fresh water to stay healthy. Aside from aiding in digestion and absorption of food, water regulates body temperature and blood

* Quantities were taken from Wikipedia, the free encyclopedia.

circulation, carries nutrients and oxygen to cells, and removes toxins and other wastes. This water also protects tissues and organs, including the spinal cord, from shock and damage. Conversely, lack of water (dehydration) can be the cause of many problems for the body, including hypertension, asthma, allergies, and migraine headaches.

Since water plays such a vital role in life on Earth, good quality water is a precious resource. Often water quality is more important than water quantity. The quality of the water affects the use we make of it, but the reverse is also true. Once we have used the water, we affect its quality. This circular process indicates that the traditional habit of discharging untreated sewage and chemical wastes directly into rivers, lakes, and oceans is no longer acceptable either technically or morally.

2.2 Water Distribution*

The planet's fresh water is also very unevenly distributed. Today the distribution is approximately as follows: 68.7 ice caps and glaciers, 30.1% ground water, 0.3% surface water, 0.86% ground ice and permafrost and 0.04% in the atmosphere. Of these sources, only rivers water is generally considered valuable because most of the water in lakes is in very inhospitable regions. As shown in Table 1, the distribution of renewable rivers water across the earth's surface is very uneven.

Here in Canada we are fortunate. We have extensive supplies of water but today, under the pressures of human development; many of these waters are losing their

* Quantities were taken from Wikipedia, the free encyclopedia.

unspoiled quality. It is no wonder. We dispose of domestic wastes, animal wastes and chemical substances into the environment at such a rate that even some of the largest lakes and river systems cannot tolerate. The Great Lakes and the St. Lawrence River, for example are having serious difficulty cleansing themselves and sustaining life (Environment Canada, 2003).

Canada has more lake areas than any other country in the world, with 563 lakes larger than 100 square kilometers. The Great Lakes, straddling the Canada-U.S. boundary, contain 18% of the world's fresh water. The Great Lakes basin (the lakes plus the area of land draining into the lakes) contains 18% of the world's fresh surface water and is home to almost a third of the Canadian population.

Table 1: The distribution of renewable river water across the Earth's surface.

Continent or region	Renewable river water (km^3)	Percent of world total
Sub-Sahara Africa	4,000	9.20
Middle east and North Africa	140	0.32
Europe	2,900	6.70
Asia (excluding middle east)	13,300	30.6
Australia	440	1.01
Oceania	6,500	14.9
North America	7,800	17.9
South America	12,000	27.6

2.3 Occurrence of Heavy Metals in Water

A wide variety of toxic inorganic and organic chemicals are discharged to the water sources causing a quickly growing pollution problem for our oceans, lakes, and rivers due to rapid urbanization and industrialization and their consequences. Ontario, which has the biggest heavy metals mining operations such as nickel and copper, is now having an acidification and heavy metals contaminations in more than 7000 lakes, causing severe environmental problems (Gregory, G. et al., 2005). Over 360 chemical compounds have been identified in the Great Lakes. Many are toxic chemicals such as alkylated lead, DDT, mercury, which are potentially dangerous to humans and already destructive to the aquatic ecosystems (Environment Canada, 2001).

Tables 2 and 3 show the concentration of heavy metals in water samples collected during 2001 and 1993-1994 respectively from lakes in the Sudbury basin (Gregory, G. et al., 2005; Nriagu, J. et al., 1998). Comparing concentrations of Cu, Ni, and Zn in lakes Ramsey and Kelley as shown in Table 4, it is obvious that the situation in the two lakes improved with respect to these cations and it could improve more if we were aware of the problems heavy metals create, so we all, in our little ways, can contribute to the solutions.

The origin of heavy metals contamination in water is mainly a result of uncontrolled disposal of several industries wastewater such as painting, pigments, metallic coating passivation, mining, extractive metallurgical industries, agriculture phosphorous fertilizer, antibacterial, insecticides, fungicides, and other industries

(Korngolg, E. et al., 1996; Sayari, A. et al., 2005; Dąbrowski, A. et al., 2004; Apak, R. et al., 1998). Other sources of heavy metals contamination are the corrosion of pipes used to transfer water (Korngolg, E. et al., 1996), electrical wiring, plumping, heating, roofing and building constructions (Apak, R. et al., 1998).

Table 2: Dissolved trace metal concentrations in water samples collected in 2001 from 12 lakes in the Sudbury basin, Ontario, Canada.

Lake	Total Metal Concentration (µg/L)									
	Al	As	Ba	Cu	Fe	Ni	Rb	Se	Sr	Zn
Barlow	238.7	ND*	12.7	4.3	389	9.7	2.0	ND	20.0	10.3
Big Marsh	128.7	0.7	10.3	3.7	421	9.0	1.7	ND	16.3	7.3
Birch	172.7	ND	14.3	2.0	714	7.0	2.0	ND	18.3	7.0
Waubamac	80.0	ND	10.0	2.0	412	8.0	1.7	0.6	28.3	5.8
Kelly	ND	2.4	38.4	15.0	477	338.2	19.2	5.8	365.0	11.7
Mud	70.7	3.3	33.3	17.0	653	257.3	15.3	4.7	291.0	7.3
Simon	ND	2.3	33.3	9.7	422	318.7	15.7	5.0	271.3	9.0
Hannah	ND	2.0	23.7	25.0	71	181.0	3.0	2.3	64.7	10.0
Kusk	46.0	2.0	14.3	6.0	261	60.0	3.0	1.2	56.7	6.0
McCharles	ND	1.7	19.7	6.0	203	111.3	5.3	1.0	102.0	4.7
Rasmsey	ND	1.3	14.0	9.7	36	52.0	2.0	2.0	48.7	5.7
Whitson	ND	0.7	21.3	19.0	53	155.0	2.3	ND	36.3	17.7

* ND: Not detected

Table 3: Dissolved trace metal concentrations in water samples collected in 1993-1994 from 10 lakes in the Sudbury basin, Ontario, Canada.

Lake	Total Metal Concentration (µg/L)				
	Ni	Cu	Zn	Mn	Cd
Ramsey	116	16	7.8	1.2	0.099
Kelley	379	30	21	223	0.091
Silver	631	282	83	175	1.1
McFarlane, east Basin	76	7.7	2.7	0.96	0.003
McFarlane, west Basin	73	8	3.6	2.5	0.051
Clearwater	188	86	23	240	0.45
Lohi	142	87	22	147	0.34
Richard	86	6.6	1.3	2.1	0.036
Windy	13	2.3	4.6	4.8	0.036
Nelson	5.7	2.7	3.3	14	0.029

Table 4: Dissolved trace metal concentrations in water samples collected in 1993-1994 and in 2001 from lakes Ramsey and Kelley in the Sudbury basin, Ontario, Canada.

Lake	Total Metal Concentration (µg/L)					
	Cu		Ni		Zn	
	1994	2001	1994	2001	1994	2001
Ramsey	16	9.7	116	52	7.8	5.7
Kelley	30	15	379	338	21	11.7

2.4 Hazard Identification

Pollution is not always visible. A river or lake may seem clean, but still be polluted. In groundwater, on which over one quarter of all Canadians relies for their water supply (Environment Canada, 2001), pollution is especially difficult to distinguish. Also, the effects of pollution are not necessarily immediate; they may take years to appear.

When pollution makes water unsuitable for drinking, recreation, agriculture and industry, it eventually also diminishes the beauty quality of lakes and rivers. Even more seriously, when contaminated water destroys aquatic life and reduces its reproductive abilities, it eventually affects human health. Nobody escapes the effects of water pollution.

The presence of heavy metals in water has great effects on the fauna and flora of lakes and streams. Heavy metals in water have clear effects on water acidity, they decrease the value of pH, which in turn adversely affects fish stocks and vegetation (Ahmad, S. et al., 1998). For example, various species of fish now suffer from tumors and lesions, and their reproductive capacities are decreasing (Environment Canada, 2001). Populations of fish consuming birds and mammals also seem to be on the decline. Of the ten most highly valued species of fish in Lake Ontario, seven have now almost totally vanished (Environment Canada, 2003). Freshwater mussels, Elliptio Complanata, were caged in various locations in several storm water treatment facilities and control sites in southeastern Ontario. Mussels were sampled at 2, 5.5, 8, 11, and 14 weeks and Ni, Cr, Cu, Cd, and Pb concentrations in soft tissues were determined by

ICP-MS (Anderson, B.C. et al., 2004) and that make the public health and environmental agencies in the Great Lakes states and the province of Ontario to warn against human consumption of certain fish. Some fish cannot be sold commercially because of high levels of mercury or other substances (Environment Canada, 2003). Also heavy metals may contribute to a health decline when they accumulate in the body tissues (Alpatova, A. et al., 2004). In general health problems related to water pollution are estimated to cost Canadians $300 million per year (Environment Canada, 2001). Actual Ontario standards of contaminants in drinking water are summarized in Table 5 (Ministry of Environment, 2001).

In 1977, Environment Canada published an environmental code of practice for mines and explanatory notes in a single report entitled Metal Mining Liquid Effluent Regulations and Guidelines (EPS1-WP-77-1) MMLER and the MMLEG. The legal reference to the regulations is the consolidated regulations of Canada 1978, chapter 819 (Government of Canada, 1978). The MMLER prescribed authorized concentration limits for hazardous substances in mine effluents that discharged to waters frequented by fish. The limits were based on best practicable technology as determined by a state of the art review by a joint federal provincial industry task force. Some of the regulated parameters were arsenic, copper, lead, nickel, and zinc. The regulations applied to new, expanded and reopened metal mines are shown in Table 6. In Ontario region some of the mines still don't meet the MMLER regulations as shown in Figure 1.

Table 5: Ontario Drinking Water Standards*.

Element	MAC[1] (mg/L)	IMAC[1] (mg/L)	Effects
Arsenic		0.025	Carcinogenic.
Cadmium	0.005		Highly toxic non-essential metal that affects the action of enzymes and impedes respiration, photosynthesis, transpiration and chlorosis, kidney diseases.
Mercury	0.001		The most hazardous contaminant in natural environment because it spreads easily and will be accumulated in living organisms causing damage to the nervous system.
	AO[1] (mg/L)	OG[1] (mg/L)	
Aluminium		0.1	No clear evidence that residual aluminium has any effects on health. But high residual can cause coating of the pipes in the distribution system resulting in increased energy requirement for pumping.
Copper	1		Due to its toxicity inhibit natural growth and development of plants and effect negatively self-purification of water and living organism in the water environment.
Lead	0.01		Toxic, harmful to pregnancy and children.
Iron	0.3		Brown colour of water, a bitter and a stringent taste in water, promote the growth of iron bacteria in water.
Zinc	5		

* (Ministry of Environment, 2001)
MAC (Maximum Acceptable Concentration) established for parameters which when present above a certain concentration, have known or suspected adverse health effects. The length of time the MAC can be exceeded without health effects will depend on the nature and concentration of the parameter.
IMAC (Interm Maximum Acceptable Concentration): established for parameters either when there are insufficient toxicological data to establish a MAC with reasonable certainity, or when it is not feasible, for practical reasons, to establish a Mac at the desired level.
[1]OG (Operational Guidelines) established for parameters that, if not controlled, may negatively effect the efficient and effective treatment, disinfection and distribution of water.
[1] AO (Aesthetic Objective): established for parameters that may impair the taste, odor or color of water or which may interfere with good water quality control practices. For certain parameters, both aesthetic objectives and health-related MACs have been derived.

Table 6: Authorized Levels of Hazardous Substances Prescribed in the MMLER

Substance	Maximum Authorized Monthly Mean Concentration (mg/L)
Arsenic	0.5
Copper	0.3
Lead	0.2
Nickel	0.5
Zinc	0.5

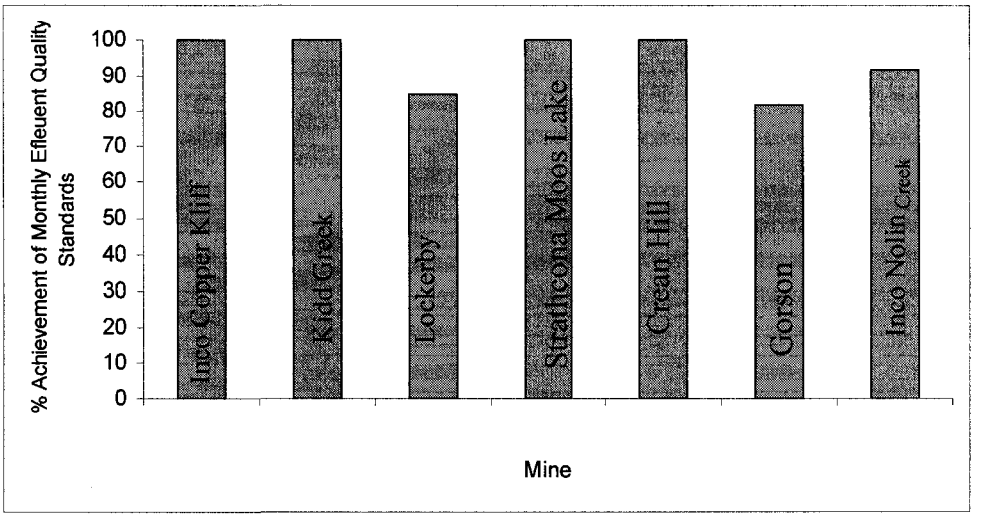

Figure 1: Performance of mines subject to the MMLER in the Ontario region in 2001.

2.5 Conventional Methods for Removal of Heavy Metals from Water

The removal and separation of toxic and environmentally relevant heavy metal ions are technological challenges with respect to industrial and environmental applications. Many researchers have made efforts to remove heavy metals from industrial water using several processing methods such as precipitation, membrane, evaporation, ion exchange and sorption. The development of these processes has been accelerated in recent years and has begun to find applications in the treatment of industrial wastewaters.

2.5-1 Precipitation Processes

Chemical precipitation is the most widely used method for the removal of heavy metals from water. Charerntanyarak, L. (1999) applied hydroxide precipitation and found that the optimum pH for chemical coagulation and precipitation by lime treatment was more than 9.5, and was able to decrease the heavy metals content to the wastewater standards level. However, the disadvantages of this method include high residual effluent metal concentrations (0.5-2 mg/L) (Veeken, A. et al., 2003). Another good alternative is sulphide precipitation, which can result in very low effluent concentrations (< 0.01 mg/L) (Veeken, A. et al., 2003). Another advantage of sulphide precipitation is the ability to separate different metals and reuse them by controlling pH, sulphide concentration and redox potential. Pott, B. and Mattiasson, M. (2004) were able to separate copper from cadmium by the use of redox potential control. However, sulphide precipitation shows many drawbacks because the dosing of sulphide cannot be controlled, and excess sulphide in the effluent is toxic and corrosive (Veeken, A. et al., 2003). One technique to overcome this is to use a combination of lime and sulphide, which could precipitate all the heavy metals completely (Feng, D. et al., 2000). One major problem with precipitation is the formation of large amounts of sediments containing heavy metal ions.

2.5-2 Ion Exchange

By ion exchange undesirable ions are replaced by others, which don't contribute to contamination of the environment. This method is able to remove Pb (II), Hg (II), Cd (II), Ni (II), Cr (II), Cu (II), and Zn (II) by means of modern types of ion exchangers.

Many authors have studied the ion exchange process (Dąbrowski, A. et al., 2004). Korngold, E. et al. (1996) studied the possibility of removing heavy metals, such as Cu, Co, Ni, Cd, and Pb. They concluded that a cation-exchange resin possessing an important iminodiacetic acid group could selectively remove these metals from relatively high initial concentrations of calcium and magnesium. Ahmed, S. et al. (1998) studied the removal of lead and cadmium from aqueous solution by batch ion exchange with a solid Na-Y zeolite under competitive and non-competitive conditions. Base, A. et al. (1996) carried out experiments to determine the relative ability of sodium and different heavy metal cations in replacing protons from inorganic sites of a modified coconut coir cation exchanger. The relative preference they found follows the sequence: Pb >Cu >Ni >Mn >Ca >Na.

2.5-3 Membrane Processes

Membrane processes, especially reverse osmosis (RO) and nanofiltration (NF) were proved to be a promising alternative to technologies based on precipitation and ion exchange. These processes, which were mainly used for desalination purposes are relatively new (Abu Qudais, H. and Moussa, H., 2004). However, many developments have been achieved recently in order to be able to use this technique in the treatment of industrial wastewaters. The advantages of this process are the high separation selectivity and low energy consumption (Trivunac, K. and Stevanovic, S., 2006). These separation processes involve bonding the metals to a special bonding agent and then separating the loaded bonding agent from the wastewater by membrane filtration (Blőcher, C. et al., 2003). Trivunac, K. and Stevanovic, S. (2006) studied the effects of

type of complexing agent, pH value and applied pressure on the retention. At best operating conditions the removal of Cd^{2+} and Zn^{2+} was more than 95% and 99% respectively. Blőcher, C. et al. (2003) studied the use of hybrid flotation-membrane filtration process. The feasibility of this system was proven since all toxic metals, copper, nickel and zinc, were reduced from 474, 3.3, and 167 mg/L respectively to below 0.05 mg/L which is acceptable value. Abu Qudais, H. and Moussa, H. (2004) showed that high removal efficiency of the heavy metals could be achieved by RO (99%). NF, however, was able to remove only 90%. The effectiveness for treating water containing more than one metal was also investigated. RO was able to decrease the concentration from 500 ppm to about 3 ppm (99.4%), while NF achieved 97% removal. Nenov, V. and Petro, S. (2004) studied the complexation of Cu^{2+}, Pb^{2+}, Fe^{2+}, and Mn^{2+} by carboxyl methylcellulose (CMC) from synthetic solutions and real wastewater followed by ultrafiltration (UF) used as complex separation step. The results obtained showed that a low Cu:CMC ratio favors both ultrafiltrate permeability during the first stage of the process and the separation following the next step of complex destruction at lower pH.

2.6 Conventional Adsorbents for Wastewater Treatment

Adsorption is now considered the most effective, economic and selective method for water treatment and analysis purposes. Many solid substances have the capability of attracting molecules of gases or solutions with which they are in contact to their surfaces. Solids that are used to adsorb gases or dissolved substances are called adsorbents. Activated carbons (Űçer, A. et al., 2006; Kadirvelu, K. et al., 2001) are

among the most effective adsorbents for heavy metals in wastewater. This is mainly because of their very high surface area (Sayari, A. et al., 2005). In recent years, many researchers concentrated their efforts to develop more effective adsorbents. Currently, there is an increasing emphasis on adsorbents based on naturally occurring materials. Natural supports have many advantages such as, availability in large quantities, relatively cheap, and can be chemically modified to increase their binding capacity. Among these adsorbents chelating resins (Abd El-Moniem, N. et al., 2005; Lin, S. et al., 2000), cellulose (O'Connell, D. et al., 2006; Zhou, D. et al., 2004), peat resin (Sun, Q. et al., 2004), clays and soil constituents (Zhao, H. and Vance, G., 1998; Dho, N. and Lee, S., 2003; Bradl, H., 2004), red mud (Apak, R. et al., 1998; Cho, H. et al., 2005), and fly ashes (Cho, H. et al., 2005; Jang, A. et al., 2005). Another approach is to utilize adsorbents from biomass sources. These raw biomasses can be chemically modified by various methods to increase their sorption capacity. Some of these biomasses are mulsh (Jang, A. et al., 2005), wheat bran (Farajzadeh, M. and Monji, A., 2004), modified lignin (Demirbas, A., 2004; Celik, A. and Demirbaş, A., 2005), fish scales (Mustafiz, S. et al., 2003), crab shell (An, H. et al., 2001), and marine alga (Feng, D. and Aldrich, C., 2004). Many authors tried different materials to be used as adsorbents, for example crown ether (Tzeng, D. et al., 1987), graphitic carbons (Groszek, A.J., 1997), carbon aerogel (Goel, J. et al., 2005), and organically modified montmorillonite for adsorption of phenol and alkylphenols from aqueous solutions (Huh, J. et al., 2000). However, these adsorbents show many disadvantages because of their wide distribution of pore sizes, heterogeneous pore structure (Zhang, L. et al., 2003; Kruk, M. et al., 2000), low

selectivity and low capacity due to their weak interactions with metallic ions (Sayari, A. et al., 2005).

Whether dealing with adsorption of heavy metal ions or with adsorption of other pollutants, there is need to develop novel adsorbents with well-designed pore size, pore geometry, and binding capacity. Mesoporous materials such as MCM-41 are considered to be superior in this area of research because of their high surface area, controlled pore sizes and narrow pore-size distributions (Kruk, M. et al., 2000). This topic will be discussed in the following section.

3 MCM-41 Silica

Discovery of Periodic Mesoporous Silica

In 1990, Kuroda and coworkers (Yanagisawa, T. et al., 1990) first reported the preparation of periodic mesoporous silica with uniform pore size distribution through ion-exchange of cetyltrimethylamonium cations within the layered polysilicate kanemite (idealized formula $NaHSi_2O_5.3H_2O$), followed by calcination to remove the organic moiety. These novel materials were also known as Folded Sheet Materials (FSM-16). The calcined silica had pores 2-4 nm in diameter, and surface area of 900 m^2/g.

In 1993, Kuroda and coworkers (Inagaki, S. et al., 1993) reported the successful formation of highly ordered mesoporous materials derived from layered polysilicate kanemite by optimizing the reaction conditions of the ion exchange reaction. They found that the FMS-16 pore diameter could be controlled by varying the alkyl chain length of the cationic surfactants. A schematic presentation of their work is shown in Figure 2.

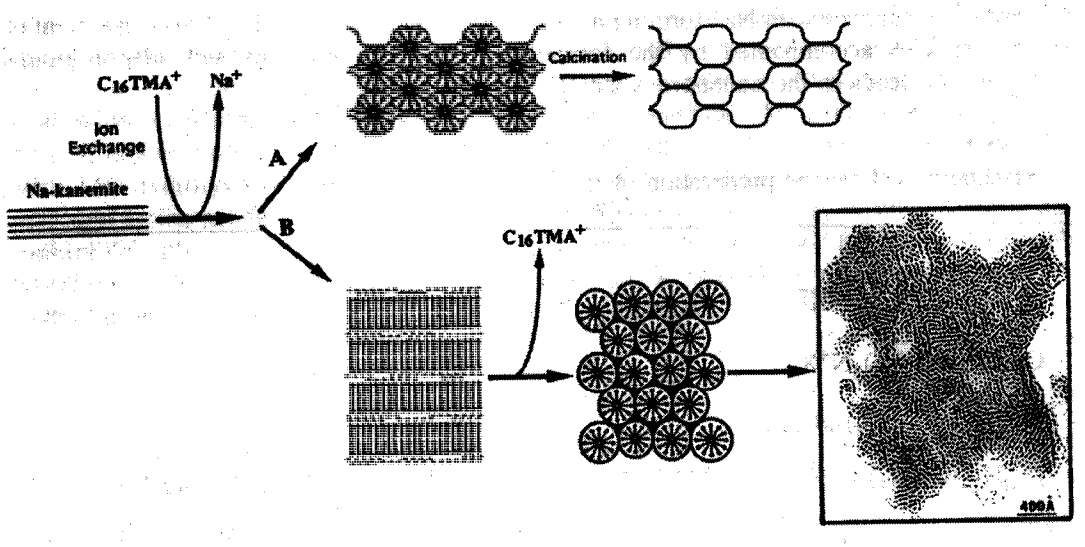

Figure 2: Formation mechanisms of FSM-16 according to Inagaki, S. et al., 1993.

In 1992, scientists of Mobil described the synthesis, characterization, and proposed mechanism of formation of a new family of silica and aluminosilica mesoporous molecular sieves designated as M41S (Beck, J. et al., 1992). They reported that MCM-41, one member of this family, exhibits a hexagonal arrangement of uniform cylindrical mesopores whose dimensions may be engineered in the range of 20 A to greater than 100 A. Also they synthesized other members of this family, including a material exhibiting cubic symmetry, MCM-48. They found that these mesoporous materials have typical surface areas above 700 m^2/g and hydrocarbon sorption capacities of 0.7 mL/g or greater. In support of this templating mechanism, it was demonstrated that the structure and pore dimensions of MCM-41 materials are intimately linked to the properties of the surfactant, including surfactant chain length and solution chemistry. The presence of variable pore size MCM-41, cubic material and other phases, indicates that M41S is an extensive family of materials. Also in 1992, the same group reported similar synthesis of periodic mesoporous aluminosilicate in the presence of surfactants. The material they obtained possessed regular arrays of uniform channels with dimensions in the range of 1.6 to 10 nm through the choice of surfactant, auxiliary chemicals and reaction conditions (Kresge, C.T. et al., 1992).

Since the discovery of FSM-16 and M41S much interest has been put into the synthesis of materials with well defined mesoporous structure, because of their potential applications in catalysis (Reynhardt, J. et al., 2004; Sayari, A., 1996; Armengol, E. et al., 1997; Morey, M. et al., 1998; Pater, J. et al., 1999), separation science (Hata, H. et al., 1999; Newalkar, B. et al., 2002; Mattigod, S. et al., 1999; Zhao, D. et al., 1998;

Shiraishi, Y. et al., 2002), and environmental protection such as adsorption of heavy metals from aqueous solutions (Olkhovyk, O. et al., 2004; Sayari, A. et al., 2005; Olkhovyk, O. and Jaroniec, M., 2005; Mercier, L. and Pinnavaia, T., 1998; Algarra, M. et al., 2005; Brown, J. et al., 1999; Yanatasee, W. et al., 2003; Liu, A. et al., 2000; Antochshuk, V. and Jaroniec, M., 2002), adsorption of carbon dioxide (Franchi, R. et al., 2005; Harlick, P. and Sayari, A., 2006) and adsorption of organic pollutants (Sayari, A. et al., 2005; Zhao, Y.X. et al., 2005, and Serna, R. and Sayari, A., 2007). This strong interest in these materials is due to their flexibility in terms of synthesis conditions, pore sizes, particle geometry and advanced materials applications. Figure 3 shows a microscopic view of MCM-41.

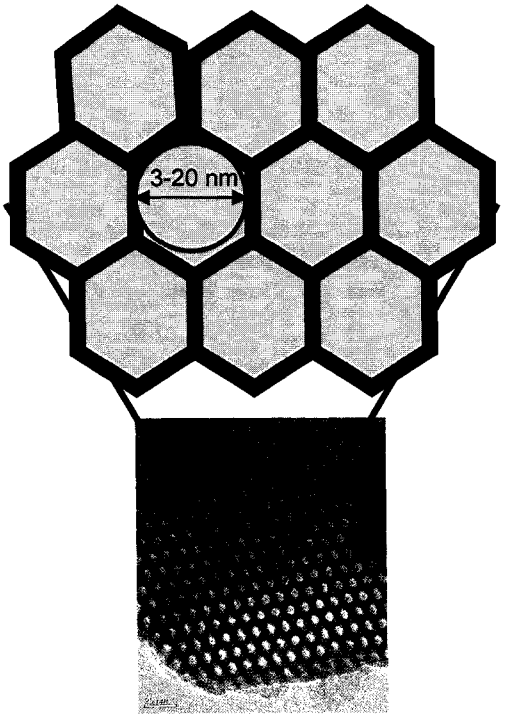

Figure 3: Microscopic view of MCM-41

Synthesis and Modification of MCM-41 Mesoporous Silica

MCM-41 is prepared by hydrothermal treatment of a gel, typically at 80 to 120 °C for 24 to 48 h (Sayari, A., 1996). An array of surfactant molecules, which are an amphilphile molecule with hydrophophilic head and hydrophopic tail, play the role of template. A template is a structure around which a material nucleates and grows, then after the removal of the templating structure, its geometric and physical characteristics reflect the nature of the template. In this case, the surfactant array, i.e. liquid crystal, dictate the pore structure including the shape of the pores, their size and their connectivity. A hexagonal array of cylindrical micelles gives rise to MCM-41 silica mesophase. Figure 4 shows a schematic representation for this process.

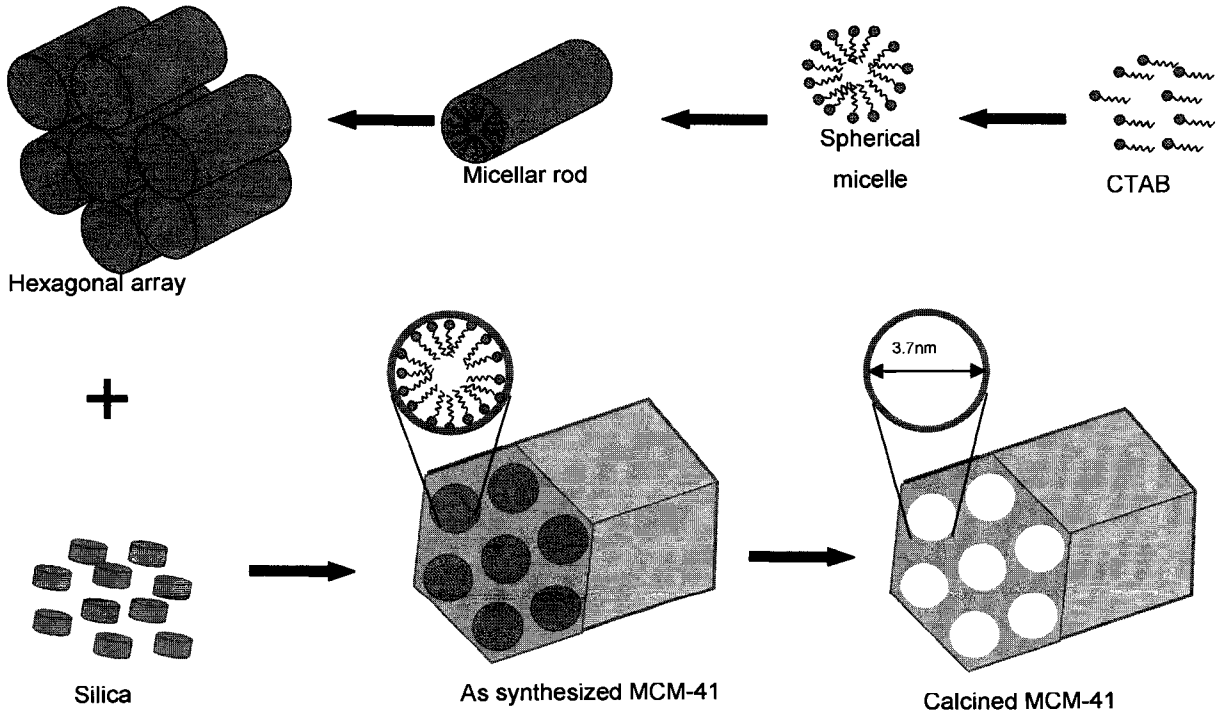

Figure 4: Scheme of synthesis of periodic mesoporous silica.

The preparation of MCM-41 requires three ingredients in appropriate amounts: A solvent, a source of silica and a surfactant. Other reagents such as acids, bases, salts, co-solvents, and expanders may be used. These materials can vary from one application to another of the target MCM-41.

Surfactant aggregation in water is the first stage. Figure 5 shows a schematic phase diagram of surfactants in water (Sayari, A., 1996). As shown in the figure, the surfactant aggregation is mainly a function of temperature and concentration. At very low concentration these surfactants tend to be randomly dispersed in the solution. At the first critical micelle concentration (CMC1), spherical micelles are formed and when the concentration reaches the second critical micelle concentration (CMC2), further aggregation takes place forming cylindrical rod-like micelles, which play an important role in the formation of MCM-41. As the concentration increases further, a higher level of aggregation takes place leading to liquid crystals with different structure, e.g., lamellar, hexagonal and cubic.

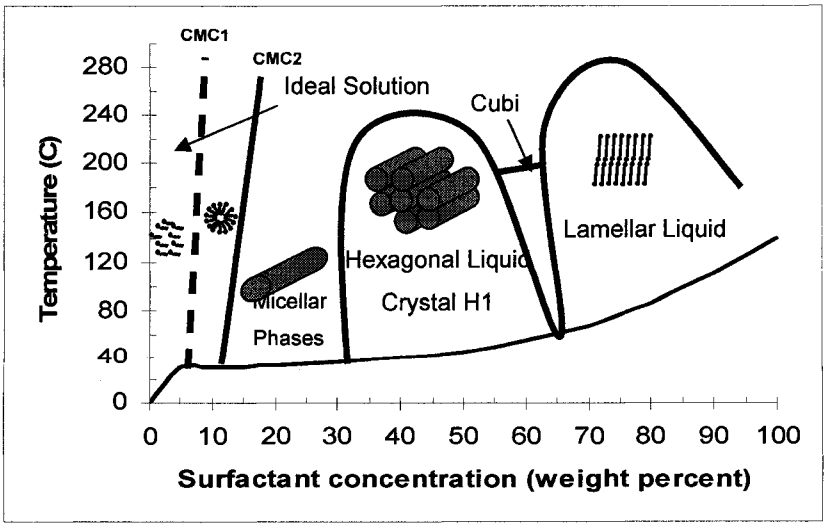

Figure 5: Schematic phase diagram of surfactant in water (Sayari, A., 1996).

Hexagonal MCM-41 phase can be prepared using different kinds of surfactants; the most common being alkyltrimethylammonium (ATA) salts. Low molecular weight surfactants seem to be more difficult to self organize, thus resulting in a less ordered materials with broader pore size distributions (Sayari, A. and Yang, Y., 2000). On the other hand, too heavy surfactants were rarely used because they are difficult to dissolve. Thus, ATA salts with carbon chains with 10 to 18 carbon atoms are the most commonly used. Sayari, A. et al. (2005) used cetyltrimethylammonium bromide (CTAB) with 16 carbon atoms chain to prepare MCM-41. The same surfactant was used by Sayari, A. (2000) to prepare another type of mesoporous material, cubic MCM-48. Also he provided reproducible recipes, which afford excellent quality materials using decyltrimethylammonium bromide (DATAB) (Sayari, A. et al., 2000). The same method can be used in the presence alkyltrimethylammonium bromide (ATAB) with 12 and 14 carbon chains. Kruk, M. et al. (1997) prepared MCM-41 using ATAB with different chain lengths. The pore size was shown to increase in a regular way with the chain length of the surfactant used. Lee, B. et al. (2001) prepared their MCM-41 using dodecylamine (DDA) as a template.

It has been reported that as-synthesized (i.e. surfactant-containing) MCM-41 is mechanically stable and promising adsorbent for removing organics from liquid and gas phase (Kruk, M. et al., 2002). However, because its pore system is filled with surfactant, as-synthesized MCM-41 usually has a low surface area and restricted diffusion within the pores. These pores become accessible after the removal of surfactant. Surfactant removing procedures depend on the nature of surfactant. In the case of charged

surfactants, where electrostatic interactions between inorganic and surfactant ions are strong, calcination, which involves a high temperature treatment of the MCM-41, is the preferred method (Sayari, A. et al., 2005). This calcination results in some structure shrinkage and further condensation of the silica pore walls (Antochshuk, V. and Jaroniec, M., 1999). In the case of neutral surfactants the framework and the template interact by weak hydrogen bonding so the template can be removed by solvent extraction (Antochshuk, V. and Jaroniec, M., 1999). This method is also applied regardless of the nature of the surfactant, when the material framework is thermally unstable such as organosilicates.

The pore size can be controlled within a wide range by one of the following synthesis strategies:(i) using surfactants of appropriate chain lengths (Kruk, M. et al., 1997), (ii) direct synthesis in the presence of swelling agents such as alkylamines (Kruk, M. et al., 2000; Sayari, A. et al., 1998) and trimethylbenzene (Beck, J. et al., 1992), (iii) post-synthesis treatment in the presence of amine in water (Sayari, A., 2000; Sayari, A. et al., 1998). Several factors can affect the materials obtained by post-synthesis hydrothermal pore expansion such as MCM-41 preparation temperature, amine to silica ratio, duration and temperature of post-synthesis treatment (Sayari, A., 2000).

For environmental applications, mesoporous materials often undergo appropriate surface modification to impart that specific surface chemistry and bonding sites. It is expected that the occurrence of high density of functional groups while retaining the open structure would result in high performance. Therefore, achieving high loading of

functional groups in mesoporous silica has received much attention. Many researchers have reported surface modification with different functional groups, using different routes and for different purposes (Sayari, A. and Hamoudi, S., 2001). One way is to anchor a functional group on the surface of the pores using post-synthesis procedures. Indeed, after the removal of the surfactant the silica surface contains a certain amount of hydroxyl groups, which can react with alkoxysilane with different functionalities giving rise to grafted species through oxygen bridges as shown in Figure 6 (Yanatasee, W. et al., 2003; Olkhovyk, O. et al., 2004; Shiraishi, Y. et al., 2002; Liu, A. et al., 2000; Antochshuk, V. and Jaroniec, M., 2002; Feng, X. et al., 1997; Liu, J. et al., 1998; Lee, H. and Yi, J., 2001; Bois, L. et al., 2003). Liu, A. et al. (2000) prepared a thiol and amino-functionalised silicas with uniform mesoporositiy and they applied them for removing heavy metal ions from wastewater; the thiolated adsorbent was found to exhibit a higher complexation affinity for mercury ions, while other ions such as Cu^{2+}, Ni^{2+} and Co^{2+} showed exceptional binding ability with its aminated analogue. Antochshuk, V. and Jaroniec, M. et al. (2002) used 1-allyl-3-propylthiorea modified mesoporous silica and they showed that this material has high adsorption capacity towards mercury ions and its regeneration can be accomplished under mild conditions in the presence 10% thiourea aqueous solution. Feng, X. et al. (1997) synthesized a mercaptopropylsilane crosslinked to mesoporous silica. They reached a surface coverage up to 76% and a distribution coefficient up to 340,000 for mercury and other heavy metal ions. Liu, J. et al. (1998) developed a new approach so that organized functional monolayers are covalently bound to mesoporous supports. Their functionalised hybrid materials showed exceptional selectivity and capacity for removing heavy metals from waste streams.

Lee, B. et al. (2001) immobilized 3-(2-aminoethylamino) propyltrimethoxyisilane (AAPTS) on the mesoporous surface. They were able to remove copper ions from aqueous solution up to 10 times more efficiently than commercial silica. Using a triaminesilane, Harlick, P. and Sayari, A. (2005) carried out a systematic study of the amine loading as a function of grafting temperature and the relative amount of triamine and water used during the grafting procedures. They found that the optimally grafted MCM-41 was obtained under the conditions of 3.0 mL silane/g silica, 0.3 mL water/g silica and 85 °C grafting temperature. Harlick, P. and Sayari, A. (2006) used conventional MCM-41 and pore-expanded MCM-41 silicas as supports for grafting triamine. They found that when both supports were grafted under the same conditions, the pore-expanded silica was grafted with slightly larger quantities of amine than the conventional one for all controlled silane additions. Because the surface area of the two supports they used was similar, this result may be due to the density of reactive hydroxyl group or due to the pore size and pore volume effect.

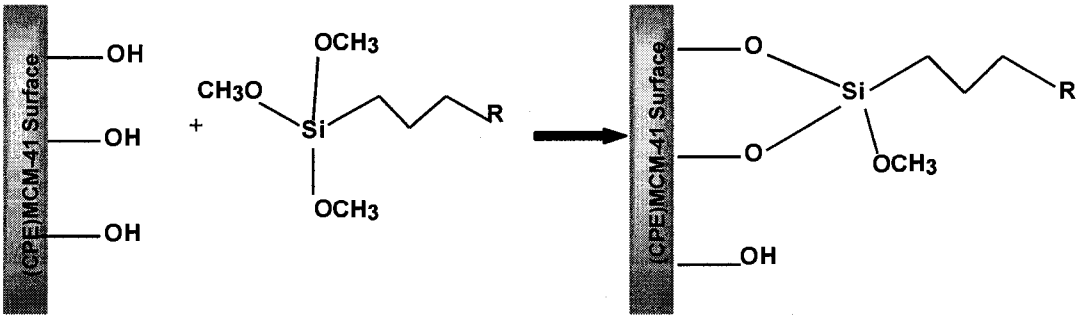

Figure 6: Schematic representation of post-synthesis grafting of alkoxysilane with different functionalities.

The second approach to achieve surface functionalization is the cocondensation of alkoxysilane with the silica source, often tetraethylorthosilicate (TEOS) (Bois, L. et al., 2003; Inumaru, K. et al., 2004; Inumary, K. et al., 2000; Fowler, C.E. et al., 1997). Mercier, L. and Pinnavaia, T. (1997) demonstrated the superior effectiveness of functionalized mesoporous molecular sieves as heavy metal adsorbents over those prepared from materials with disordered pore networks such as silica gel. In 1998 they prepared a thiol-functionalized nanoporous silica and used it for selective adsorption of Hg^{2+}. They found that this material exhibit selective complexation affinity for Hg^{2+}, while other metal ions (Cd^{2+}, Pb^{2+}, Zn^{2+}, Co^{3+}, Fe^{3+}, Cu^{2+}, and Ni^{2+}) have little or no binding ability with the adsorbent (Mercier, L., and Pinnavaia, J. 1997). Bois, L. et al. (2003) used cocondensation to prepare functionalised porous silica with different organic groups. These organo-silicas were used for the removal of heavy metal ions from aqueous solutions. Samples synthesized with [amino-ethylamino] propyl- and (2-aminoethylamino) ethylamino] propyl- functions show high loading capacity for Cu^{2+}, Ni^{2+} and Co^{2+}. The samples synthesized with a mercaptopropyl function have high loading capacity for Cd^{2+}. Inumaru, K. et al. (2004) studied the molecular selective adsorption of alkylphenols and alkylanilines onto n-alkyl grafted MCM-41 with different chain lengths. They found that octyl groups gave better adsorption performance than pentyl and dodecyl groups. They identified two major factors that determine the molecular affinity. One is the hydrophobicity of the alkyl groups of the molecule, where molecules with large hydrophopic alkyl groups were found preferentially adsorbed. The other major factor they studied was the hydrophilic groups of the molecule alkylanilines, which have a stronger hydrophilic group than alkylphenols, and are preferably adsorbed

due to stronger hydrogen bonding. Inumaru, K. et al. (2000) reported the grafting of alkylsilanes with intermediate chain lengths. They found that the octyl-silane-grafted mesoporous silica effectively removed nonylphenol from water, while it showed no detectable adsorption of phenol. Yokoi, T. et al. (2004) compared two methods of introducing mono-, di-, and tri-amine functionality to MCM-41 via direct co-condensation and post-synthesis grafting. They found that the amount of Co^{2+} and Fe^{2+} adsorbed on the amino-functionalised samples via the co-condensation method increased with an increase in the surface density of the amino groups regardless of the amino-alkoxysilanes. When mono and diamine were grafted onto the surface of MCM-41 by post-synthesis the adsorption capacity increased with an increase in the surface density of amino groups. However, when triamine was grafted, the adsorption capacity decreased with an increase in the surface density of the amino groups, which indicates that the locations of the amino groups introduced by the two methods are different. Lim, M. and Stein, A. (1999) compared the structures, stability and the reactivity of vinyl-functinalized MCM-41 samples prepared either by a post-synthesis grafting process or direct co-condensation. They found that the vinyl groups were non-uniformly distributed in the grafted samples while uniform distribution was obtained by the co-condensation method. Also they reported that the mesoscopic order of products from the direct synthesis (co-condensation) depend on the type of alkoxysilane precursor used and on the ratio of vinylsiloxane to alkoxysilane in the reaction mixture. Toshitake, H. et al. (2002) compared aminosilane functionalized cubic mesoporous silica (SBA-1) and MCM-41. They found that SBA-1 fixes amino silanes more densely than MCM-41 and

that all amino groups work as adsorption sites, which make it superior to MCM-41 in this area.

Another way to introduce functional groups is the template-displacement (Olkhovyk, O. and Jaroniec, M., 2005). Antochshuk, V. and Jaroniec, M., (1999) applied a one-step silylation of uncalcined MCM-41, they were able not only to obtain external surface modification, but also to remove the surfactant template from the mesopores and to chemically modify the internal pore walls as shown in Figure 7. Thus, through template-displacement one can achieve several goals by one step: (i) preparation of functionalized mesoporous materials with hydrophobic surfaces; (ii) removal of surfactant molecules from the mesopores; (iii) avoiding high temperature calcination or solvent extraction procedures; and (iv) avoiding structure shrinkage during the calcination process.

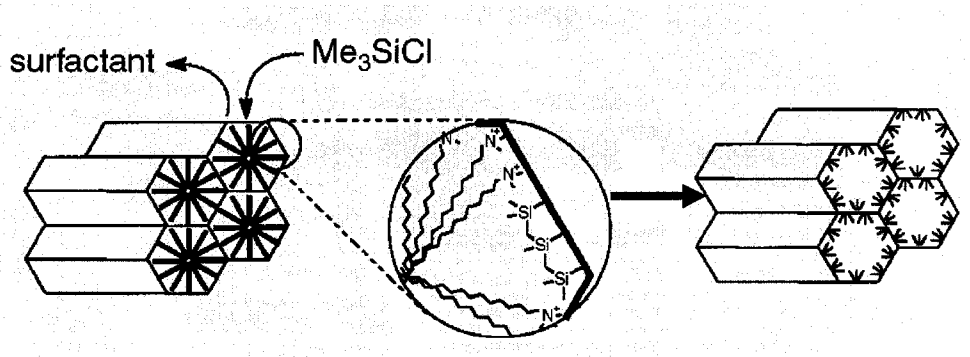

Figure 7: Schematic representation of one step modification of uncalcined MCM-41 (Antochshuk, V. and Jaroniec, M., 1999).

Jaroniec, M. et al. (1999) compared physical coating of MCM-41 with 4'-cyano-4-biphenyl[4(4-pentenyloxy)] benzoate and chemical modification using trimethylethoxysilane. They concluded that physical coating procedures did not allow to obtain a uniform surface coverage. While chemical modification led to significant changes of surface properties and pore size of the MCM-41.

4 Objectives of the Work

Because of its open structure and suitable surface properties, (PE)MCM-41 may generate fast and high-capacity adsorbents. However, since most applications in separation science and environmental remediation take place in aqueous solutions, it is important for this material to have good stability in such solutions. In this context, one objective in this thesis work was to study the stability of (PE)MCM-41 in aqueous solutions and the factors affecting this stability such as mixing time and pH.

Another objective of the work was to develop novel adsorbent to remove Copper from aqueous solutions. This adsorbent should exhibit suitable pore size, geometry, adsorption capacity and good stability when being in contact with water. The development of novel adsorbents was achieved by introducing amine functionality to the calcined pore-expanded MCM-41 via surface grafting and optimizing the grafting conditions (amount of water and silane added to the grafting mixture) to achieve the maximum amine loading without adverse effect on the adsorption performance with minimum possible cost. Also it was important from economic point of view to study the ability of the obtained adsorbent to be regenerated.

5 Experimental Work

5.1 Preparation of MCM-41

This recipe for preparation of MCM-41 was reported by Sayari, A. (2000). According to this method CTAB (cetyltrimethylammonium bromide) was used as a surfactant and 25% TMAOH (tetramethyl ammonium hydroxide) solution in water for pH adjustment and SiO_2 (Cab-O-Sil) as a silica source. The composition of the synthetic mixture was:

1 SiO_2: 0. 32 TMAOH: 0.45 CTAB: 66.67 H_2O

To prepare 1000 g of as-synthesized MCM-41, 622 g of 25% TMAOH was added to 6 L of distilled water and stirred. CTAB (874 g) was then added under vigorous stirring for 15 minutes. Then SiO_2 (320 g) was added to the mixture regularly and the total mixture was stirred for about 2 hours. The mixture was sealed in a stainless steel vessel and left under stirring in an oven at 80 °C for 2 days. The mixture was filtered, and thoroughly washed with distilled water. Finally the resulting powder was spread out in the fume hood and dried at ambient conditions for 24 hours. This is as-synthesized MCM-41 or (AS)MCM-41.

5.2 Pore Expansion of As-synthesized MCM-41

The pore expansion was achieved through post-synthesis treatment in the presence of N,N-dimethyldecylamine (DMDA) as swelling agent. The procedure as reported by Sayari, A. et al. (2005) was as follows:

175 g of (AS)MCM-41 was added to an emulsion of DMDA (218.75 g) in distilled water (2,625 g) under vigorous stirring. The mixture was stirred for 30 minutes. Subsequently, the vessel was sealed and placed in an oven at 393 K under static conditions for 3 days. The product was recovered by filtration, washed with distilled water, and dried under ambient conditions for 24 hours. The resulting powder is the pore-expanded MCM-41 or (PE)MCM-41. Figure 8 shows a schematic diagram of this process.

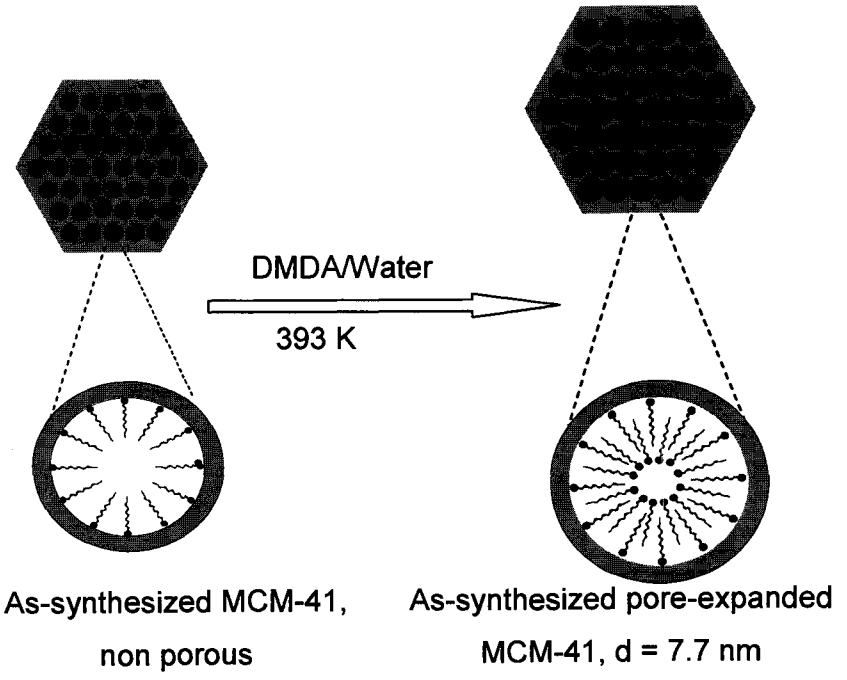

Figure 8: Scheme of material pore expansion.

5.3 Selective Extraction of DMDA

Ethanol was used to extract the expander (DMDA) selectively. This is achieved by contacting the material with ethanol under stirring at room temperature followed by filtration, washing and drying. The amount of ethanol used in extraction 18.5 and 9.25 mL ethanol/g (AS)MCM-41 for the first and second extraction respectively. The resulting powder is an extracted pore-expanded MCM-41 or (EPE)MCM-41. This process is illustrated in Figure 9.

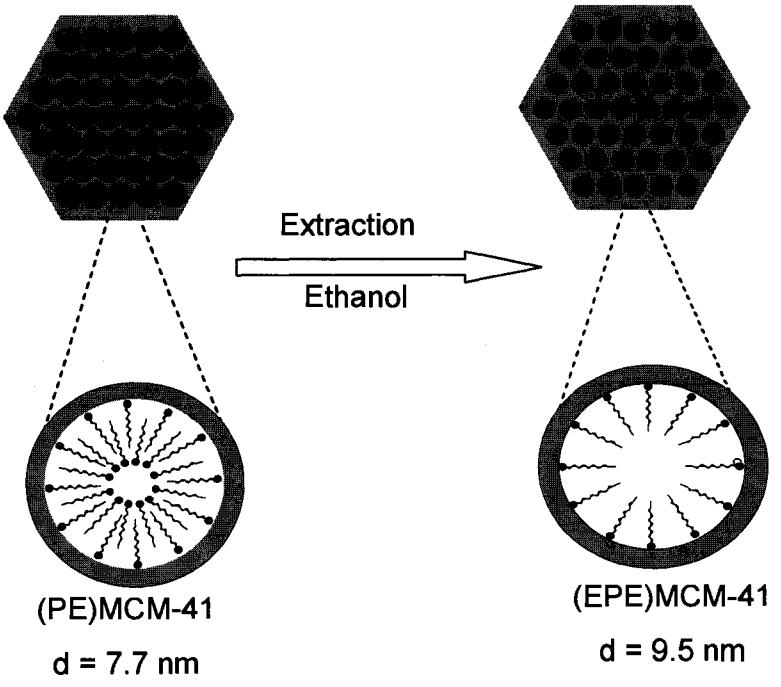

Figure 9: Scheme of material extraction.

5.4 Calcination

Samples from (AS)MCM-41, (PE)MCM-41 and (EPE)MCM-41 may be calcined to remove the surfactant(s) completely. Calcination was performed in flowing N_2 under a thermal ramp of 1 °C/min to 550 °C, and then held at 550 °C in flowing air for five hours. The letter C such as (C)MCM-41, (CPE)MCM-41 and (CEPE)MCM-41 denotes the calcined samples. This step is illustrated in Figure 10.

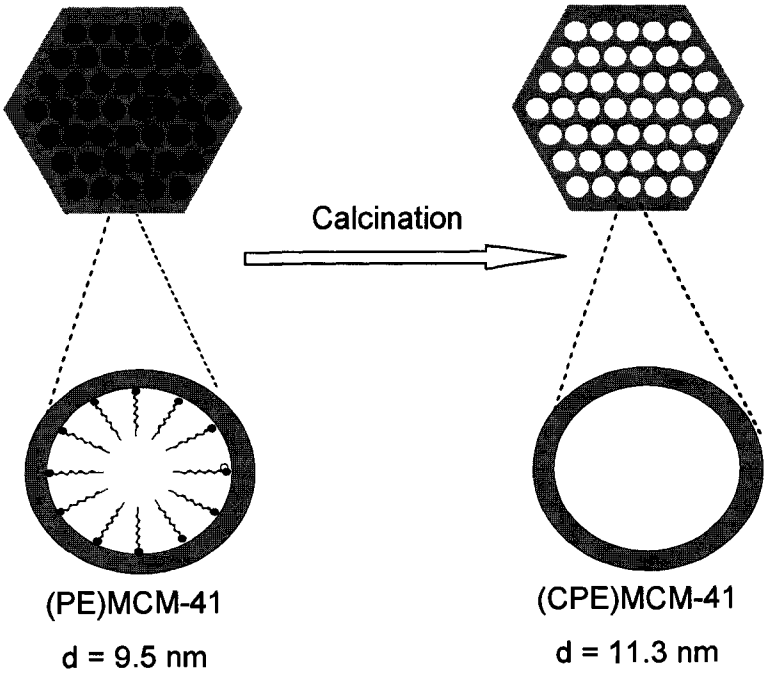

Figure10: Scheme of material calcination.

5.5 Surface Analysis

Nitrogen adsorption experiments were performed at 77 K using a Coulter Omnisorp 100 gas analyzer. Prior to nitrogen adsorption measurements, (C)MCM-41, (CPE)MCM-41, and (CEPE)MCM-41 were degassed down to 10^{-5} torr at 100 °C, whereas uncalcined materials that contain surfactant and DMDA such as (AS)MCM-41, (PE)MCM-41 and (EPE)MCM-41 were degassed at room temperature.

The specific surface area, SBET, was determined using the highly popular Brunauer-Emmett-Teller (BET) method (Thomas, J. M. and Thomas, W. J., 1997) within the P/P_o range of 0.05-0.15. The pore size distributions and mean pore sizes were determined using the KJS method developed by Kruk, Jaroniec and Sayari (Kruk, M. et al., 1997).

5.6 Copper adsorption Measurements

Aqueous solutions of Cu cations were prepared by dissolving copper acetate in distilled water. Adsorption was performed batchwise under vigorous stirring at room temperature. The slurries were filtered, and the obtained solutions were analyzed by Inductively Coupled Plasma, (ICP), using a 1000 µg/mL reference copper standard solution to calibrate the instrument. The amount of metal retained in the adsorbent phase (mg/g) was calculated by:

$$q_e = (C_i - C_e)\, V/m \qquad \text{(Tûtem, E. et al., 1998)}$$

Where C_i and C_e are the initial and final (equilibrium) concentrations of the Cu ions in solution (mg/L), V is the solution volume (L), and m is the mass of adsorbent (g).

5.7 Stability Test of (PE)MCM-41

Since the DMDA is attached within the (PE)MCM-41 material by electrostatic forces (Figure 8), it is essential to investigate the stability of the (PE)MCM-41 adsorbent and the regeneration ability of the material. For this purpose two approaches were used.

5.7-1 Total Organic Carbon (TOC) Measurements

25 mg of (PE)MCM-41 were stirred in 25 mL of distilled water at ambient temperature for different periods of time, then filtered. The total organic carbon (TOC) in the filtrates was measured using a TOC-VCSH Shimadzu Total Organic Carbon Analyzer after being calibrated with special standard solutions.

In order to identify the origin of TOC sources in water, several experiments were performed by changing the sorbent/water ratio and by changing the sorbent itself using (AS)MCM-41, (E)MCM-41, (EPE)MCM-41, (C)MCM-41 and (CEPE)MCM-41. An amount of 25 mg of each of these samples was stirred in 25 mL distilled water for 24 hours then filtered and the TOC in the filtrate was measured each time. Also the effect of pH was studied by performing the same set of experiments under different pH values and the same mixing time. The pH was measured using an Orion 5 stars instrument.

5.7-2 Adsorption-Desorption Cycles

Consecutive adsorption-desorption cycles were performed using Cu^{+2} containing solution with the same concentration (150 ppm) and the same solution/adsorbent ratio. After one hour of stirring the fresh adsorbent in copper solution, it was filtered, washed and dried at room temperature. The copper-loaded sample was then stirred in 0.5 M ethylenediamine tetra acetic acid tetra sodium salt (EDTA) solution. Stirring continued for 1 hr then it was filtered, washed and dried at room temperature. The first adsorption–desorption cycle was followed by four other cycles using the same Cu^{+2} solution/adsorbent and EDTA solution/adsorbent ratio.

The second approach used for recycling was washing with acid solution. An amount of 50 mg of copper loaded (PE)MCM-41 was added to 50 mL of diluted HNO_3 (pH = 3) and stirred for 30 minutes at room temperature. After filtration and washing the sample was stirred in 50 mL of distilled water and the mixture was neutralized to pH = 7 followed by stirring for 5 minutes, then it was filtered and dried. The first adsorption–desorption cycle was followed by three other cycles using the same Cu^{2+} solution/adsorbent and acid solution/ adsorbent ratio.

5.8 Amine Grafting on (CPE)MCM-41

Grafting, in this context, refers to post-synthesis modification of a surfactant-free silica support by attachment of organic moieties having appropriate functional groups to the surface of the mesopores. To introduce amine functionality to the MCM-41 materials, the method reported by Harlick, P. and Sayari, A. (2006) was applied.

Specifically, a batch of the support material was first dehydrated at 120 °C for 3 hours under vacuum. This drying procedure was necessary so that the quantity of water on the surface of the support was due only to the controlled addition during grafting and not from water physically adsorbed during preparation or storage. From this dried batch, 1.0 g was dispersed in 75 mL of toluene in a 100 mL multi-neck flask by mixing for 30 minutes at room temperature. Next, a specific quantity of water (0.1-1.0 mL/g silica) was rapidly added to the mixture and allowed to equilibrate at room temperature for 2-3 hours to make sure that water added was evenly distributed on the surface of the support material. After that time frame, the temperature was increased rapidly to the desired grafting temperature (85 °C) and a quantity of 3-aminopropyltrimethoxysilane (AMP), 0.2-10 mL/g silica, was added, and the system was held for 18 h with vapor reflux. These grafted materials were then filtered in a Büchner funnel and washed with toluene followed by pentane. The materials were dried at 120 °C in a natural convection oven for 4 hours and subsequently stored in capped vials until use.

5.9 Characterization of Grafted Materials

5.9-1 Surface Analysis

The grafted materials were characterized by N_2 adsorption using a Micromeritics, ASAP 2020 surface area and porosity analyzer. All materials were first degassed at 50 °C in order to remove all moisture attached to the surface.

5.9.2 Thermogravimetry-Mass Spectrometry Analysis (TGA-MS): CO_2 Adsorption and Thermal Decomposition

To determine the amount of amine that was grafted, thermal decomposition method using thermogravimetric analysis coupled with mass spectrometry (TGA-MS) was applied. Harlick, P. and Sayari, A. (2006) reported that the unbound methoxy ligands could be totally removed at temperature below 200 °C. As shown by mass spectrometry, above this temperature the amine chains start to decompose. Thus, the amount of grafted amine should correspond to the total weight loss beyond 200 °C. To correctly determine this amount, the sample was first treated in a flow of ultra high purity N_2 (UHP) at 200 °C for a period of 2 hours to remove any moisture attached to the surface. Then it was equilibrated at 25 °C in a flow of 5% CO_2 in N_2 for 2 hours, this step was done to study the adsorption capacity and the accessibility of the adsorption sites in the grafted materials. A thermal ramp of 10 °C/min to 800 °C was then applied in a flow of N_2 (UHP). Then, another ramp of 10 °C/min to 1000 °C in flowing air was carried out and the material was kept under isothermal conditions for 15 min.

5.9-3 Copper Adsorption Capacity

A set of experiments was undertaken to measure the copper adsorption capacity of samples prepared in the presence of different amounts of water and amine. Typically 100 mg of adsorbent was added to a 25 mL of 500 ppm copper acetate solution and stirred for 30 minutes. Subsequently, it was filtered and the filtrate was analyzed with the Inductive Coupled Plasma (ICP) technique to determine the concentration of solution after treatment.

5.9-4 FT-IR Characterization

The IR spectra were recorded using a Nicolet spectrometer Magna 550. Different types of samples were investigated to confirm the structural characteristics of (PE)MCM-41, (CPE)MCM-41 and AMP grafted MCM-41 using KBr pellets.

6 Results and Discussion

6.1 Support Structural Characterization

Figures 11 and 12 show the nitrogen adsorption-desorption isotherms and the corresponding pore size distributions (PSDs) for materials (C)MCM-41, (PE)MCM-41, (EPE)MCM-41 and (CPE)MCM-41. The BET surface area, pore size, and pore volume are given in Table 7. As can be seen in Figure 11, the adsorption isotherm of (C)MCM-41 corresponds to type IV of the International Union of Pure and Applied Chemistry (IUPAC) classification, which is characteristic of mesoporous materials with narrow pore size distribution (W.J. Thomas and B. Chrittenden, 1998). This shape is very similar to the profiles obtained by Sayari, A. et al. (2005), Sayari, A. and Yang, Y. (2000) and Sayari, A. et al. (1998). As shown in Figure 12 the corresponding pore size distribution was very narrow. As expected this material has higher surface area (1126 m^2/g) since it has the smallest pore size (3.7 nm). Sayari, A. et al. (2005) obtained 1025 m^2/g for surface area and 3.5 nm for the pore diameter, while Harlick, P. and Sayari, A. (2006) obtained 1140 m^2 /g for surface area and 3.5 nm for the pore diameter.

After the post-synthesis hydrothermal treatment, the material had a limited surface area (36 m^2/g) and a very small pore volume (0.08 mL/g) since this material still contains the CTAB and the DMDA inside its pores. For similar material, Sayari, A. et al. (2005) obtained 89 m^2/g for surface area and 0.2 mL/g for pore volume. Figure 9 also shows that this material has very wide pore size distribution. By selectively removing the DMDA using ethanol as extraction agent, the pore-expanded material now has a large pore size (9.5 nm), comparable to the 8.5 nm obtained by Sayari, A. et al. (2005) with

relatively narrow distribution as shown in Figure 9. This material also has a higher surface area (365 m^2/g) and a larger pore volume (0.9 mL/g), also comparable to the 509 m^2/g and 1.08 mL/g obtained by Sayari, A. et al. (2005). As expected, the calcined material exhibited highly enlarged pores (11.3 nm) with relatively narrow pore size distribution. The pore volume has also increased by a factor of 2 and the surface area remained very high (950 m^2/g). Sayari, A. et al. (2005) obtained 1192 m^2/g for surface area, 11.0 nm pore diameter and 2.6 mL/g for pore volume. Harlick, P. and Sayari, A. (2006) obtained 950 m^2/g for surface area, 10 nm for the pore diameter and 2.2 mL/g pore volume.

The (CPE)MCM-41 exhibits a much higher N_2 adsorption capacity than the (C)MCM-41 at relative pressure (P/P_o) = 1, thus demonstrating the increased pore volume. Also the point of inflection of the adsorption isotherm corresponding to the nitrogen condensation step shifted from 0.3 for (C)MCM-41 to 0.65 for (CPE)MCM-41, which is directly related to the increased in pore diameter. Therefore, it is expected that (CPE)MCM-41 should exhibit less mass transfer resistance and, thus, higher diffusional constants which make it superior over (C)MCM-41 for adsorption applications.

The nonexpanded calcined MCM-41 has no hysterysis loop. This is due to the relatively small pore size of this material (W.J. Thomas and B. Chrittenden, 1998). It was shown elsewhere that nitrogen hysteresis loops appear only for materials with mesopores larger than 4 nm (Kruk, M., et al., 2002 and Sayari, A., et al., 1997). On the other hand, (EPE)MCM-41 and (CPE)MCM-41 showed hysteresis loops, indicating a

change in the pore size after each stage of preparation. The nitrogen adsorption isotherms and pore size distributions shown in Figures 11 and 12 were consistent with results obtained by other researchers using similar synthesis, expansion, extraction and calcination procedures (Kruk, M. et al., 1997; Kruk, M. et al., 2000, Sayari, A. et al., 2005). The broadening of the hysteresis loop has been related to a loss of pore diameter uniformity (Sayari, A. et al., 1998). All these results indicate successful preparation of pore-expanded MCM-41.

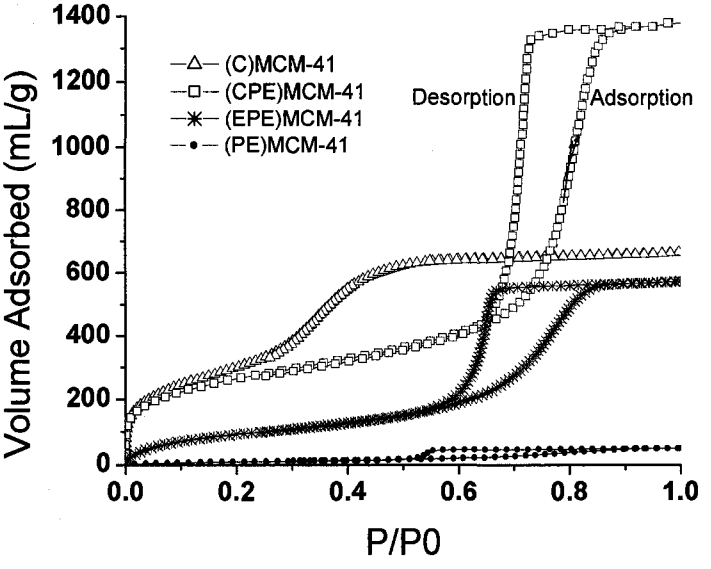

Figure 11: Nitrogen adsorption-desorption isotherm for MCM-41 after different stages of preparation.

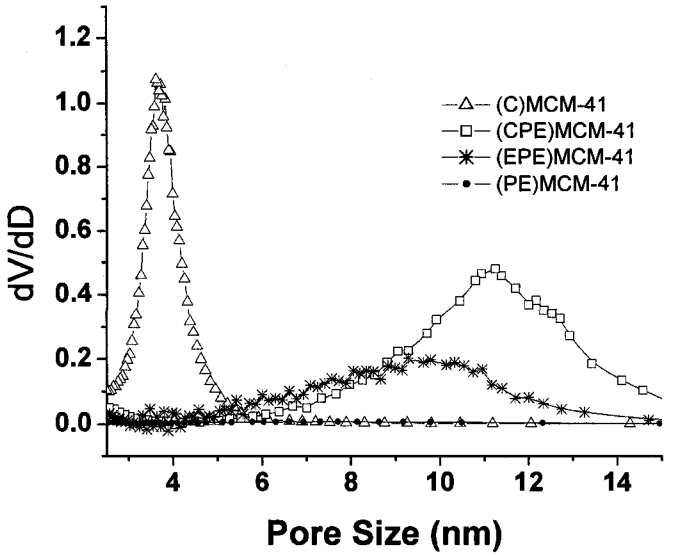

Figure 12: Pore size distribution for MCM-41 after different stages of preparation.

Table 7: Materials Characterization

Sample	Surface area (m^2/g)	Pore size (nm)	Pore volume (mL/g)
(C)MCM-41	1126	3.7	1.04
(CPE)MCM-41	950	11.3	2.16
(EPE)MCM-41	365	9.5	0.90
(PE) MCM-41	36	7.7	0.08

6.2 (PE)MCM-41 Stability in Aqueous Solution

Data of total organic carbon (TOC) released from the (PE)MCM-41 in the aqueous solution as a function of time is shown in Figure 13. As seen, the TOC changed rapidly during the first few hours then it increased slowly before leveling off. Figure 13 shows two cycles, the first cycle was obtained after stirring (PE)MCM-41 for 7

days. The (PE)MCM-41 was then filtered, dried, and then stirred for other 7 days (second cycle in Figure 13). It is obvious that (PE)MCM-41 followed the same profile during the two cycles which indicates the presence of equilibrium relation between the DMDA on the (PE)MCM-41 surface and that in the solution. As a result, the (PE)MCM-41 is expected to loose DMDA each time it is stirred in a solution as long as the equilibrium state has not been reached yet.

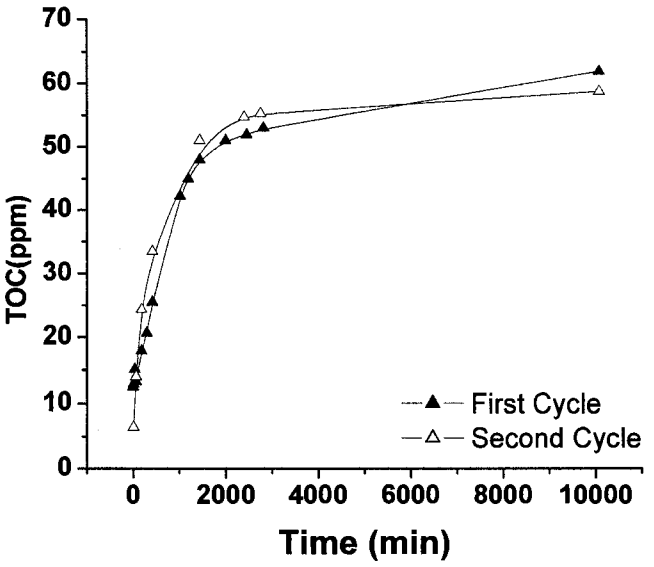

Figure 13: DMDA released from (PE)MCM-41 as a function of time for two cycles.

Table 8 shows results obtained after stirring 25 mg of different samples in 25 mL distilled water for 24 hours. The (AS)MCM-41 seems to be the least stable material and this can be explained by the large amount of loosely bonded surfactants due to insufficient washing of this material after preparation. When this material was extracted all the loosely bonded surfactants were removed so a value that is comparable to the

previous results was obtained. TOC values for (E)MCM-41, (PE)MCM-41 and (EPE)MCM-41 are close to each other even though the contents of each sample are different from the other which gives an indication that the measured TOC value does not attributable to the DMDA released only, but, CTAB also contributes in this value. As expected, for the calcined samples (C)MCM-41 and (CPE)MCM-41, the TOC was negligible or very close to the TOC contents of the distilled water used. It is thus clear that hardly any DMDA or CTAB remained in the solid material after calcination. However, changing the pH of the solution has a clear effect on the stability of this material as will be discussed next.

Table 8: TOC Values for different MCM-41 samples

Sample	Pore Contents	TOC (ppm)
(AS)MCM-41	CTAB with excess loosely bound	270
(E)MCM-41	CTAB	43
(C)MCM-41	None	1
(PE)MCM-41	DMDA + CTAB	52
(EPE)MCM-41	CTAB	49
(CPE)MCM-41	None	1

6.3 Effect of pH on the Stability of (PE)MCM-41 in Aqueous Solution

Using the (PE)MCM-41 and solutions with different initial pH, the TOC and the weight loss data shown in Table 9 were obtained. Starting the experiment from initial pH (pH_i) of 7, the final value of pH (pH_e) has increased to 9.96, which stems from the amine released to the solution as 17.04 ppm TOC to reach the equilibrium state at pH_e of 9.96. With $pH_i < pH_e$, the larger the difference between pH_i and pH_e, the stronger the driving force to release more DMDA which is apparent from the TOC measurements. The

maximum TOC value was obtained at the most acidic condition, and as the starting solution pH gets closer to pH of 9.96 the value of TOC gets lower and lower. For solutions of pH_i > 9.96, the driving force to release DMDA is almost zero and this is clear from the value of TOC which remained the same as the TOC of distilled water. The same results were obtained by measuring the sample weight before and after stirring to calculate the weight loss. By comparing the measured weight loss, and the theoretical one, which is calculated from TOC assuming that all the TOC originated from DMDA only, the average difference between measured and theoretical weight loss was found to be 13 %. To explain this difference, 1 g of fumed silica was stirred in 1L of distilled water for 5 minutes then it was filtered and dried at room conditions for 24 hours. Then it was weighed and the weight loss was found to be 15 %, which is very close to the average difference of weight loss obtained and this indicates that silica also dissolves partially in water and contributes to the weight loss, which cannot be detected using TOC only.

Table 9: Stability test as a function of pH.

Sample	Initial pH	Final pH	ΔpH	TOC (ppm)	Measured weight loss % (MW)	Theoretical weight loss % (TW)	MW-TW
1	2.63	2.89	0.26	309.70	47.1	39.9	9.1
2	2.77	3.15	0.38	300.20	47.5	38.0	7.6
3	3.04	5.19	2.15	292.10	44.2	37.6	6.6
4	3.33	8.50	5.17	167.00	32.6	21.5	11.1
5	3.81	9.12	5.31	71.53	29.5	9.3	20.2
6	7.00	9.96	2.96	17.04	19.6	2.2	17.4
7	10.32	10.33	0.01	5.80	14.2	0.8	13.4
8	11.05	11.02	0.03	6.00	13.7	0.8	12.9
9	12.21	12.13	0.08	4.80	17.9	0.6	17.3
10	12.60	12.62	0.02	3.86	16.9	0.5	16.4

6.4 Regeneration of Copper Loaded (PE)MCM-41

Since (PE)MCM-41 contains amine groups belonging to the pore expander DMDA, the material was used to adsorb copper from copper acetate solution. The adsorption capacity was calculated to be 88.8 mg Cu^{2+}/g adsorbent. To regenerate the copper-loaded (PE)MCM-41, two approaches have been investigated. The first one was to control the pH of the solution in order to release copper under acidic conditions. Values in Table 10 were obtained by reading the pH meter directly after changing the pH of the acidic solution, pH_i (first column) and after 30 minutes of stirring, pH_e (second column). It is clear from the table that for copper to be released to the solution it is not

enough to control the initial pH of the acidic solution since the values of pH increased to values that were no longer suitable for releasing copper. It is known, that amine protonates under acidic pH and its affinity to water increases (Sayari, A. et al., 2005) so it moves into the solution which in turn increases the value of pH as shown in Table 10, preventing the release of copper to the solution. By further addition of acid to the solution a point is reached where no more DMDA is released to the solution and so copper can be released. Table 11 shows that the biggest drop in the adsorption capacity occurred after the first regeneration since most of the amine was lost during that cycle. For comparison, the results for recycling the copper loaded (PE)MCM-41 obtained by Sayari, A. et al. (2005) are shown in Table 12. It is also seen that 60 % of the adsorption capacity is lost during the first adsorption-desorption cycle.

Table 10: Effect of copper-loaded material on the pH of the solution

Initial pH	Final pH
5.03	6.41
4.76	6.44
4.50	6.40
4.26	6.38
4.05	6.31
3.52	6.31
2.50	5.86

Table 11: Adsorption-desorption cycles using acidic solution as a regeneration agent.

Cycle	Adsorbent	Cu^{2+} (ppm) Initial	Final	Adsorbed amount (mg/g)	Sol./Ads. (mL/g)
1	Fresh (PE)MCM-41	150	89.3	60.7	965
2	R1(PE)MCM-41	150	134.6	15.4	965
3	R2(PE)MCM-41	150	138.2	11.8	965
4	R3(PE)MCM-41	150	140.3	9.7	965

Table 12: Adsorption-desorption cycles using acidic solution as a regeneration agent obtained by Sayari, A. et al. (2005)

Cycle	Adsorbent	Cu^{2+} (ppm) Initial	Final	Adsorbed amount (mg/g)	Sol./Ads. (mL/g)
1	Fresh (PE)MCM-41	254	1.5	50.5	200
2	R1(PE)MCM-41	254	208	20.91	200
3	R2(PE)MCM-41	254	219	19.5	200
4	R3(PE)MCM-41	254	243	7.42	200

The second approach to regenerate the Cu-loaded (PE)MCM-41 was to use EDTA as complexing agent. Data for the cycling and regeneration of the adsorbent is shown in Table 13. As seen, the adsorbed amount of copper decreased continuously from 59.7 mg/g for the first cycle to 12.0 mg/g for the fifth one. It is also clear that the maximum loss in capacity and in weight also occur within the first cycle, which may be due to the loss of the very loosely bonded amine covering the outer surface of the adsorbent. A second set of adsorption-desorption cycles was performed as before except the stirring time was reduced to 5 minutes and the weight loss [(fresh -cu-loaded)/fresh] was measured after each cycle. The results shown in Table 14 indicate that even at shorter stirring time the weight loss did not improve since most of the DMDA loss occurred within the first few minutes as the driving force to reach equilibrium state was maximum.

Table 13: Adsorption-desorption cycles using EDTA solution as a regeneration agent for 1 hour stirring period.

Cycle	Adsorbent	Cu^{2+} (ppm) Initial	Final	%Wt loss	Adsorbed amount (mg/g)	Sol./Ads. (mL/g)
1	Fresh (PE)MCM-41	148.3	86.4	46.2	59.7	965
2	R1(PE)MCM-41	147.9	128.1	26.6	19.1	965
3	R2(PE)MCM-41	146.1	130.1	30.7	15.4	965
4	R3(PE)MCM-41	146.4	132.0	24.5	13.9	965
5	R4(PE)MCM-41	143.8	131.4	23.8	12.0	965

Table 14: Adsorption-desorption cycles using EDTA solution as a regeneration agent for 5 minutes stirring period.

Cycle	Adsorbent	%Wt loss	Sol./Ads. (mL/g)
1	Fresh (PE)MCM-41	32.0	965
2	R1(PE)MCM-41	26.6	965
3	R2(PE)MCM-41	17.5	965
4	R3(PE)MCM-41	26.0	965
5	R4(PE)MCM-41	24.8	965

6.5 Surface Characterization of Grafted Materials

The effect of amine and water added on the surface area, pore volume and pore size was examined by nitrogen adsorption. Samples prepared by adding different amounts of amine ranging from 0.0 to 10.0 mL/g silca and different amounts of water ranging from 0.0 to 1.0 mL/g silica were tested. The main objective of this investigation was to identify the optimum amount of silane to be added to the reaction mixture to achieve the highest amine loading without affecting the open pore structure of the support. Minimizing the amount of silane added is crucial not only for performance control but also for cost consideration.

Figure 14 shows the surface area, pore size and pore volume for the materials grafted under dry conditions (dry grafted) as a function of amine added. It is clear from the figure that the surface area, pore size and pore volume decreased significantly from 950 m^2/g, 11.3 nm and 2.16 mL/g for 0.0 mL of AMP/g silica addition to 783 m^2/g, 7.4 nm and 1.54 mL/g for 1.0 mL of AMP/g silica addition. Beyond this amount of AMP

added, the changes were negligible which gives an indication that the maximum AMP loading is achieved at this point.

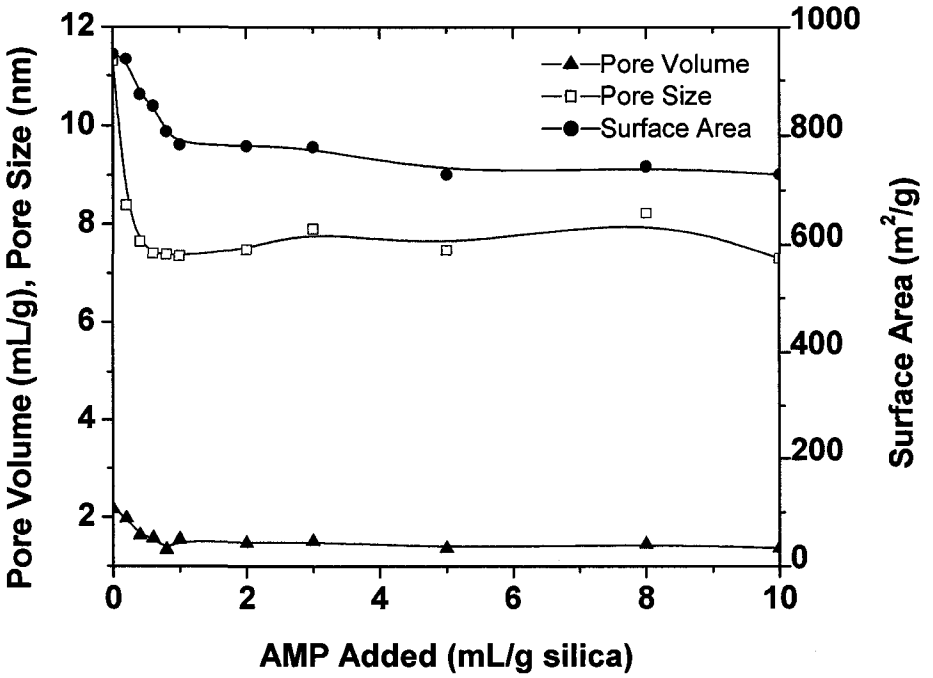

Figure14: Effect of AMP added on the structural characteristics of the dry grafted material.

The dry grafting procedure can be considered as a reaction between the hydroxyl groups covering the surface and the alkoxy ligands of the silane to form a layer of functional group bearing species as shown in Figure 15 (Harlick, P. and Sayari, A., 2007). For dry grafting, one or two alkoxy group may not react because there is not enough hydroxyl groups covering the surface as a result of calcination procedure used to remove CTAB and DMDA from the framework (Mercier, L. and Pinnavaia, T.J., 1998; Antochshuk, V. and Jaroniec, M, 1999). It is thus conceivable that the surface coverage

by functional groups can be increased by adding water to the support material in order to produce a hydrated surface with higher number of hydroxyl groups.

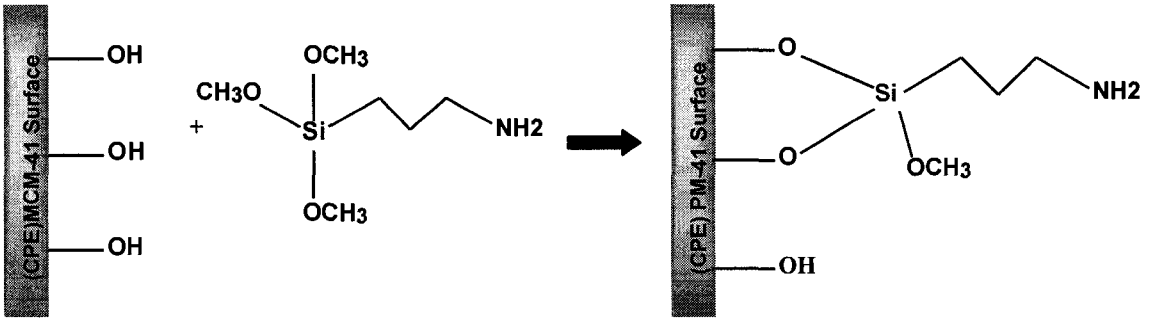

Figure15: Assumed surface species obtained by dry grafting.

The effect of the hydration step on the surface characteristics of the obtained materials is shown in Figure 16, which represents samples obtained by adding different amounts of AMP to the grafting mixture in the presence of 0.3 mL of water added per gram of silica. As the hydrated surface contains more hydroxyl groups, more AMP reacted with the support and thus causing additional effects on the surface area, pore size and pore volume. As shown in Figure 16, the surface area, pore size and pore volume, decreased from 950 m^2/g, 11.3 nm and 2.16 mL/g for 0.0 mL of AMP/g silica addition to 730 m^2/g, 6.34 nm and 0.77 mL/g for 2.0 mL of AMP/g silica addition. These changes are higher than the changes shown in Figure 14 for dry grafting. Another feature in Figure 16 is the random changes in surface area, pore size and pore volume beyond 2 mL/g of AMP addition. This can simply be explained by the promotion of silane polmerization in the presence of excess water, which produces some silane condensation in the grafting mixture that may cause random pore blockage. This

random pore blockage cause random changes in pore size, pore volume and surface area as shown in Figure 16. Similar findings were also reported by Yokoi, T. et al. (2004) who found that in grafting, most amino-organic moieties may be concentrated near the opening of channels and/or on the external surface leading to such random changes.

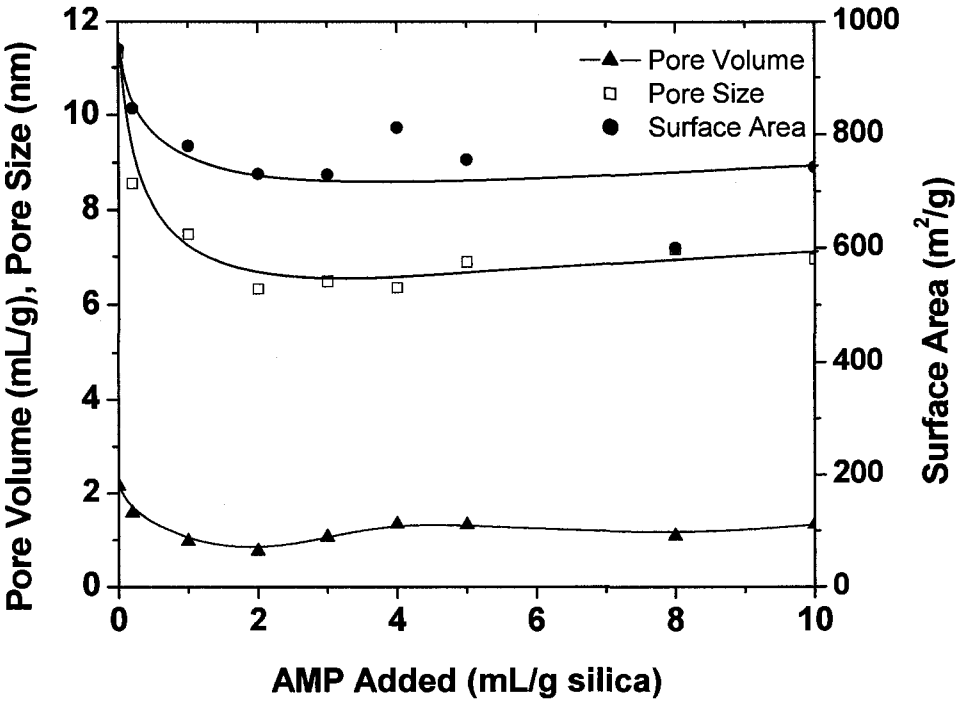

Figure16: Effect of AMP added on the structural characteristics of the wet grafted material in the presence of 0.3 mL water/g silica.

To study the effect of water on the surface characteristics, different amounts of water were added to the reaction mixture and the results are shown in Figure 17. It is obvious from the figure that the best amount of water added without large negative

effect on surface characteristics was 0.4 mL/g silica. Beyond this value, random changes occur due to the effect of polymerization explained previously.

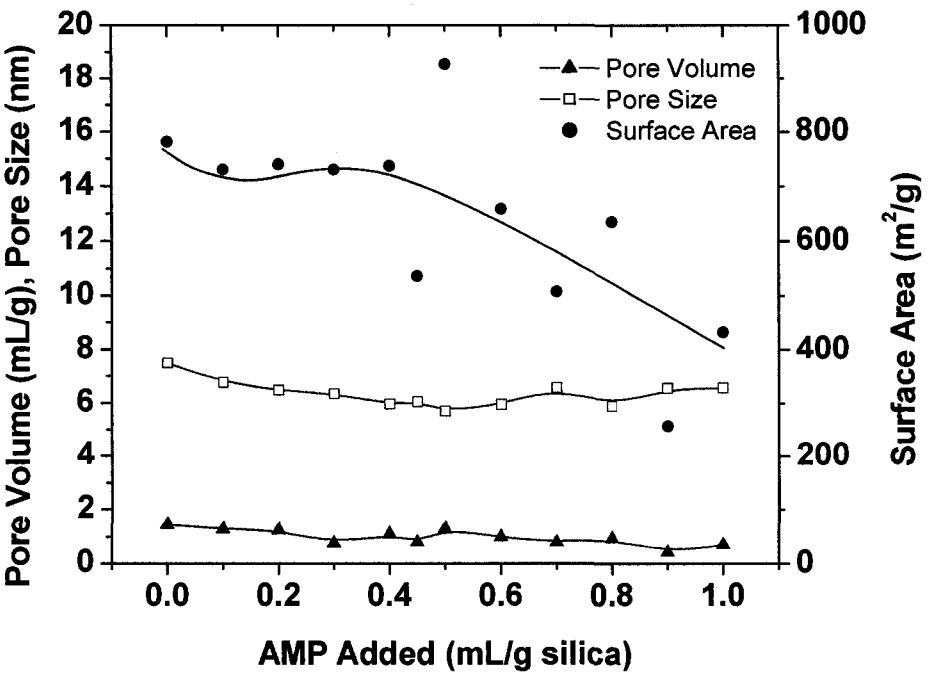

Figure17: Effect of water added on the structural characteristics of the wet grafted material with 2 mL AMP/g silica.

A few researchers have used amine-grafted mesoporous silica for heavy metals adsorption (Olkhovyk, O. et al., 2004; Mercier, L. and Pinnavaia, T.J., 1998; Shiraishi, Y. et al., 2002; Liu, A. M. et al, 2000; Yokoi, T. et al., 2004; Toshitake, H. et al., 2002). A summary of their work such as: support material characteristics, functional group, resulting loading of the adsorbent and their remarks about recycling and selectivty is show in Table 15.

Table 15: Summary of amine-grafted silica based adsorbents prepared under different grafting conditions and applied for the removal of heavy metal cations and anions.

Support material	Functional Group*	BET area (m^2/g)	Loading (mg/g)					Application	Reference	Notes
			Co^{2+}	Fe^{2+}				Co^{2+} Fe^{++}	Yokoi, T. et al. 2004	
MCM-41	-	1281	-	-						
MCM-41	Mono	662	41.8	73.1						
MCM-41	Di	471	15.9	58.0						
MCM-41	Tri	367	4.1	10.0						
			Loading (mg/g)					CrO_4^{2-} $HASO_4^{2-}$	Yoshitake, H.et al.,2002	SBA-1 was superior to MCM-41 because all amino groups work as adsorption sites in SBA-1, but not in MCM-41
			CrO_4^{2-}	$HasO_4^{2-}$						
MCM-41	-	1283	-	-						
MCM-41	Mono	1037	52.9	64.4						
MCM-41	Di	586	92.1	86.4						
MCM-41	Tri	481	115.2	109.9						
SBA-1	-	1221	-	-						
SBA-1	Mono	689	94.2	132.7						
SBA-1	Di	606	178.4	214.3						
SBA-1	Tri	126	210.8	262.7						
MCM-41	-	900	-					Hg^{2+}	Antochshuk , V. and Jaroniec, M., 2002	50 % of the initial capacity was restored after treating with 10 % thiorea in 0.05 M HCl.
MCM-41	ATU	320	300.9							
HMS-C12	-	854	-					Hg^{2+}	Mercier, L. and Pinnavaia, T.J., 1998	Functionalized HMS was more efficient for adsorbing Hg^{+2} than MCM-41
HMS-C12	MP	722	300.9							
HMS-C8	-	1200	-							
HMS-C8	MP	640	180.5							
MCM-41	-	1264	-							
MCM-41	-	1061	114.3							
MCM-48	-	1075	-					Hg^{2+}	Olkhovyk, O. et al., 2004	90 % of the initial capacity was restored after treating with 10 % thiorea in 0.05 M HCl.
MCM-48	BTU	505	268							
			Loading (mg/g)					Hg^{2+} ,Cu^{2+}, Zn^{2+}, Cr^{2+} and Ni^{2+}	Liu, A. et al., 2000	60 % of the initial adsorption capacity was retained by washing with concentrated HCl .
			Hg^{2+}	Cu^{2+}	Zn^{2+}	Cr^{2+}	Ni^{2+}			
SBA-15	MP	461	204.3	12.8	1.2	2.5	30.0			
	Mono	279	159.6	32.7	6.61	27.1	6.0			
	-	814	0	0.57	0	0.42	0			

*Mono: 3-Aminopropyltrimethoxysilane.
MP: 3-mercaptopropylsilyl groups
Di: [1-(2-amino-ethyl)-3-aminopropyl]triethoxysilane.
Tri: (Trimethoxysilyl)propyldiethylenetriamine.
ATU: 1-allyl-3-propylthiourea
BTU: 1-benzol-3-propylthiourea

6.6 FT-IR Characterization

Using a Nicolet MAGNA 550 FT-IR instrument, spectra were recorded for three types of samples to confirm the structural characteristics of (PE)MCM-41, (CPE)MCM-41 and AMP grafted (CPE)MCM-41. Considerable changes are apparent in the range of 690 cm^{-1} to 2930 cm^{-1} as can be seen in Figure 18. All samples exhibited two itense peaks at 805 and 1230 cm^{-1} corresponding to OSiO stretching and SiO stretching (Jin, S., et al., 2007), respectively which are typical of Si-O-Si network. (PE)MCM-41 showed a band at 984 cm^{-1}, corresponding to Si-OH bending (Jin, S. et al., 2007; Wang, L., 2006). However, this band was absent in (CPE)MCM-41 suggesting the reduction of silanols on the surface after calcination of the sample. The same band was also absent in the spectra of the AMP grafted (CPE)MCM-41; only very small shoulder was observed, providing a proof that the surface hydroxyl groups were consumed during the grafting process. The reduction in the bands at 2930 and 2860 cm^{-1}, which correspond to CH_3 and CH_2 stretching (Joseph, T. et al., 2007) respectively, and the band at 1470 cm^{-1}, which corresponds to C-H bending (Wang, L., 2006), in the (CPE)MCM-41 spectrum suggests the removal of all organics (CTAB + DMDA) from the sample by calcinations. The appearance of these peaks again in the spectra of AMP-grafted sample suggests successful grafting of AMP on the surface. The NH_2 stretching vibration of the primary amine which usually appears at 3390 and 3310 cm^{-1} (Wang, L., 2006) could not be observed because of its overlapping with the Si-OH stretching vibration. However, the N-H bending vibration at 690 cm^{-1} (Wang, L., 2006) and NH_2 symmetric bending vibration at 1550 cm^{-1} (Wang, L., 2006) in the case of AMP-grafted

sample provide strong evidence for the successful grafting of the 3-aminopropyl-trimethoxysilane on the surface of (CPE)MCM-41

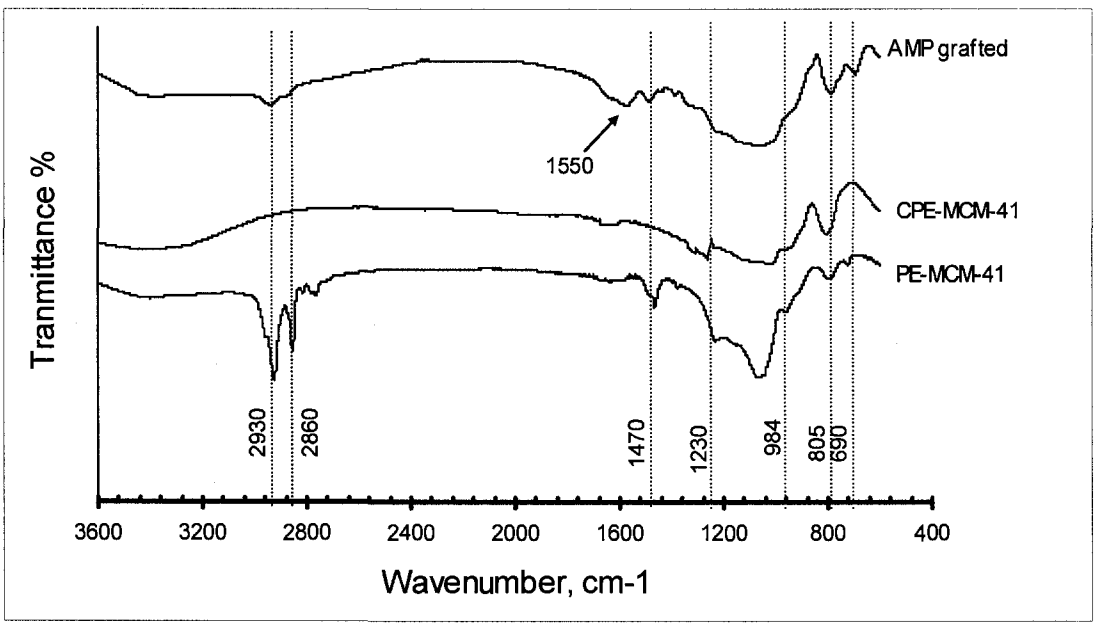

Figure 18: FT-IR spectra of (PE)MCM-41, (CPE)MCM-41 and AMP grafted MCM-41.

6.7 ^{13}C NMR Characterization

Figure 19 shows the ^{13}C NMR spectra of (CPE)MCM-41 and AMP grafted (CPE)MCM-41. The (CPE)MCM-41 does not exhibit any resonance peaks because this material does not contain any carbon as a result of calcination procedure. On the other hand, the AMP-grafted (CPE)MCM-41 shows resonance peaks at chemical shifts δ = 10, 27, and 43 ppm which represent the three C atoms in the grafted AMP (Wang, L., 2006). The peak at 10 ppm was assigned to the carbon atom attached to the silicon atom, whereas the peaks at 27 and 43 ppm were assigned to the carbon atom attached to NH_2 group and to the middle carbon atom of the propylamine respectively (Wang, L., 2006).

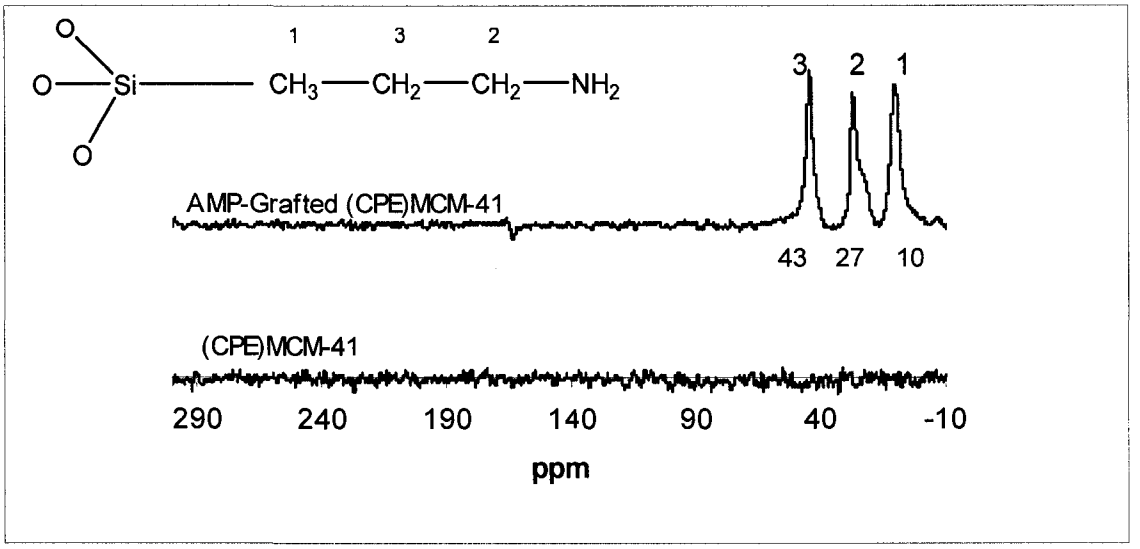

Figure 19: ^{13}C NMR spectra of (CPE)MCM-41 and AMP-grafted (CPE)MCM-41.

6.8 Thermogravimetry- Mass Spectrometry Analysis; CO_2 Adsorption

In order to determine the amount of amine that was grafted and the accessibility of the grafted material within the pores, a thermal decomposition method using a thermogravimetric analyzer (Q500 TGA, TA instruments) coupled with a mass spectrometer (Thermostar, PFeiffer Vacuum) was applied. The results for AMP-grafted (CPE)MCM-41 are shown in Figure 20 for the weight loss (TG) and in Figure 21 as the corresponding mass spectrometry profiles of selected amu/e values as a function of time. All the grafted materials exhibited the same profile.

From the data shown in Figures 20 and 21, the various species contributing to the weight loss can be determined. The first loss was obtained at temperatures lower than 200 °C, the MS profile for the same temperature range showed that the dominant species were 44 which corresponds to CO_2, 18 for H_2O, and 32 for CH_3OH. The release of trace amount of CO_2 can be related to CO_2 adsorbed on the surface of the grafted

materials from the ambient air since CO_2 is expected to have high affinity to amine (Franchi, R., 2005). However, the release of water in this temperature range is most likely related to water adsorbed on the surface (Harlick, P. and Sayari, A., 2006). The formation of water via surface dehydration and formation of siloxane bridge as shown in Figure 22 is unlikely to occur in such a low temperature range. The release of methanol supports the fact discussed previously, that not all the methoxy ligands react with the surface hydroxyl groups during grafting and thus, some are left unreacted. As the temperature increases, the remaining methoxy ligands react with adjacent hydroxyl groups to produce CH_3OH (Harlick, P. and Sayari, A., 2006) as shown in Figure 23.

Once the sample weight has been stabilized at 200 °C for about 2 h, the grafted material was cooled back to 25 °C then exposed to 5 % CO_2 in N_2 for 2 hours in order to study the adsorption capacity of the material, and the accessibility of the functional groups within the pores. This gas mixture was chosen for this study because it was reported by Franchi et al. (2005) that the amine-grafted adsorbent would have high affinity for CO_2 even in low partial pressure region. CO_2 reacts chemically with the amine which is clear from the rapid increase in the material weight at the moment of switching to CO_2 as shown in Figure 20. The amount of CO_2 adsorbed is directly related to the weight gain. The material was then heated up to 800 °C with a ramp of 10 °C/min in N_2 atmosphere. At the time of switching to N_2 and increasing the temperature, CO_2 desorbed very fast as shown from the rapid decrease in the weight in Figure 20. Above 200 °C, the amine chain starts to decompose and is removed from the surface completely when the temperature of 650 °C is reached. The decomposition products

monitored by MS consisted of water (18 amu), methanol (32 amu), and the propylamine species, $C_3H_6NH_2$ (58 amu). At 800 °C, the N_2 was replaced with air and another temperature ramp of 10 °C/min up to 1000 °C was carried out in order to burn any coke deposited on the sample surface. This burn off can be detected from the increase in the MS profile of CO_2 (44 amu) and water (18 amu). In summary, the grafted amine species seems to be stable up to 200 °C in a nitrogen atmosphere. Thus, the amount of AMP grafted could be calculated from the weight loss beyond 200 °C, and any weight loss below 200 °C should not be included.

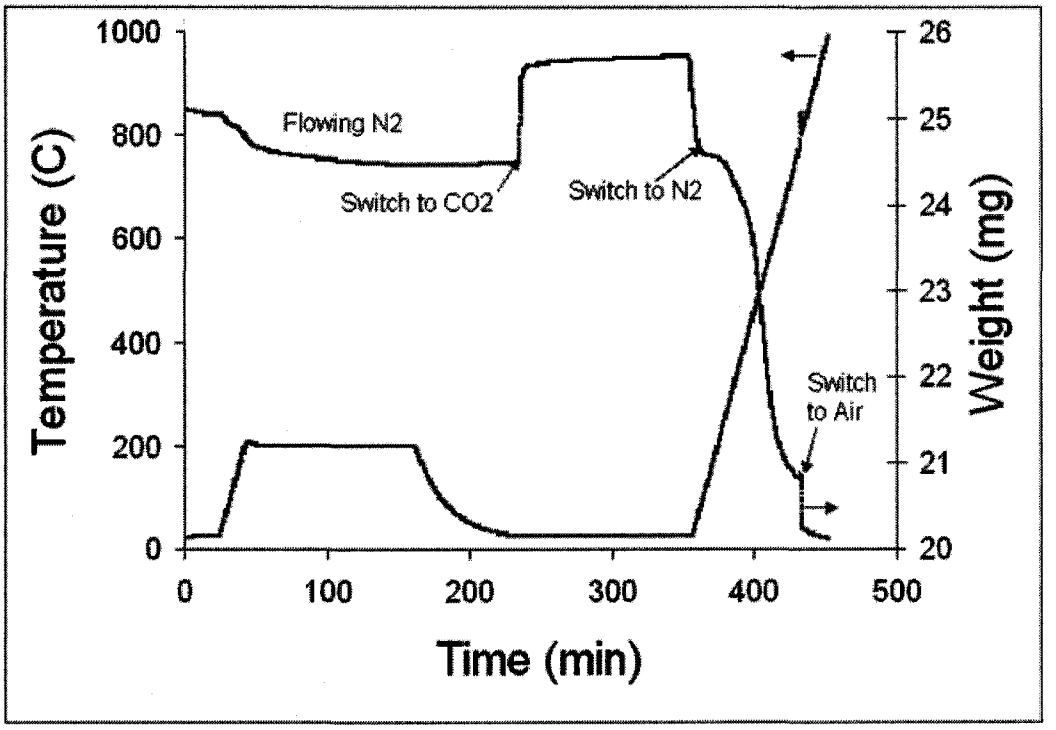

Figure 20: TG profile for AMP-grafted material.

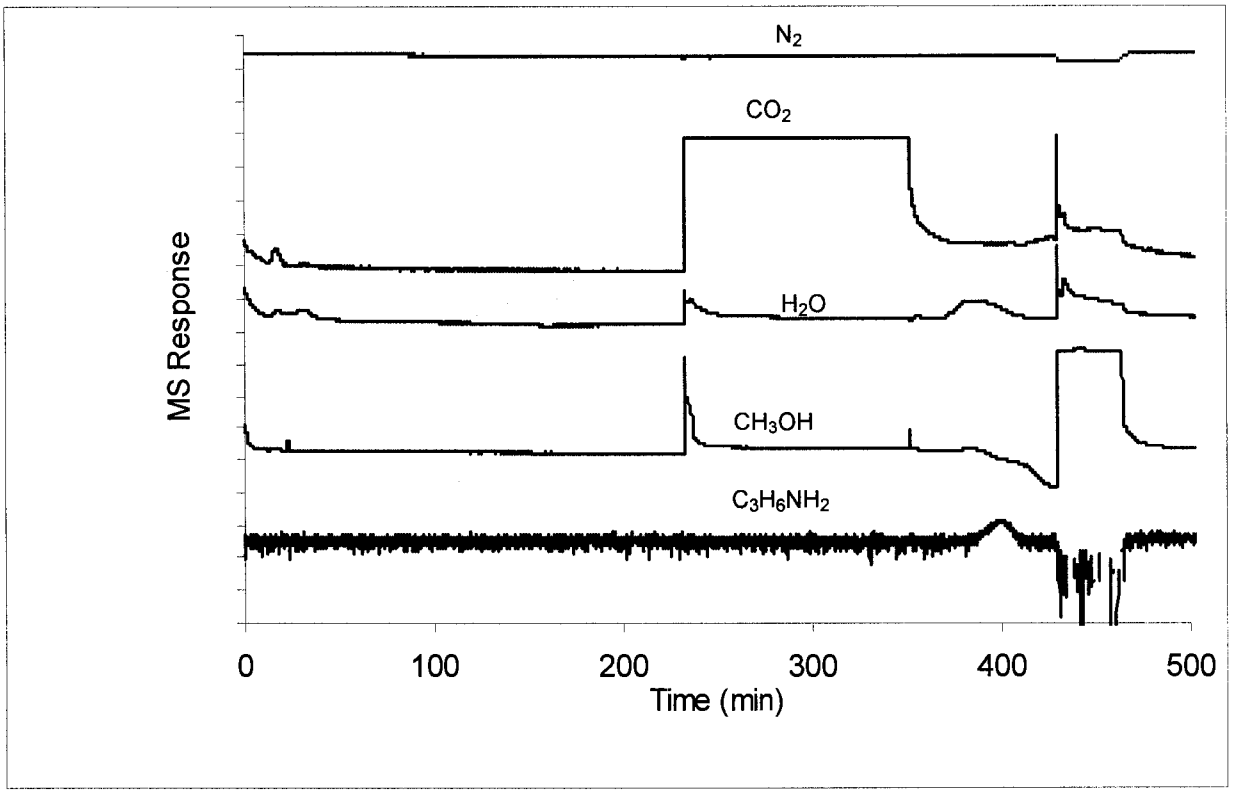

Figure 21: MS response profile for AMP-grafted material.

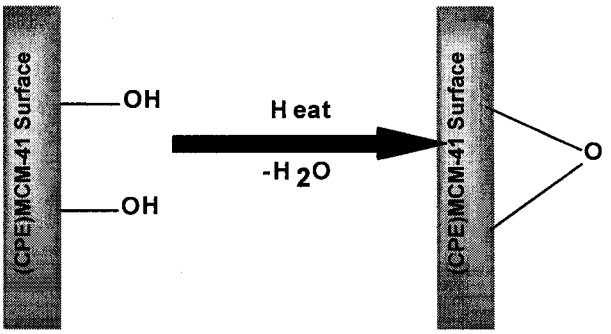

Figure 22: Schematic representation of dehydroxylation process which takes place at high Temperature.

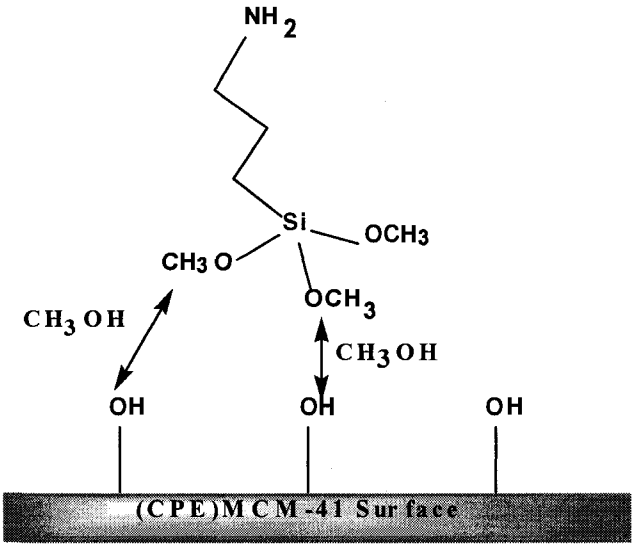

Figure 23: Schematic representation of the AMP grafting on the silica surface.

6.9 Effect of Grafting Conditions

Optimization of the grafting conditions involved multiple constrains. The goal is the minimization of the amount of silane added with respect to (PE)MCM-41 to achieve the best adsorption properties of the grafted material. The benefit from minimizing silane addition is twofold: (i) to lower the cost of silane required to prepare the adsorbent, and (ii) to prevent any potential adverse effect on the adsorption performance such as adsorption rate and/or adsorption capacity.

6.9-1 Effect of Grafting Conditions on the Amount of Amine Grafted

Figure 24 shows the effect of the amount of monoamine added to the grafting mixture on the grafted quantity of amine under dry condition. The figure shows that addition of 1 mL of silane/g silica to the grafting mixture was appropriate. Further addition of silane did not improve the amount of amine grafted. Figure 25 shows data for

similar grafting experiment except that 0.3 mL of water/g silica was added to the grafting mixture (wet grafting) each time. The figure shows that the maximum amine loading occurred at 2 mL of silane/g silica added with significant improvement in the grafted amount from 2.29 mmol AMP/g total in the case of dry grafting to 4.12 mmol AMP/g in the case of wet garfting.

Grafting in the presence of different amount of water (0-1) mL/g silica was undertaken to examine the effect of the quantity of water added to the grafting mixture on the amount of amine that can be grafted. The quantity of silane added was kept constant at 2 mL/g silica, and the results are shown in Figure 26. From these data, it is evident that the amount of water added has a significant impact on the quantity of amine that can be grafted. The amount of grafted amine increased significantly from 2.29 mmol AMP/g total in the case of dry grafting to 4.44 mmol AMP/g total in the case of wet grafting in the presence of 0.4 mL of water/g silica then decreased slightly as water added increased.

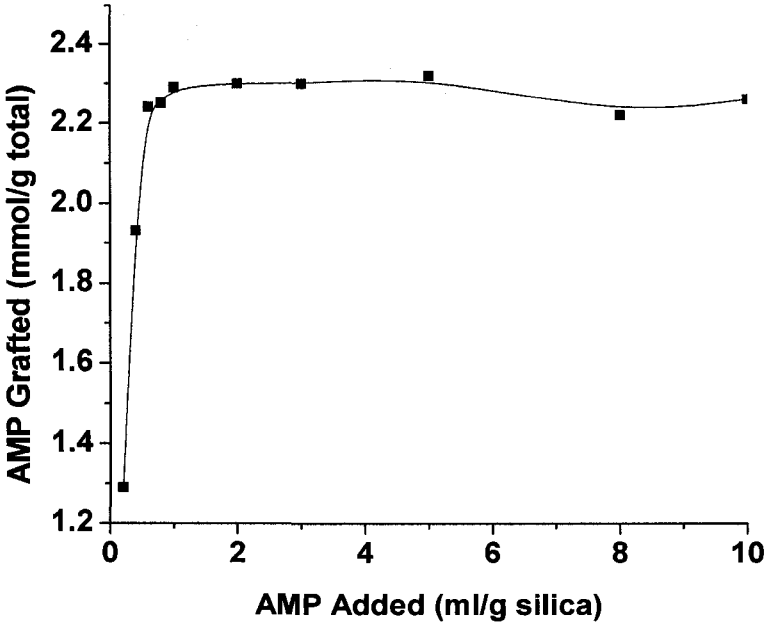

Figure 24: Effect of AMP added to the dry grafting mixture on the amount of AMP grafted.

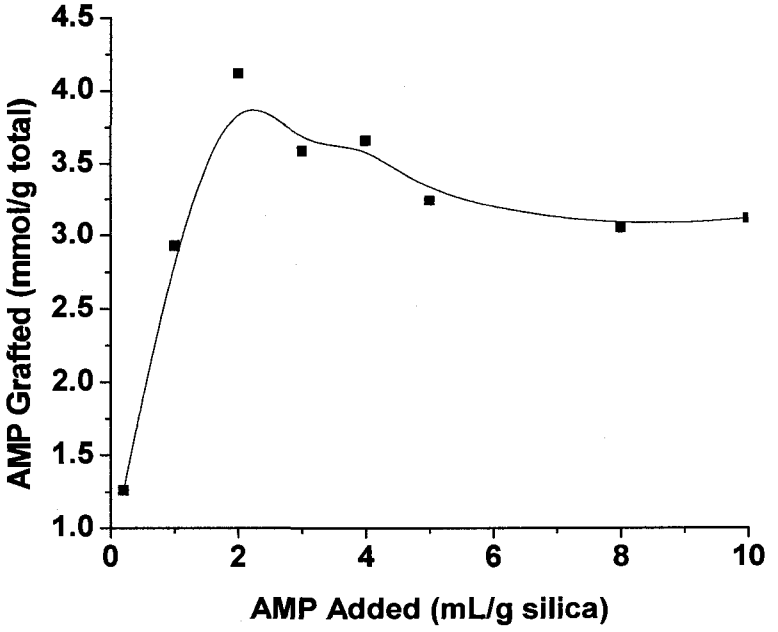

Figure 25: Effect of AMP added to the wet grafting mixture (0.3 mL water/g silica) on the amount of AMP grafted.

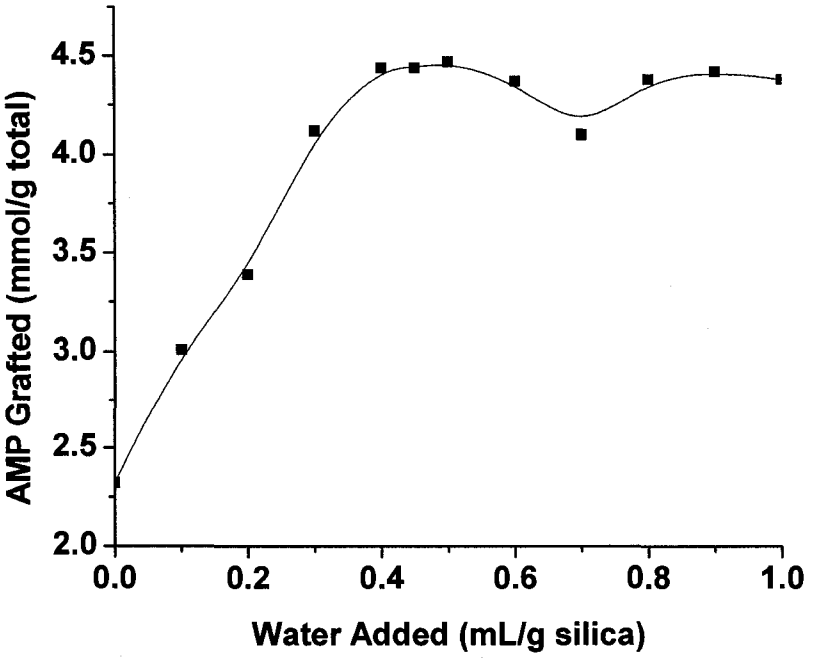

Figure 26: Effect of water added to the grafting mixture (2 mL AMP/g silica) on the amount of AMP grafted

6.9-2 Effect of Grafting Conditions on CO_2 Adsorption Capacity

Figure 27 shows the effect of the amount of monoamine added to the dry grafting mixture on the accessibility of the amine functional groups to CO_2. The figure shows that addition of 1 mL of silane/g silica to the grafting mixture was the most appropriate. Further addition of silane did not improve the amount of CO_2 adsorbed; on the contrary, some adverse effect on CO_2 adsorption capacity started to appear beyond 1 mL of silane/g silica added (Figure 27) although the amount of amine was almost constant (Figure 24). This adverse effect can be related to amine accumulation on the surface, which may cause decrease in the adsorption due to mass transfer limitations and limited amine accessibility. Figure 28 shows the results of a similar test using materials

prepared in the presence of 0.3 mL of water/g silica added to the grafting mixtures. The figure shows that the maximum CO_2 capacity of 2.06 mmol/g total occurred for the material prepared using 2 mL of silane/g silica added. Comparison of CO_2 capacity of 0.482 mmol CO_2/g for the corresponding material prepared under dry grafting conditions show the importance of adding the appropriate amount of water during grafting.

Addition of more silane beyond 2 mL/g silica causes a negative effect for both dry and wet grafting. Comparing Figure 27 and Figure 28, it is clear that, the effect of increasing amount of silane added to the grafting mixture is more significant in the case of wet grafting. In the case of dry grafting, any excess silane in the grafting silane may be accumulated on the external surface and at the pore mouth, causing mass transfer limitation. However, in the case of wet grafting, the presence of water in the grafting mixture provides suitable conditions for the silane to undergo polymerization and condensation not only with the hydroxyl groups covering the support surface, but also with the free water present in the mixture. This additional polymerization may cause some random pore blockage, which affects CO_2 adsorption in a random pattern. Because the best results were obtained by adding 2 mL of amine/g silica in wet condition; materials grafted with 2 mL of silane/g silica were examined for the effect of water added.

Grafting in the presence of different amounts of water (0-1) mL/g silica was carried out to examine the effect of the quantity of water added to the grafting mixture on the amount of CO_2 that can be adsorbed. The quantity of silane added was kept

constant at 2 mL/g silica, and the results are shown in Figure 29. From these data, it is evident that the amount of water added has a significant impact on the adsorption capacity. The amount of CO_2 adsorbed increased significantly from 0.482 mmol CO_2/g total in the case of dry grafting to 2.23 mmol CO_2/g total in the case of wet grafting in the presence of 0.4 mL/g silica of water then decreased a bit as water added increased. From the above discussion, it is possible to consider the optimum grafting conditions for monoamine to be 2 mL of silane/g silca and 0.4 mL of water/g silica.

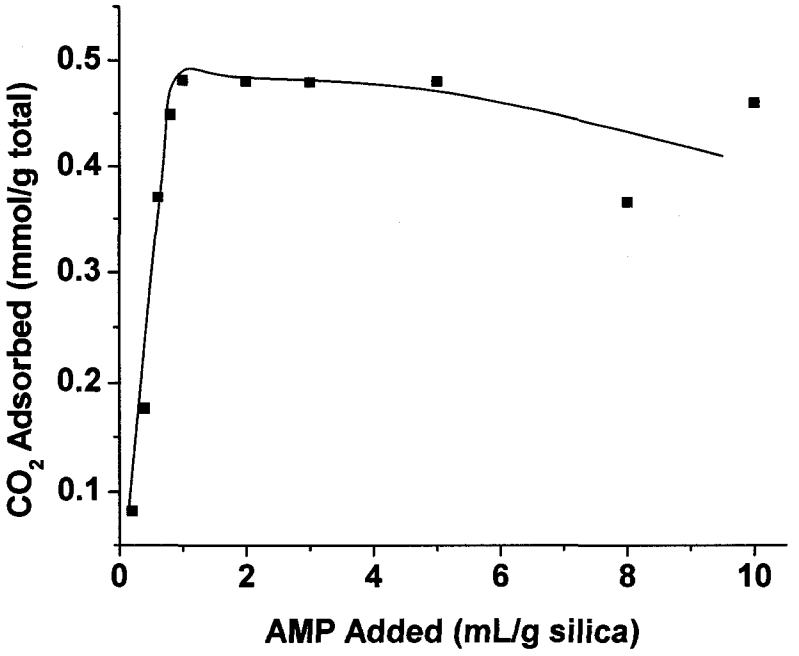

Figure 27: Effect of AMP added to the dry grafting mixture on CO_2 adsorption capacity.

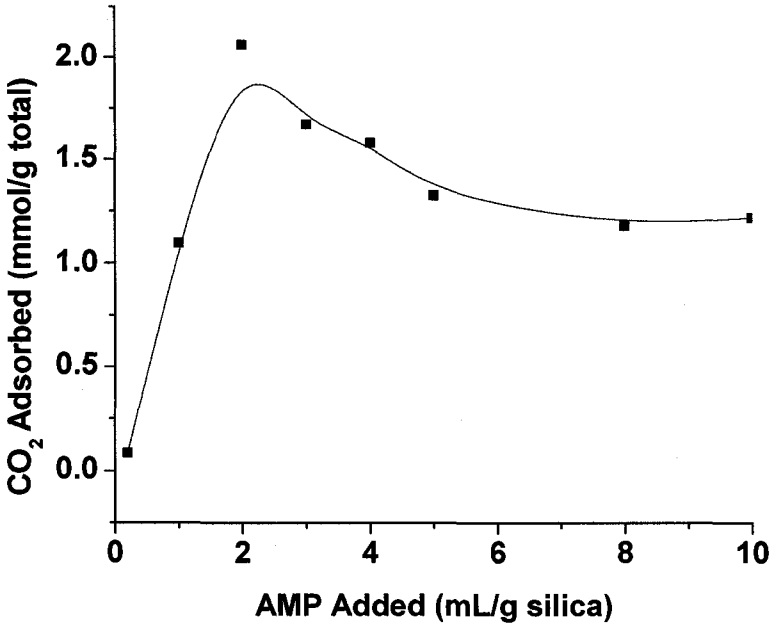

Figure 28: Effect of AMP added to the wet grafting mixture (0.3 mL water/g silica) on CO_2 adsorption capacity.

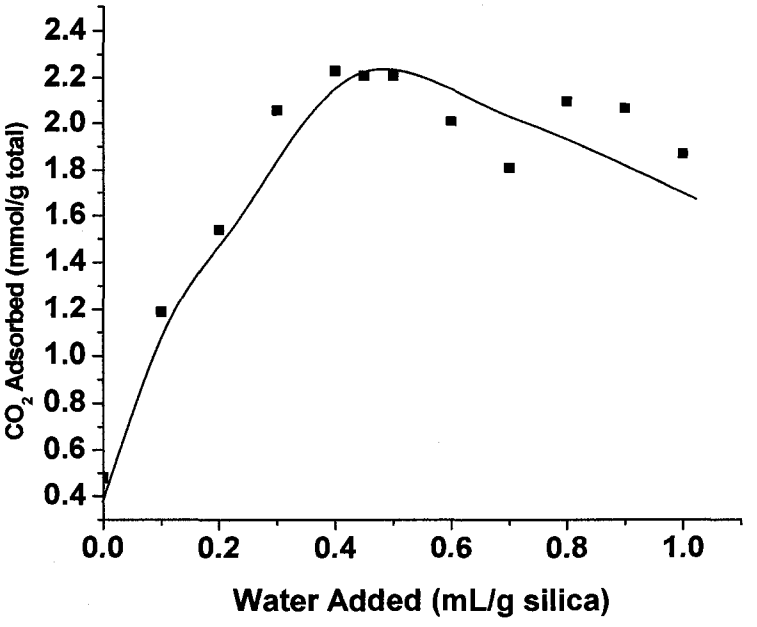

Figure 29: Effect of water added to the grafting mixture (2 mL AMP/g silica) on CO_2 adsorption capacity.

6.9-3 Effect of Grafting Conditions on Adsorption of Cu^{2+}

Data for the adsorption of Cu^{2+} is shown in Figure 30. As shown, the adsorption capacity depends on the composition of the adsorbent. It varied between 6 and 77 mg/g for the material with optimum grafted AMP (4.44 mmol AMP/g total) and from 12 to 31 mg/g with minimum grafted AMP (1.26 mmol AMP/g total). At saturation, the N/Cu ratio was 3.6 and 3.1 for the minimum and optimum AMP loading, respectively. Experiments using very dilute solutions such as 25 ppm indicate that under our conditions 93% of the copper was removed with the material with minimum AMP loading and 96% with the material with the optimum AMP loading. This indicates the high sensitivity of the AMP-grafted (CPE)MCM-41 as adsorbent even at very low copper concentration and minimum amine loading.

Figure 30 shows the adsorption isotherm of the minimum and maximum AMP loading adsorbent. These isotherms can be described by Freundlich adsorption isotherm model, $\ln(q_e) = \ln(k) + (1/n)\ln(C_e)$, as shown in Figure 31. The Freundlich constants k and n are presented in Table 16 for both the minimum and optimum AMP loading adsorbent. For comparison, the results obtained by Sayari, A. et al. (2005) for adsorption of Cu^{2+} using (PE)MCM-41 are included in Table 17. Comparing results in Tables 16 and 17 leads to the conclusion that the copper adsorption capacity of the as-synthesized (PE)MCM-41 is higher than that of the AMP-grafted (CPE)MCM-41 materials.

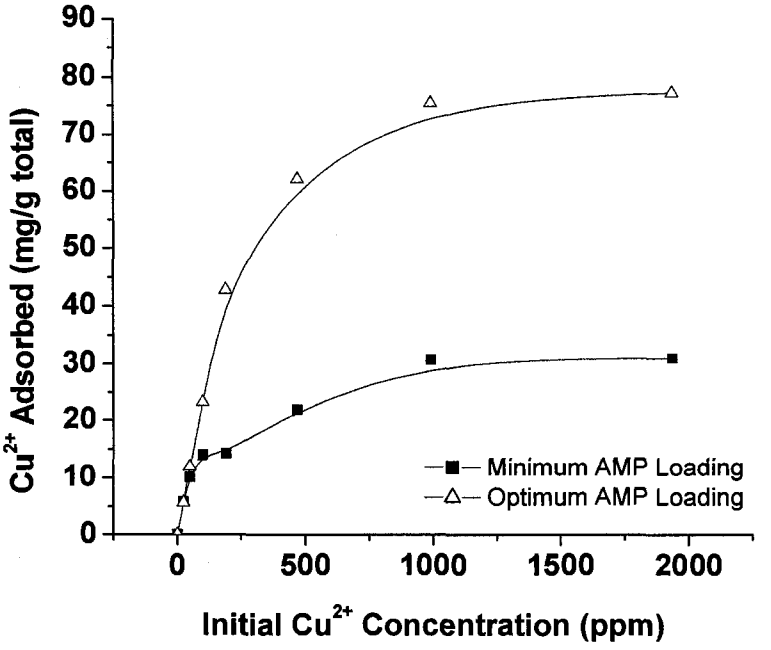

Figure 30: Adsorption isotherm of Copper on AMP-grafted material.

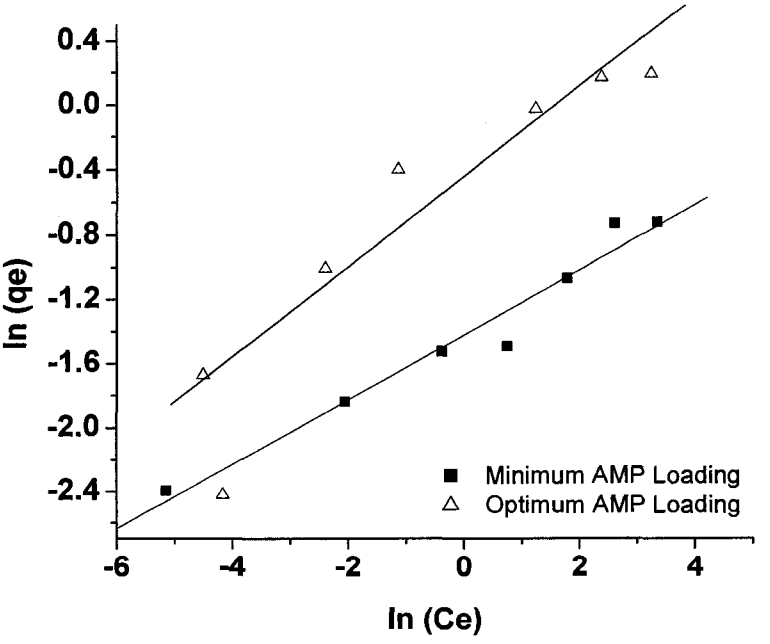

Figure 31: Adsorption isotherm of Copper on AMP-grafted material according to Freundlich model.

Table16: Freundlich isotherm constants

Adsorbent	K (mmol/g)	1/n (l/g)	qe (mmol/g)
Optimum AMP loaded	0.602	0.301	1.21
Minimum AMP loaded	0.241	0.203	0.49

Table17: Freundlich isotherm constants obtained by Sayari, A. et al. (2005) for (PE)MCM-41.

Metal Cation	K (mmol/g)	1/n (l/g)	qe (mmol/g)
Cu^{2+}	0.947	0.518	1.62

6.9-4 Effect of Grafting Conditions on the Adsorption Performance for Cu^{2+}

Data for the adsorption of Cu^{2+} are shown in Figures 32, 33 and 34. Each data point was done twice, and the average is represented by the solid line. Figure 32 represents the data obtained from the dry grafted materials prepared by adding different amount of AMP to the grafting mixture. The maximum Cu^{2+} capacity was 42 mg/g and was achieved when 1 mL/g silica of the AMP was added.

Figure 33 shows the results obtained from samples prepared exactly as those in Figure 32 except that 0.3 mL of water/g silica was added to the grafting mixture. The adsorption capacity increased significantly with a maximum of 77 mg/g obtained was at 2 mL of AMP/g silica added. Figure 34 shows the effect of the amount of water added. From the figure, it can be shown that the best adsorption capacity was achieved by

adding 0.4 mL water/g silica with adsorption capacity of 90 mg/g. This value of water added was also found to be the optimum amount from the surface characterization analysis discussed earlier.

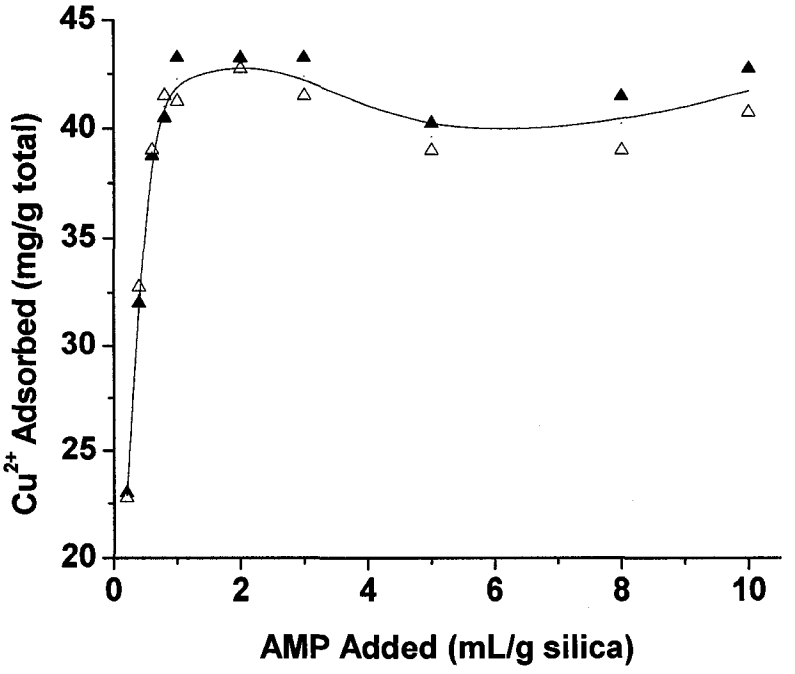

Figure 32: Effect of amount of AMP added to the dry grafting mixture on the Cu^{2+} adsorption capacity.

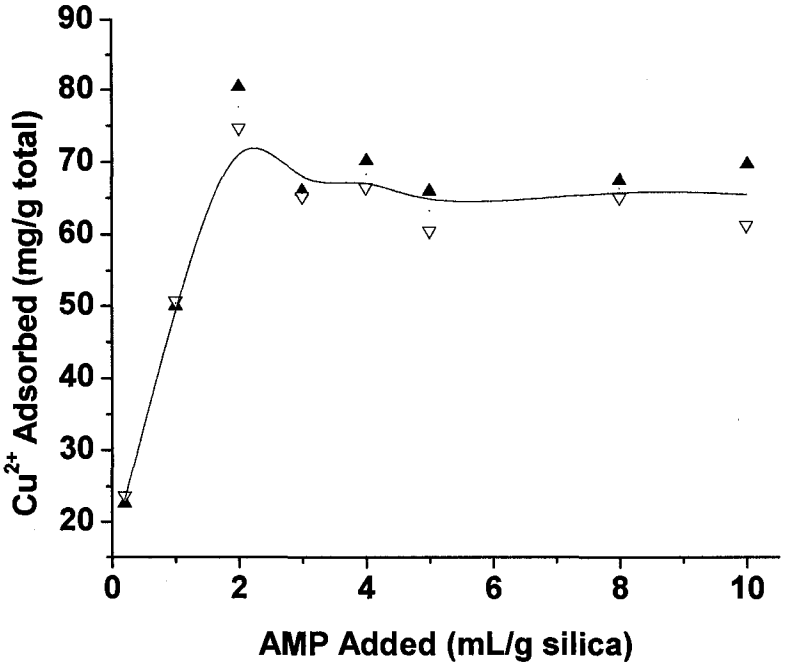

Figure 33: Effect of amount of AMP added to the wet grafting mixture (0.3 mL water/g silica) on the Cu^{2+} adsorption capacity.

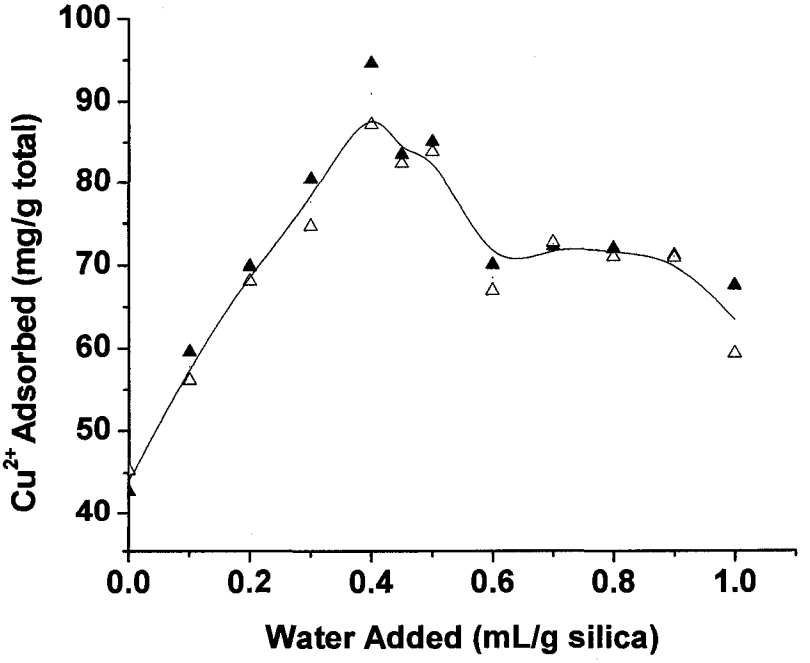

Figure 34: Effect of amount of water added to the grafting mixture mixture (2 mL AMP/g silica) on the Cu^{2+} adsorption capacity.

The adsorption data were also examined in terms of atom efficiency, i.e., moles adsorbed per mole of amine grafted. Figures 35, 36 and 37 show the effect of AMP and water added to the grafting mixture on Cu^{2+} and CO_2 adsorption efficiency (mol/mol). For Cu^{2+}, the ratio Cu^{2+}/N was almost constant around 0.3 mol/mol, which indicates that Cu^{2+} forms a complex with an average of three amine groups regardless of the amount of AMP grafted on the surface. This could be a mixture of different complexes with 2 and 4 amines groups for Cu^{2+} cation. On the other hand, the CO_2/N ratios vary widely between the three series of samples and even within the same series. For dry grafting (Figure 35) it changed from 0.06 for sample prepared with 0.2 mL of AMP/g silica up to about 0.21 when 1 mL of AMP/g silica was added. For wet grafting in the presence of 0.3 mL of water/g silica (Figure 36), the ratio changed from 0.37 for the sample prepared with 1 mL of AMP/g silica to 0.46 when 3 mL of AMP/g silica was added. For grafting in the presence of 2 mL of AMP/g silica and different amounts of water (Figure 37), the ratio changed from 0.21 for sample prepared under dry condition to the highest ratio of 0.50 for sample prepared under optimum conditions (2 mL AMP/g silica and 0.4 mL water/g silica). For monoamine-grafted materials, the CO_2/N ratios also vary widely in literature data. Leal, O. et al. (1995) obtained a CO_2/N ratio of 0.42 using silica gel as support material. Hiyoshi, N. et al. (2005) obtained a ratio of 0.19 for SBA-15 and Huang, H. and Yang, R. (2003) obtained 0.5 with MCM-48 as support. Harlick, P. and Sayari, A. (2006) obtained a ratio between 0.14 and 0.24 using (PE)MCM-41 as support for grafted triamine.

Harlick, P. and Sayari, A. (2007) assumed that the CO_2 adsorption takes place via carbamate formation as shown in Figure 38, which corresponds to a ratio of 0.5. However, the CO_2/N ratios obtained by dry grafting, Figure 35, were significantly below the stoichiometric ratio (0.5). This can be related to the low amount of grafted AMP obtained under dry conditions and the lack of two amine groups in close proximity for carbamate formation. The same explanation applies for the low ratios obtained initially in Figures 36 and 37. Figure 36 shows that a ratio of 0.5 was obtained using grafting mixture containing 2 mL of AMP/g silica and 0.3 mL of water/g silica. Figure 37 on the other hand shows that the best ratio (0.5) can be reached at 0.4 mL of water/g silica addition. Harlick, P. and Sayari, A. (2007) suggested that the low CO_2/N ratio may be due to several reasons. First, the reaction between CO_2 and amine is CO_2 partial pressure dependent and since it was relatively low in this work, 5%, the ratio is expected to be lower than the stoichiometric value. Second, the amine-CO_2 interaction may be suppressed by the formation of hydrogen bonds between amine groups and between amine and free hydroxyl groups.

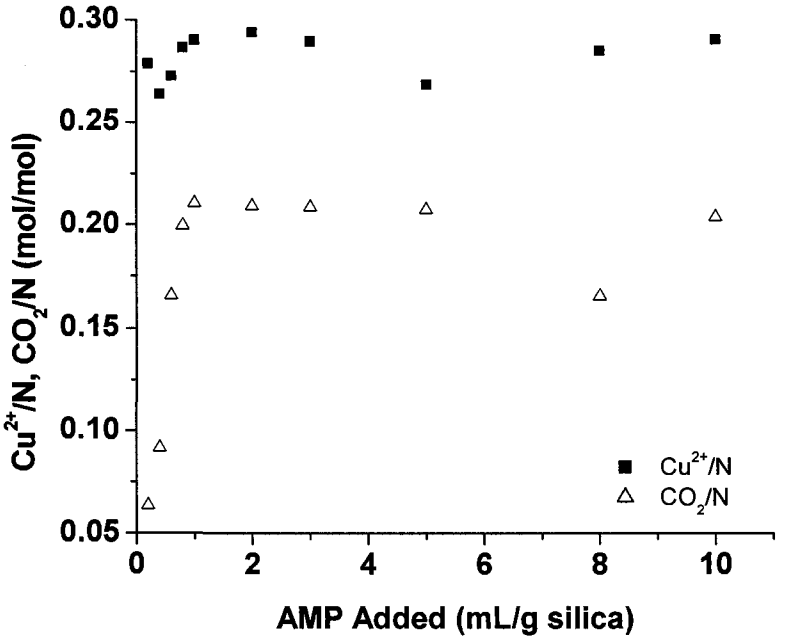

Figure 35: Effect of the amount of AMP added to the dry grafting mixture on the CO_2 and Cu^{2+} adsorption efficiency.

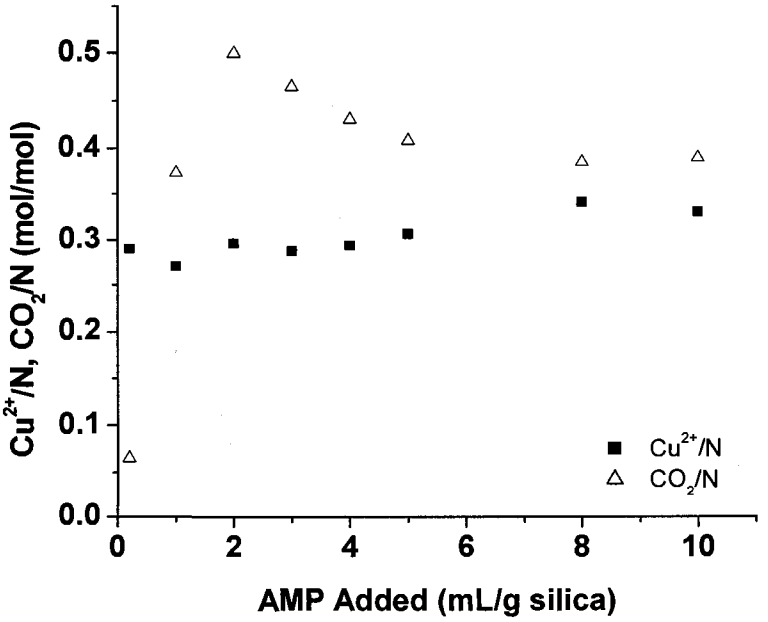

Figure 36: Effect of the amount of AMP added to the wet grafting mixture (0.3 mL water/g silica) on the CO_2 and Cu^{2+} adsorption efficiency.

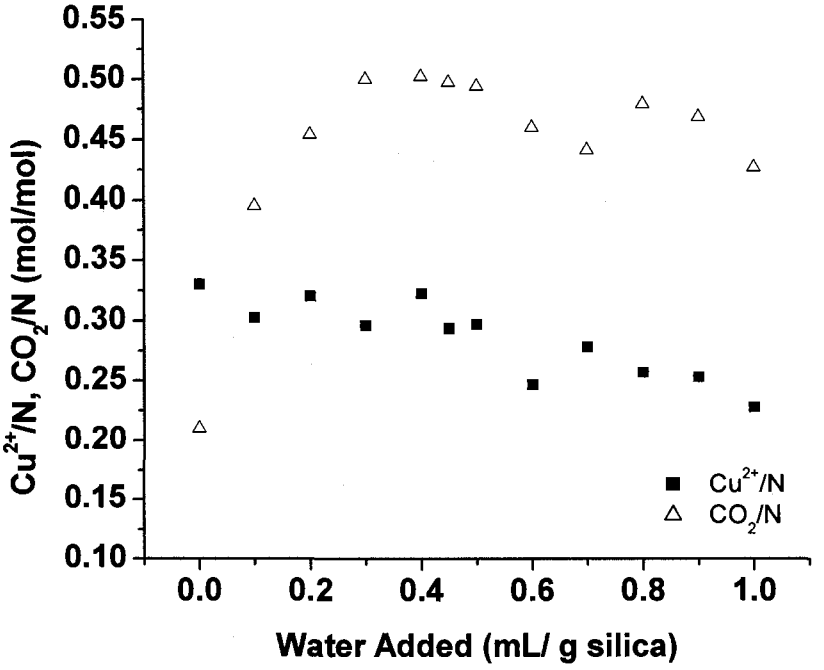

Figure 37: Effect of the amount of water added to the grafting mixture (2 mL AMP/g silica) on the CO_2 and Cu^{2+} adsorption efficiency.

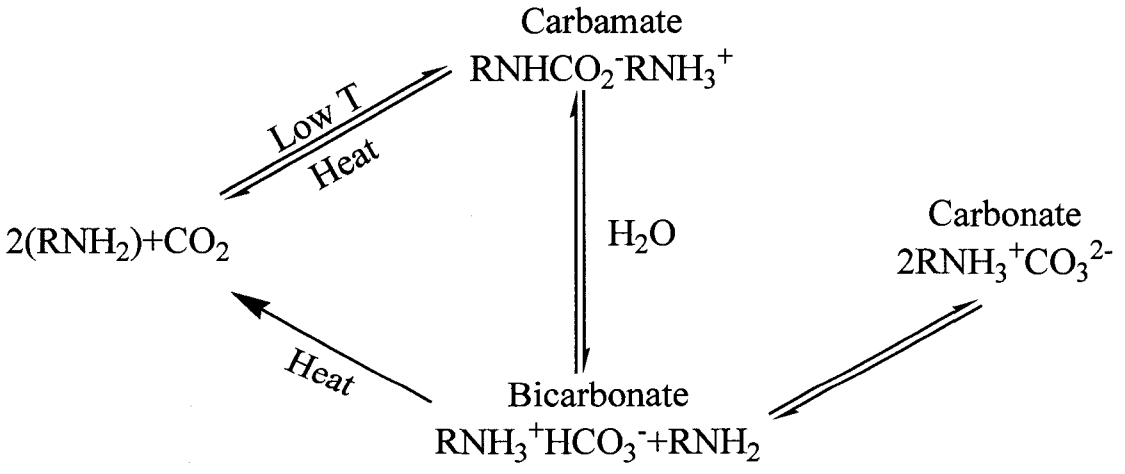

Figure 38: Scheme of CO_2 reaction pathways with primary amines (Harlick, P. and Sayari, A., 2006).

Another factor to examine when using grafted material for adsorption is to measure the maximum rate, in this case CO_2 adsorption, since this rate gives an indication about the time efficiency of the adsorbent. To do so, the maximum rates obtained for different materials were plotted against the amount of AMP added to the grafting mixture as in Figures 39, 40, and amount of water added to the grafting mixture as in Figure 41. For dry grafting, the maximum rate was obtained at 1 mL of AMP/g silica addition, then the rate started to decline which may be due to mass transfer limitations caused by the increased amount of AMP grafted on the pore mouth. For wet grafted materials, the maximum rate was obtained at 1 mL of AMP/g silica added then leveled off. The maximum rate obtained in the case of wet grafting, about 1.3 mmol/g.min, was higher than that obtained in the case of dry grafting, about 0.8 mmol/g/min. Changing the amount of water added (Figure 41) had an effect on the rate of adsorption of CO_2 that reflects the effect on surface characteristics obtained in Figure 17. It is clear from this figure that the maximum rate of CO_2 adsorption was reached when 0.1 mL of water/g silica was added to the grafting mixture with a rate of about 1.3 mmol/g.min. Increasing the amount of water added beyond 0.4 mL/g silica may cause a negative effect on the rate due to pore blockage by polymerization of the amine.

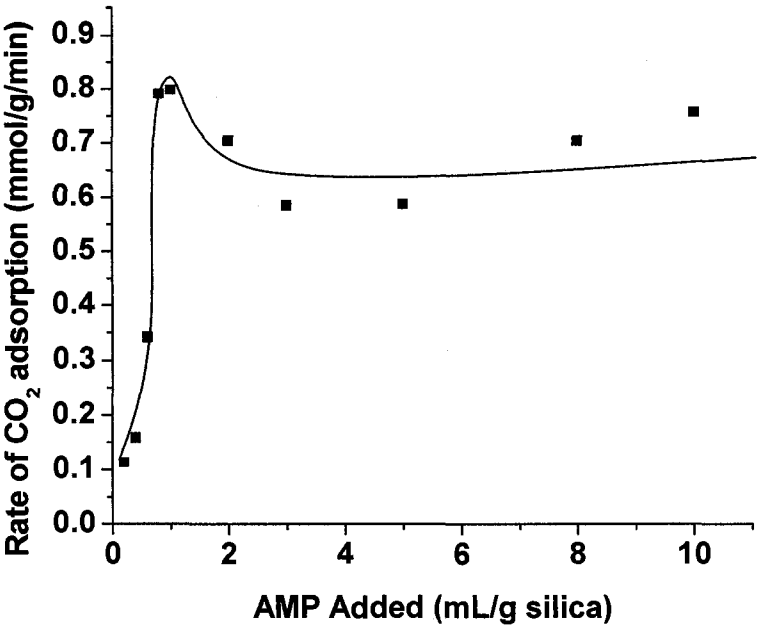

Figure 39: Effect of the amount of AMP added to the dry grafting mixture on the CO_2 adsorption rate.

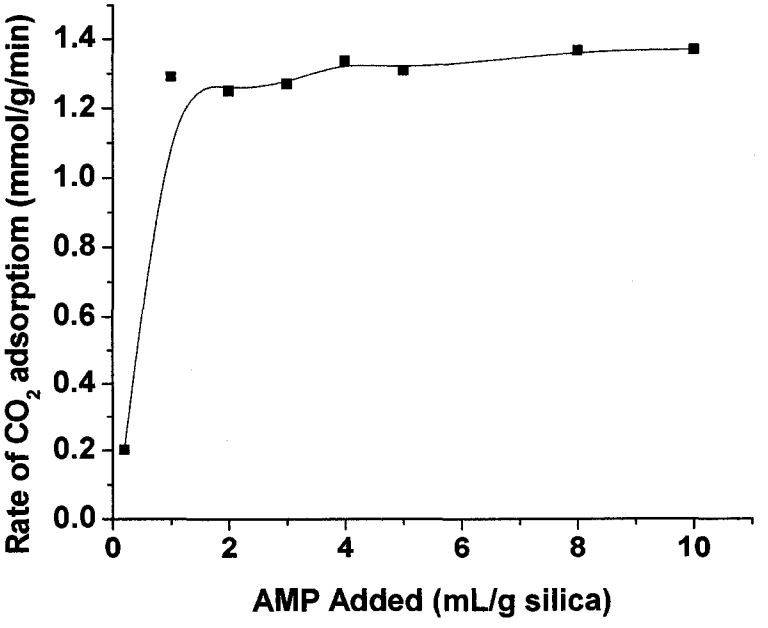

Figure 40: Effect of the amount of AMP added to the wet grafting mixture mixture (2 mL water/g silica) on the CO_2 adsorption rate.

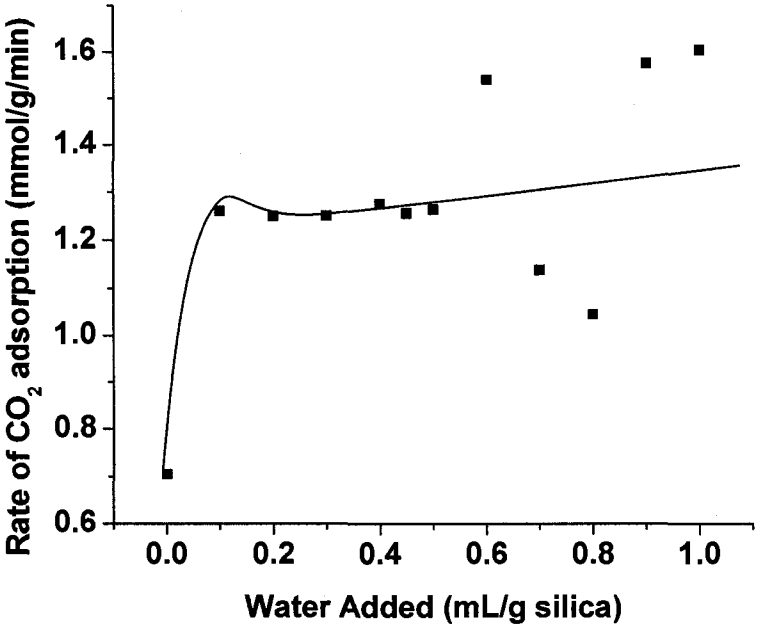

Figure 41: Effect of amount of water added to the grafting mixture mixture (2 mL AMP/g silica) on the CO_2 adsorption rate.

Figures 42, 43, and 44 show the effect of surface density of the grafted monoamine (amount of AMP grafted per unit surface area of the support, mmol/m^2) on the density of Cu^{2+} and CO_2 adsorbed (amount of Cu^{2+} and CO_2 adsorbed per unit surface area of the support, mmol/m^2). In both cases there were approximately direct relationships between the surface density of the AMP grafted amine, and the density of the adsorbed Cu^{2+} and CO_2.

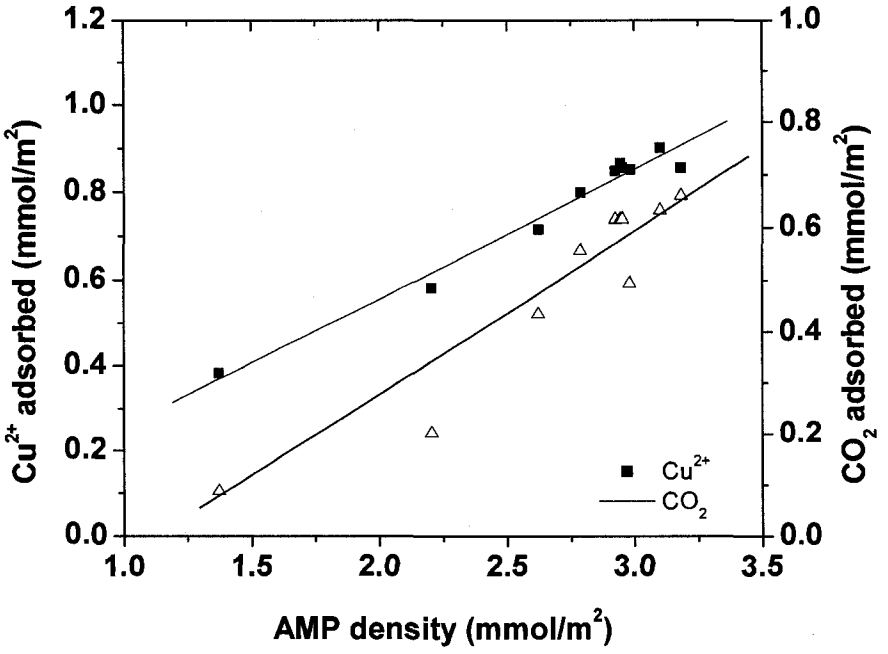

Figure 42: Effect of the AMP surface density on the Cu^{2+} and CO_2 adsorption capacity for dry grafted materials.

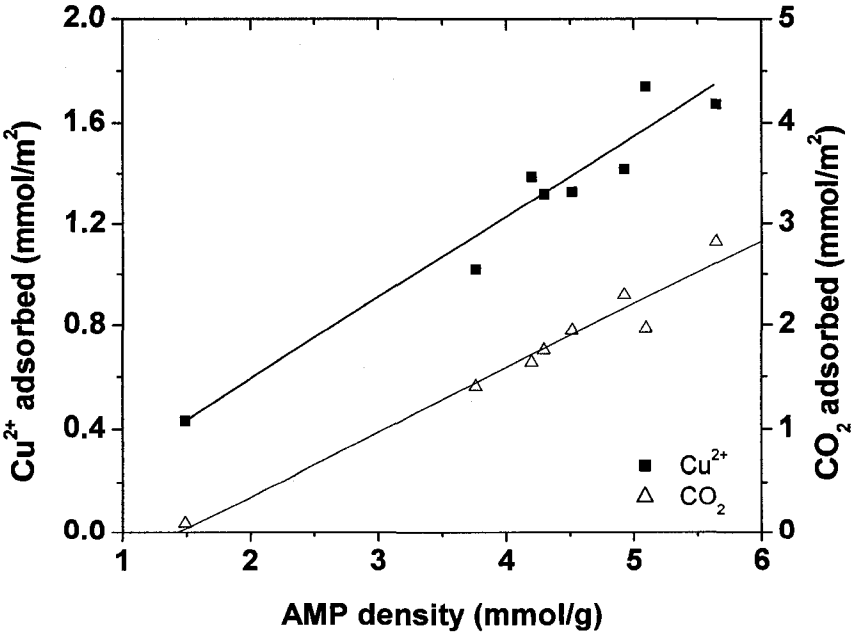

Figure 43: Effect of the AMP surface density on the Cu^{2+} and CO_2 adsorption capacity for wet grafted materials (0.3 mL water/g silica; 0.2-10 mL AMP/g silica).

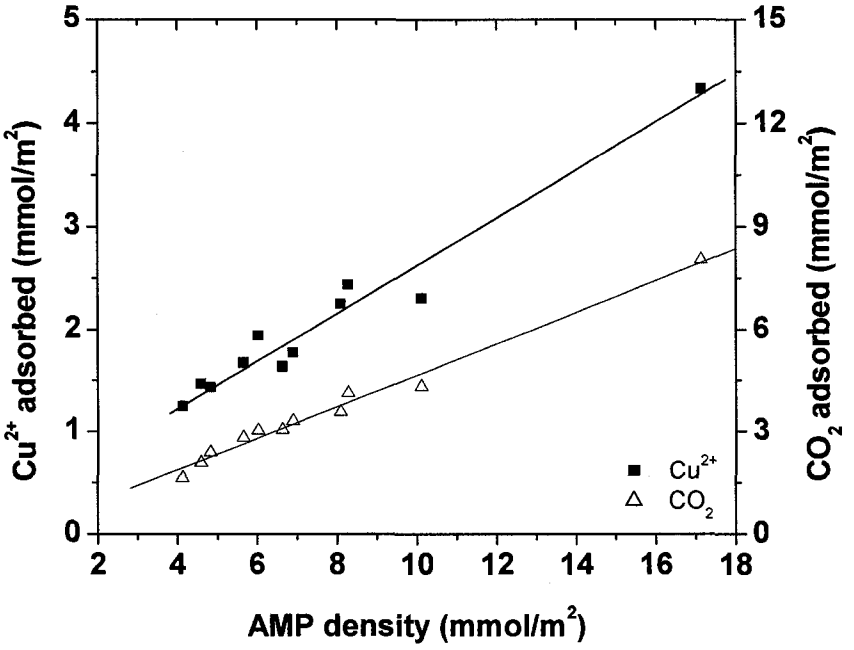

Figure 44: Effect of the AMP surface density on the Cu^{2+} and CO_2 adsorption capacity for wet grafted materials (3 mL AMP/g silica, 0-1 mL water/g silica).

6.10 Recycling of Amine-Grafted Material

Treatment of Cu^{2+}-loaded adsorbents with 1M HNO_3 for 30 min followed by filtration then washing with distilled water and titration to neutral pH (7.0) with 1 M NH_4OH allowed complete removal of the adsorbed Cu^{2+} from the materials. This was confirmed through the appearance of the original white color of the material. As shown in Figure 45, the leaching process did not affect the nature of the functional group of the adsorbent. All the IR peaks of amine modified materials were obtained indicating that the characteristics of the grafted amine groups remained unchanged after protonation of the NH_2 groups with HNO_3 and after treatment with NH_4OH. However, the TGA analysis showed a large drop in CO_2 adsorption capacity from 2.10 mmol/g for the fresh

adsorbent to 0.34 mmol/g for the leached adsorbent even though the two samples have almost the same amine content. Also, when the regenerated material was used to adsorb copper, very weak change in the color of the material was noticed, which indicates a large decrease in the copper adsorption capacity. To explain the reduction in adsorption capacity, a sample from the fresh adsorbent was stirred in distilled water for 30 min then it was filtered and dried. The TGA analysis of the sample was then carried out. The results showed the same amount of amine grafted with large drop of the CO_2 adsorption capacity, which confirmed that even the amine still available in large quantity on the surface of the adsorbent it is no longer accessible for the CO_2 or Cu^{2+} molecules suggesting structural changes occurr in contact with water regardless of the acidity of that solution; or the amine remains protonated even after treatment with NH_4oH, according to the following equations:

$$-NH_2 + HNO_3 \rightarrow -NH_3^+NO_3^-$$

$$-NH_3^+NO_3^- + NH_4OH \rightarrow -NH_3^+OH^- + NH_4NO_3$$

Another approach used for recycling was the treatment with 0.3 M EDTA solution. 1 g of the copper loaded sample was stirred in 20 mL of EDTA solution for 10 min then it was filtered and dried and used for adsorption of copper again. From the color change of the material, it was noticed that complete leaching of copper did not occur. Results in Table 18 show that the adsorption capacity decreased rapidly from 78.7 mg/g for fresh material to 22.5 mg/g for the material recycled only one time. This decrease in adsorption capacity may be related to incomplete leaching of copper during EDTA treating or to the structural changes discussed earlier.

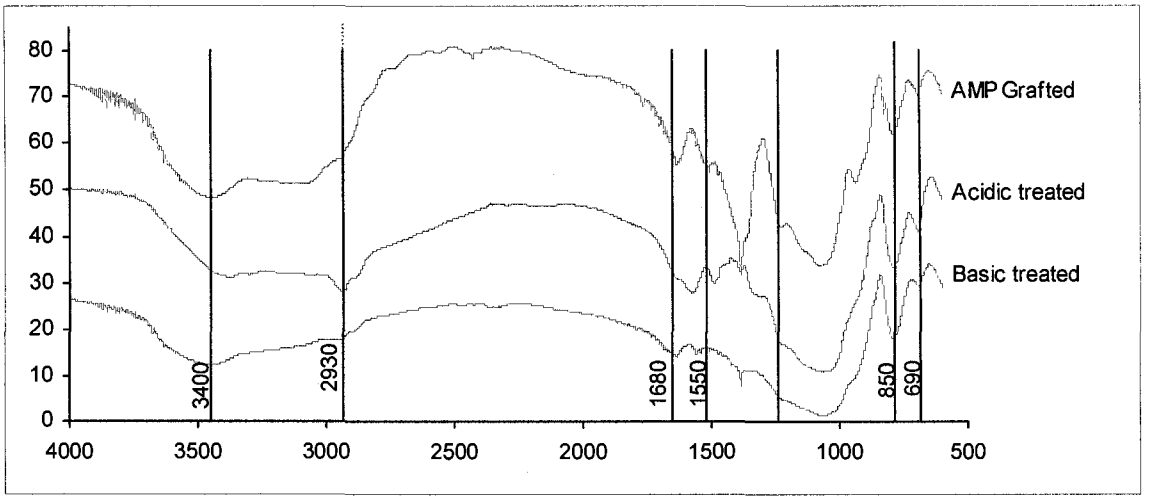

Figure 45: FT-IR spectra of AMP-grafted (CPE)MCM-41, acid treated AMP-grafted (CPE)MCM-41 and base treated AMP-grafted (CPE)MCM-41.

Table 18: Cu^{2+} and CO_2 adsorption-desorption cycles of amine-grafted adsorbent using EDTA solution as a regeneration agent.

Cycle	Adsorbent	Cu^{2+}Adsorbed (mg/g)	CO_2Adsorbed (mmol/g)
1	Fresh AMP-loaded (PE)MCM-41	78.7	2.114
2	R1 AMP-loaded (PE)MCM-41	22.5	0.942
3	R2 AMP-loaded (PE)MCM-41	12.7	0.621
4	R3 AMP-loaded (PE)MCM-41	8.0	0.436

7 Conclusions and Recommendations

The as-synthesized (PE)MCM-41 material is a fast and high capacity adsorbent for copper cations because of its open structure and suitable surface properties. However, because the amine-bearing surfactant, DMDA, is weakly held, there is a progressive loss of amine when this material is stirred in water. Moreover, more amine is lost when the adsorbent is treated with acid to release metals. Amine loss can be reduced under high pH (around 9), but this pH is not suitable for adsorption of heavy metals because they will precipitate under such a high pH. Thus this material may not be suitable for the removal of heavy metals from aqueous solution because of its poor stability.

The grafting of 3-aminopropyltrimethoxy silane to the surface of pore-expanded MCM-41 was examined through the control of the amount of water and amine added to the grafting mixture. The effects of these parameters were investigated in terms of the amount of amine grafted, the CO_2 adsorption capacity and Cu^{2+} adsorption capacity. The results showed that there exists an optimal condition under which the (CPE)MCM-41 should be grafted in order to obtain the most efficient use of the grafted amine in conjunction with the target application.

Under appropriate conditions for grafting monoamine, 0.4 mL of water/g silica and 2 mL of monoamine/g silica, the (CPE)MCM-41 was loaded to very high amine content of 4.44 mmol/g with high CO_2 and Cu^{2+} adsorption capacity of 2.23 mmol/g and 90 mg/g respectively.

Coaddition of water to the grafting mixture also exhibited a pronounced effect on the adsorption performance. In comparison to the dry grafting procedure, the wet grafting afforded material with 90% higher in amine loading with 364% and 100% higher CO_2 and Cu^{2+} adsorption capacities respectively.

Excess amount of either water or monoamine in the grafting mixture has a negative effect on the quality of the grafted material since it promotes amine polymerization within the grafting mixture causing some pore blockage. In order to minimize the effect of water addition in promoting polymerization, it is recommended to add water to the grafting mixture in multiple dozes separated by sufficient stirring time instead of single doze.

Although the initial uptake of copper by AMP-grafted (CPE)MCM-41 was quite high, attempts to recycle it using an acid, then base treatment or using EDTA met limited success. Work is now in progress using large pore (6 nm) water stable mesoporous silica prepared at high temperature, i.e., 130 ° C (Corma, A. et al., 1997). The recycling problem may be overcome.

Since the unstability of the material in water seems to be a major handle for its use as adsorbent of heavy metals in wastewaters, it is recommended to investigate the stability of the materials to be used as support before doing any grafting to ensure better quality of the obtained material.

8 References

Abd El-Moniem, N.M.; El-Sourougy, M.R.; Shaaban, D.A.F. "Heavy metal ions removal by chelating resin", *Pigment and Resin Technology* 34 (2005) 332.

Abu Qudais, H.; Moussa, H. "Removal of heavy metals from wastewater by membrane processes: a comparative study", *Desalination* 164 (2004) 105.

Ahmad, S.; Chughtai, S., Keane, M. "The removal of cadmium and lead from aqueous solution by ion exchange with Na-Y zeolite", *Separation and Purification Technology* 13 (1998) 57.

Algarra, M.; Jimènez, M.V.; Rodriguez-Castellón, E.; Jiménez-López, A.; Jiménez-Jiménez, J. "Heavy metals removal from electroplating wastewater by aminopropyl-Si MCM-41 ", *Chemosphere* 59 (2005) 779.

Alpatova, A.; Verbych, S.; Bryk, M.; Nigmatullin, R.; Hilal, N. "Ultrafiltration of water containing natural organic matter: heavy metal removing in the hybrid complexation-ultrafiltration process", *Separation and Purification Technology* 40 (2004) 155.

An, H.K.; Park, B.Y.; Kim, D.S. "Crab shell for the removal of heavy metals from aqueous solution", *Water Research* 35 (2001) 3551.

Anderson, B.C., T. Bell, P. Hodson, J. Marsalek and W. Edgar Watt. "Accumulation of trace metals in freshwater invertebrates in storm water management facilities", *Water Quality Research Journal of Canada* 39 (2004) 362.

Antochshuk, V.; Jaroniec, M. "1-allyl-3-propylthiorea modified mesoporous silica for mercury removal", *Chemical Communications* (2002) 258.

Antochshuk, V.; Jaroniec, M. "Simultaneous modification of mesoporous and extraction of template molecules from MCM-41 with trialkylchlorosilanes", *Chemical Communications* (1999) 2373.

Apak, R.; Gűçlű, K.; Turgut, M.H. "Modeling of Copper (II), Cadmium (II), and Lead (II) adsorption on red mud", *Journal of Colloid and Interface Science* 203 (1998) 122.

Apak, R.; Tűtem, E.; Hűgűl, M.; Hizal, J. "Heavy metal cation retention by unconventional sorbents (red mud and fly ashes)", *Water Research* 32 (1998) 430.

Armengol, E.; Corma, A.; Fernandez, L.; Garcia, H.; Primo, J. "Acid zeolites as catalysts in organic reactions. Acetylation of cyclohexene and 1-methylcyclohexene ", *Applied Catalysis A: General* 158 (1997) 323.

Armengol, E.; Corma, A.; Garcia, H.; Primo, J. "Acid zeolites as catalysts in organic reactions. Tert-butylation of anthracene, naphthalene and thiathrene", *Applied Catalysis A: General* 149 (1997) 411.

Baes, A.U.; Umali, S.J.P.; Mercado, R.L. "Ion exchange and adsorption of some heavy metals in a modified coconut coir cation exchanger", *Water Science and Technology* 34 (1996) 193.

Beck, J. S.; Vartuli, J. C.; Roth, W. J.; Leonowicz, M. E.; Kresge, C. T.; Schmitt, K. D.; Chu, C. T-W. ; Olson, D. H.; Sheppard, E. W.; McCullen, S. B.; Higgins, J. B.; and Schlenker J. L. "A New Family of Mesoporous Molecular Sieves Prepared with Liquid Crystal Templates", *Journal of the American Chemical Society 114 (*1992) 10834.

Blőcher, C.; Dorda,J.; Mavrov, V.; Chmiel, H.; Lazaridis, N.K.; Matis, K.A. "Hybrid ultrafiltration process for the removal of heavy metal ions from wastewater", *Water Research* 37 (2003) 4018.

Bois, L.; Bonhommé, A.; Ribes, A.; Pais, B.; Raffin, G.; Tessier, F. "Functionalized silica for heavy metal ions adsorption ", *Colloids and Surfaces A: Physicochemical and Engineering Aspects* 221 (2003) 221.

Bradl, H.B. "Adsorption of heavy metal ions on soils and soils constituents", *Journal of Colloid and Interface Science* 277 (2004) 1.

Brown, J.; Mercier, L.; Pinnavaia, T.J. "Selective adsorption of Hg^{2+} by thiol-functionalized nanoporous silica", *Chemical Communications* (1999) 69.

Celik, A.; Demirbaş, A. "Removal of heavy metal ions from aqueous solutions via adsorption onto modified lignin from pulping wastes", *Energy Sources* 27 (2005) 1167.

Charerntanyarak, L. "Heavy metal removal by chemical coagulation and precipitation", *Water Science and Technology* 39 (1999) 135.

Cho, H; Oh, D.; Kim, K. "A study on removal characteristics of heavy metals from aqueous solution by fly ash", *Journal of Hazoudous Materials B* 127 (2005) 187.

Corma, A.; Kan, Q.; Navarro, M.T.; Perez-Pariente, J.; Rey, F. "Synthesis of MCM-41 with different pore diameters without addition of auxiliary organics", *Chemistry of Materials* 9 (1997) 2123.

Dąbrowski, A.; Hubicki, Z.; Podkościelny, P.; Robens, E. "Selective removal of the heavy metal ions from waters and industrial wastewaters by ion-exchange method", *Chemosphere* 56 (2004) 91.

Demirbas, A. "Adsorption of Lead and Cadmium ions in aqueous solutions onto modified lignin from alkali glycerol delignication", *Journal of Hazardous Materials B*109 (2004) 221.

Dho, N.Y.; Lee, S.R. "Effect of temperature on single and competitive adsorptions of Cu (II) and Zn (II) onto natural clays", *Environmental Monitoring and Assessment* 83 (2003) 177.

Environment Canada: Water Pollution
http://www.ec.gc.ca/default.asp?lang=En&n=FD9B0E51-1

Environment Canada, Environmental Protection Service, Minerals and Metals Division, EPS 1/MM/10 - August 2003, "Status report on water pollution prevention and control"

Environment Canada, National report to the 2001 intergovernmental review meeting on implementation of the global programme of action, 2001.

Farajzadeh, M.A.; Monji, A.B. "Adsorption characteristics of wheat bran towards heavy metal cations", *Separation and Purification Technology* 38 (2004) 197.

Feng, D.; Aldrich, C.; Tan, H. "Treatment of acid mine water by use of the heavy metal precipitation and ion exchange", *Minerals Engineering* 13 (2000) 623.

Feng, D.; Aldrich, C. "Adsorption of heavy metals by biomaterials derived from the marine alga ecklonia maxima", *Hydrometallurgy* 73 (2004) 1.

Feng, X.; Fryxell, G.E.; Wang, L.Q.; Kim, A.Y.; Liu, J.; Kemner, K.M. "Functionalized monolayers on ordered mesoporous supports", *Science* 276 (1997) 923.

Fowler, C.E.; Burkett, S.L.; Mann, S. "Synthesis and characterization of ordered organo-silica- surfactant mesophases with functionalised MCM-41-type architecture", *Chemical Communications* (1997) 1769.

Franchi, R.S.; Harlick, P.' Sayari, A. "Applications of pore-expanded mesoporous silica. 2. Development of a high capacity, water tolerant adsorbent for CO_2 ", *Industrial and Engineering Chemistry Research* 44 (2005) 8007.

Goel, J.; Kadirvelu, K.; Rajagopal, C.; Garg, V.K. "Investigation of adsorption of lead, mercury and nickel from aqueous solutions onto carbon aerogel", *Chemical Technology Biotechnology* 80 (2005) 469.

Gregg, S.A. and Sing, K.S.W. "Adsorption, Surface Area and Porosity", Academic Press, London (1982).

Gregory, G. Pyle; James, W. Rajotte; Patrice Couture. "Effects of industrial metals on wild fish populations along a metal contamination gradient", *Ecotoxicology and Environmental Safety* 61 (2005) 287.

Groszek, A.J. "Irreversible and reversible adsorption of some heavy transition metals on graphitic carbons from dilute aqueous solutions", *Carbon* 35 (1997) 1329.

Harlick, P.; Sayari, A. "Applications of pore-expanded mesoporous silica. 3. Thiamine silane grafting for enhanced CO_2 adsorption", *Industrial and Engineering Chemistry Research* 45 (2006) 3248.

Harlick, P.; Sayari, A. "Application of pore-expanded mesoporous silica. 5. Triamine grafted material with exceptional CO_2 dynamic and equiliprium adsorption performance", *Industrial and Engineering Chemistry Research* 46 (2007) 446.

Hata, H.; Saeki, S.; Kimura, T.; Sugahara, Y.; Kuroda, K. "Adsorption of taxol into ordered mesoporous silicas with various pore diameter", *Chemistry of Materials* 11 (1999) 1110.

Hiyoshi, N.; Yogo, K.; Yashima, T. "Adsorption of carbon dioxide on organically functionalised SBA-15", *Microporous and Mesoporous Materials* 84 (2005) 357.

Huang, H. Y.; Yang, R. T. "Amine-grafted MCM-48 and silica xerogel as superior sorbents for acidic gas removal from natural gas ", *Industrial and Engineering Chemistry Research* 42 (2003) 2427.

Huh, J.K.; Song, D.I.; Jeon, Y.W. "Sorption of phenol and alkylphenols from aqueous solution onto organically modified montmorillonite and applications of dual-mode sorption model", *Separation Science and Technology* 35 (2000) 243.

Inagaki, S.; Fukushima,Y.; Kurodab, K. "Synthesis of Highly Ordered Mesoporous Materials from a Layered Polysilicate", *Chemical Communications* (1993) 680.

Inumaru, K.; Inoue, Y.; Kakii, S.; Nakano, T.; Yamanaka, S. "Molecular selective adsorption of dilute alkylanilines from water by alkyl-grafted MCM-41: tenability of the cooperative organic-inorganic function in the nanostructure", *Physical Chemistry Chemical Physics* 6 (2004) 3133.

Inumary, K.; Kiyoto, J.; Yamanaka, S. "Molecular selective adsorption of nonylphenol in aqueous solution by organo-functionalised mesoporous silica", *Chemical Communications* (2000) 903.

Jang, A.; Seo, Y.; Bishop, P.L. "The removal of heavy metals in urban runoff by sorption on mulch", *Environmental Pollution* 133 (2005) 117.

Jaroniec, M.; Kurk, M.; Jaroniec, C.P.; Sayari, A. "Modification of surface and structural properties of ordered mesoporous silicates", *Adsorption* 5 (1999) 39.

Jin, S.; Qiu, G.; Xiao, F.; Chang, Y.; Wan, C. "Investigation of the structural characterization of mesporous molecular sieves MCM-41 from sepiolite", *Journal of the America Ceramic Society* 90 (2007) 957.

Joseph, T.; Kumar, V.; Ramaswamy, A.V.; Halligudi, S.B. "Au-Pt nanoparticles in amine functionalised MCM-41: Catalytic evauation in hydrogenation reactions", *Catalysis Communications* 8 (2007) 629.

Kadirvelu, K.; Thamaraselvi, K.; Namasivayam, C. "Removal of heavy metals from industrial wastewaters by adsorption onto activated carbon prepared from an agricultural solid waste", *Biosource Technology* 76 (2001) 63.

Korngolg, E.; Belfer, S.; Urtizberea, C. "Removal of heavy metals from tap water by a cation exchanger", *Desalination* 104 (1996) 197.

Kresge, C. T.; Leonowicz, M.E.; Roth, W.J.; Vartuli, J.C.; and Beck, J.S. "Ordered mesoporous molecular sieves synthesized by a liquid crystal template mechanism", *Nature* 359 (1992) 710

Kruk, M.; Jaroniec, M.; Antochshuk, V.; Sayari, A. "Mesoporous silicate-surfactant composites with hydrophopic surfaces and tailored pore sizes", *Journal of Physical Chemistry B* 106 (2002) 10096.

Kruk, M.; Jaroniec, M.' Sayari, A. "Anew insights into pore-size expansion of mesoporous silicates using long-chain amines", *Microporous and Mesoporous Materials* 35 (2000) 545.

Kruk, M.; Jaroniec, M.; Sayari, A. "Adsorption study of surface and structural properties of MCM-41 materials of different pore sizes", *Journal of Physical Chemistry B* 101 (1997) 583.

Kruk, M.; Jaroniec, M.; Sayari, A. "Influence of thermal restructuring conditions on structural properties of mesoporous molecular sieves", *Microporous and Mesoporous Materials* 27 (1999) 217.

Kudesia,V. P. "Water Pollution: Principles of disinfiction of drinking water and its analysis)", *Paragati Prakashan*, India (1990)

Leal, O.; Boli'var, C.; Ovalles, C.; Garci'a, J.; Espidel, Y. "Reversible adsorption of carbon dioxide on amine surface-bonded silica gel", *Inorganic Chiminica Acta* 240 (1995)183.

Lee, B.; Kim, Y.; Lee, H.; Yi, J. "Synthesis of fuctionalized porous silicas via templating method as heavy metal ion adsorbents: the introduction of surface hydrophilicity onto the surface of adsorbents", *Microporous and Mesoporous Materials* 50 (2001) 77.

Lee, H.; Yi, J. "Removal of copper ions using functionalised mesoporous silica in aqueous solution", *Separation Science and Technology* 36 (2001) 2433.

Lim, M. H.; Stein, A. "Comparative studies of grafting and direct synthesis of inorganic-organic hyprid mesoporous materials", *Journal of Materials Chemistry* 11 (1999) 3285.

Lin, S.H.; Lai, S.L.; Leu, H.L. "Removal of heavy metals from aqueous solution by chelating resin in a multistage adsorption process", *Journal of Hazardous Materials B* 76 (2000) 139.

Liu, J; Feng, X.; Fryxell, G.E.; Wang. L.Q.; Kim, A.Y.; Gong, M. "Hybrid mesoporous materials with functionalised monlayers", *Chemical Engineering and Technology* 21 (1998) 1.

Liu, A. M.; Hidajat, K.; Kawi, S.; Zhao, D.Y. "A new class of hybrid mesoporous materials with functionalised organic monolayers for selective adsorption of heavy metal ions", *Chemical Communications* (2000) 1145.

Mattigod, S.V.; Feng, X.; Fryxell, G.E.; Liu, J.; Gong, M. "Separation of complexed mercury from aqueous wastes using self-assembled mercaptan on mesoporous silica", *Separation Science and Technology* 34 (1999) 2329.

Mercier, L.; Pinnavaia, T.J. "Access in mesoporous materials: Advantages of a uniform pore structure in the design of a heavy metal ion adsorbent for environmental remedation", *Advanced Materials* 9 (1997) 500.

Mercier, L.; Pinnavaia, T.J. "Heavy metal ion adsorbents formed by the grafting of a thiol functionality to mesoporous silica molecular sieves: factors affecting Hg (II) uptake", *Environmental Science and Technology* 32 (1998) 2749.

Ministry of Environment, 444e Technical Support Document for Ontario Drinking Water Standards, Objectives and Guidelines, 2001.
http://www.ene.gov.on.ca/envision/techdocs/4449e.htm

Mustafiz, S.; Rahman, M.S.; Kelly, D.; Tango, M.; Islam, M.R. "The application of fish scales in removing heavy metals from energy-produced waste streams: the role of microbes", *Energy Sources* 25 (2003) 905.

Morey, M.S.; Davidson, A.; Stucky, G.D. "Silica-based, cubic mesostructures: synthesis, characterization and relevance for catalysis", *Journal of Porous Materials* 5 (1998) 195.

Nenov, V.; Petro, S. "Removal and recovery of copper from wastewater by a comlexation- ultrafiltration process", *Desalination* 162 (2004) 201.

Newalkar, B.L.; Choudary, N.V.; Kumar, P.; Komarneni, S.; Bhat, T.S.G. "Exploring the potential of mesoporous silica, SBA-15, as an adsorbent for light hydrocarbon separation", *Chemistry of Materials* 14 (2002) 304.

Nriagu, J.O.; Wong, H.K.T.; Lawson, G.; Daniel, P. "Saturation of ecosystems with toxic metals in Sudbury basin, Ontario, Canada", *The Science of the Total Environment* 223 (1998) 99

O'Connell, D.W.; Birkinshaw, C.; O'Dwyer, T.F. "A chelating adsorbent for the removal of Cu (II) from aqueous solution", *Journal of Applied Polymer Sience* 99 (2006) 2888.

Olkhovyk, O.; Antochshuk, V.; Jaroniec, M. "Benzoythiourea-modified MCM-48 mesoporous silica for mercury (II) adsorption from aqueous solutions", *Colloids and Surfaces: Physicochemical and Engineering Aspects* 236 (2004) 69.

Olkhovyk, O.; Jaroniec, M. "Adsorption characterization of ordered mesoporous silicas with mercury-specific immobilized ligands", *Adsorption* 11 (2005) 685.

Olkhovyk, O.; Jaroniec, M "Ordered mesoporous silicas with 2,5-dimercapto-1, 3,4-thiadiazole ligands: high capacity adsorbents for mercury ions", *Adsorption* 11 (2005) 205.

Pater, J.P.G.; Jacobs, P.A.; Martens, J.A. "Oligomerization of hex-1-ene over acid aluminosilicate zeolites, MCM-41, and silica-alumina co-gel catalysts: a comparative study", *Journal of Catalysis* 184 (1999) 262.

Pott, B.M.; Mattiasson, M. "Separation of heavy metals from water solutions at the laboratory scale", *Biotechnology Letters* 26 (2004) 451.

Reynhardt, J.P.K.; Yang, Y.; Sayari, A.; Alper, H. "Periodic mesoporous silica-supported recyclable rhodium-complexed denrimer catalysts", *Chemistry of Materials* 16 (2004) 4095.

Sayari, A. "Catalysis crystalline mesoporous molecular sieves", *Chemistry of Materials* 8 (1996) 1840.

Sayari, A. "Periodic mesoporous materials: synthesis, characterization and potential applications" *Recent Advances and New Horizons in Zeolite and Technology, Studies in Surface Science and Catalysis* 102 (1996) 1.

Sayari, A. "Novel synthesis of high quality MCM-48 silica", *Journal of the American Chemical Society* 122 (2000) 6504.

Sayari, A. "Unprecedented expansion of the pore size and volume of periodic mesoporous silica", *Angewandte Chemie* 112 (2000) 3042.

Sayari, A.; Hamoudi, S. "Periodic mesoporous silica-based organic-inorganic nanocomposite materials", *Chemistry of Materials* 13 (2001) 3151

Sayari, A.; Hamoudi, S.; Yang, Y. "Applications of Pore-Expanded Mesoporous Silica. 1. Removal of heavy metal cations and organic pollutants from wastewater", *Chemistry of Materials* 17 (2005) 212.

Sayari, A.; Kurk, M.; Jaroniec, M.; Moudrakovski, I.L. "New approaches to pore size engineering of mesoporous silicates", *Advanced Materials* 10 (1998) 1376.

Sayari, A.; Liu, P.; Kruk, M.; Jaroniec, M. "Characterization of large-pore MCM-41 molecular sieves obtained via hydrothermal restructuring", *Chemistry of Materials* 9 (1997) 2499

Sayari, A.; Yang, Y. "Highly ordered MCM-41 silica prepared in the presence of decyltrimethylammonium bromide ", *Journal of Physical Chemistry B* 104 (2000) 4835.

Serna, R. and Sayari, A. "Applications of pore-expanded mesoporous silica. 7. Adsorption of volatile organic compounds", *Environment Science and Technology* 13 (2007) 4761

Shiraishi, Y.; Nishimura, G.; Hirai, T.; Komasawa, I, "Separation of transition metals using inorganic adsorbents modified with chelating ligands", *Industrial and Engineering Chemistry Research* 41 (2002) 5065.

Sun, Q.Y.; Lu, P.; Yang, L.Z. "The adsorption of lead and copper from aqueous solution on modified peat-resin particles", *Environmental Geochemistry and Health* 26 (2004) 311.

Thomas, W. J., Chrittenden, B. "Adsorption Technology and Design", *Butterworth-Heinmann, Great Britain* (1998).

Thomas, J. M.; Thomas, W.J. "Principles and Practice of Heterogeneous Catalysis" *VCH, Germany* (1997).

Toshitake, H.; Yokoi, T.; Tatsumi, T. "Adsorption of chromate and arsenate by amino-functionalised MCM-41 and SBA-1", *Chemistry of Materials* 14 (2002) 4603

Trivunac, K.; Stevanovic, S. "Removal of heavy metals ions from water by complexation- assisted ultrafiltration", *Chemosphere* 64 (2006) 486.

Tutem, E.; Apak, R.; Unal, C.F. "Adsorptive removal of chlorophenols from water by bituminous shale", *Water Research* 32 (1998) 2315.

Tzeng, D.L.; Shih, J.S.; Yeh, Y.C. "Adsorption of heavy metal ions on crown ether adsorbents", *Analyst* 112 (1987) 1413.

Űçer, A.; Uyanik, A.; Aygűn, Ş.F. "Adsorption of Cu (II), Cd (II), Zn (II), Mn (II) and Fe (II) ions by tannic acid immobilised activated carbon", *Separation and Purification Technology* 47 (2006) 113.

Veeken, A.H.M.; Vries, S.; Mark, A.; Rulkens, W.H. "Selective precipitation of heavy metals as controlled by a sulfide- selective electrode", *Separation Science and Technology* 38 (2003) 1.

Wikipedia, the free encyclopedia,
http://en.wikipedia.org/wiki/Water_distribution_on_Earth

Wang, L.' Qi, T.; Zhang, Y. "Novel organic-inorganic hybrid mesoporous materials for boron adsorption ", *Colloids and Surfaces A: Physicochemical Engineering Aspects* 275 (2006) 73.

Yanagisawa, T.; Shimizu, T.; Kuroda, K.; Kato, C. "The preparation of alkyltrimethyl-ammonium-kanemite complexes and their conversion to microporous materials", *Bulletin of the Chemical Society of Jaban* 63 (1990) 988.

Yanatasee, W.; Lin, Y.; Fryxell, G.E.; Busche, B.J.; Birnbaum, J.C. "Removal of heavy metals from aqueous solution using novel nano-engineered sorbents: Self-assembled carbaoylphosphonic acids on mesoporous silica", *Separation Science and Technology* 38 (2003) 3809.

Yokoi, T.; Yoshitake,H.; Tatsumi,T. "Synthesis of amino-functionalized MCM-41 via direct co-condensation and post-synthesis grafting methods using mono-, di-, and tri-amino- organalkoxysilane", *Journal of Materials Chemistry* 14 (2004) 951.

Zhang, L.; Zhang, W.; Shi, J.; Hua, Z.; Li, Y.; Yan, J. "A new thioether functionalized organic-inorganic mesoporous composite as a highly selective and capacious Hg^{2+} adsorbents", *Chemical Communications* (2003) 210.

Zhao, H.; Vance, G.F. "Sorption of trichloroethylene by organo clays in the presence of humic substances", *Water Research* 32 (1998) 3710.

Zhao, D.; Yang, P.; Huo, Q.; Chemelka, B.F.; Stucky, G.D. "Topological construction of mesoporous materials", *Current Opinion in Solid State and Materials Science* 3 (1998) 111.

Zhou, D.; Zhang, L.; Zhou, J.; Guo, S. "Cellulose/chitin beads for adsorption of heavy metals in aqueous solution", *Water Research* 38 (2004) 2643.

9 Appendix

Classification of pores according to their width

A convenient classification of pores according to their average width adopted by the international Union of Pure and Applied Chemistry (IUPAC) is summerized in Table A1.

Table A1: IUPAC pore size classification

Class	Width
Micropore	> 2 nm
Mesopore	2 nm - 50 nm
Macropore	> 50 nm

Classification of Adsorption Isotherms:

Adsorption isotherms can have very different shapes depending on the type of adsorbent, the type of adsorbate, and the intermolecular interactions between the gas and the surface. These isotherms are shown in Figure A1.

Type I: Characteristic of microporous adsorbents.

Type II: Characteristic of nonporous adsorbents with strong adsorbate-adsorbent interactions.

Type III: Characteristic of nonporous or macroporous adsorbents with weak adsorbate-adsorbent interactions.

Type IV: Characteristic of mesorporous adsorbents with hysteresis loop and strong adsorbate-adsorbent interactions.

Type V: Characteristic of mesorporous adsorbents with hysteresis loop weak adsorbate-adsorbent interactions.

Type VI: The stepped isotherm.

Figure A1: The six types of adsorption isotherms.

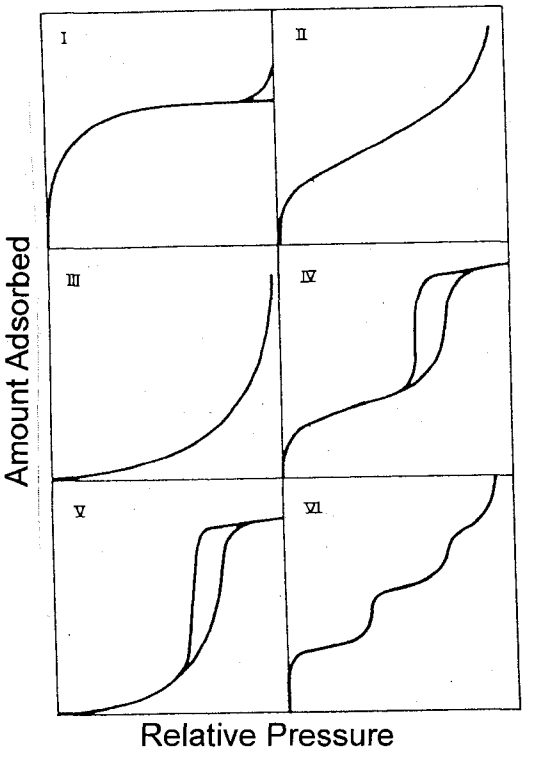

Adsorption Models:

Adsorption is usually described through isotherms, that is, functions which connect the amount of adsorbate on the adsorbent, with its pressure (if gas) or concentration (if liquid). Some of these models are:

Freundlich Isotherm:

The Freundlich isotherm model is considered to be appropriate for describing both multilayer adsorption and adsorption on heterogeneous surfaces. The Freundlich isotherm is represented by the equation:

$$q = K_f C_{eq} 1/n$$

Where:

C_{eq}: is the equilibrium concentration (mg/L)

q: is the amount adsorbed (mg/g)

K_f and n: are constants incorporating all parameters affecting the adsorption process, such as adsorption capacity and intensity respectively.

The linearised forms of Freundlich adsorption isotherm was used to evaluate the sorption data and is represented as:

$$\ln q = \ln K_f + 1/n \ln C_{eq}$$

n and K_f could be calculated from the slope and intercept of the Freundlich plots respectively.

The Brunauer, Emmett and Teller Model: BET model

The most convenient form of the BET equation for application to experimental data is given by:

$$\frac{P/p^0}{n\left(1-P/p^0\right)} = \frac{1}{n_m c} + \frac{c-1}{n_m c}\left(P/p^0\right)$$

With:

$c = \exp[(\Delta H_L - \Delta H_1)/RT]$

ΔH_L: enthalpy of adsorption for subsequent layers (kJ/mol).

ΔH_1: enthalpy of adsorption for monolayer (kJ/mol).

R: universal gas constant (L.atm/K)

T: Temperature (K)

p: applied pressure (atm)

p^0: saturation pressure (atm)

n_m: monolayer adsorption capacity (moles of adsorbate per gram of adsorbent)

n: amount adsorbed (moles of adsorbate per gram of adsorbent)

This model is linear between relative pressures of about 0.05 and 0.35 and is based on the following assumptions:

a) In all layers except the first, the heat of adsorption is equal to the molar heat of condensation.

b) In all layers except the first, the evaporation-condensation conditions are identical.

c) When $p = p^0$, the adsorptive condenses to a bulk liquid on the surface of the solid, i.e. the number of layers becomes infinite.

The plot of $(p/p^0)/n(1-p/p^0)$ against p/p^0 should therefore be a straight line with slope $s = (c-1)/n_m c$ and intercept $i = 1/n_m c$. Solution of these two simultaneous equations gives n_m and c:

$$n_m = \frac{1}{s+i}$$

$$c = \frac{s}{i} + 1$$

In practice, the monolayer capacity is of intrest, not so much in itself, but as a means of calculating the specific surface area. The BET method for calculation of specific surface area A involves two steps: evaluation of the monolayer capacity n_m from the isotherm, and conversion of n_m into A by means of molecular area a_m with the following relation:

$$A = L\, n_m\, a_m$$

a_m: average area occupied by a molecule of adsorbate in the completed monlayer (m^2/molecule).

L: Avogadro constant.

A: specific surface area of the solid (m^2/g)

Capillary Condensation and Kelvin equation:

Kelvin equation is, indeed, the basis of all the various procedures for the calculation of the pore size distribution from type IV isotherm. From the Kelvin equation it follows that the vapor pressure p over a concave meniscus must be less than the saturation vapor pressure p^o. Consequently "capillary condensation" of vapor to a liquid should occur within a pore at some pressure p determined by the value of r_m for the pore, and less than the saturation vapor pressure. Kelvin equation is given as:

$$\ln\frac{p}{p^0} = -\frac{2\gamma V_L}{RT}\frac{1}{r_m}$$

p/p^0: relative pressure

V_L: liquid molar volume (mL/mol)

r_m: mean radius of curvature (nm)

γ : surface tension (N)

It is convenient to simplify the Kelvin equation by putting $K = \gamma V_L / RT$ and to use the exponential form:

$$\frac{p}{p^0} = \exp\left(K / r_m\right)$$

Pore Size Distribution

This method of calculating the pore size distribution shown in Table A2 involves only the wall area and is applied to the desorption branch of the isotherm. It is based on an imaginary emptying of the pores by the stepwise lowering of the relative pressure, from the point where the mesopore system is taken as being full up, a relative pressure of 0.95 is frequently adopted as starting point. The steps may be chosen as to correspond to consecuitive points on the experimental isotherm (desorption branch).

Column [1] to [8] based on Table A3 and according to the following calculations:

Column [1]: p/p^0, experimental data.

Column [2]: r^k, core radius (Å) after adsorption of monolayer of N_2 as shown in Figure A2. It is calculated from p/p^0 using Kelvin equation assuming cylindrical pores with:

γ = 8.72 N

V_L = 34.68 mL/mol

T = 77.4 K

$$r^k = \frac{4.078}{\log\left(p / p^0\right)}$$

Column [3]: r^k_{avg}, average r^k:

$$r^k_{avg} = \frac{r^k_i + r^k_{i-1}}{2}$$

Column [4]: r^p, empty pore radius (Å) and calculated as:

$$r^p = r^k + t$$

Column [5]: δr^p, is the difference between consecuitive values of r^p:

$$\delta r^p = r^p_{i-1} - r^p_i$$

Column [6]: r^{p}_{avg}, average r^{p}:

$$r^{p}_{avg} = \frac{r^{p}_{i} + r^{p}_{i-1}}{2}$$

Column [7]: t, thickness of adsorbed N_2 (Å) shown in Table A3.

One method of calculating the thickness (t) of adsorbed N_2 at any relative pressure is from number of monolayers (n/n_m). The conversion is accomplished by taking the n/n_m and multiplying it with the thickness of one single N_2 layer (σ), so that:

$$\frac{t}{\sigma} = \frac{n}{n_m}$$

For N_2 , σ = 3.54 Å.

Column [8]: δt , is the difference between consecuitive values of t :

$$\delta t = t_{i-1} - t_i$$

Column [9]: factor converting core volume (v^{k}) into pore volume (v^{p}).

$$Q = \left(\frac{r^{p}_{avgi}}{r^{p}_{avgi} - t_i} \right)^2$$

Column [10]: V , adsorbed volume (mm^3) from experimental data (desorption branch).

Column [11]: δV , is the difference between consecuitive values of V :

$$\delta V = V_{i-1} - V_i$$

Column [12]: δv^{f}, correction factor due to the thinning of the adsorbed film and is calculated from the line above as:

$$\delta v^f = 0.1 \times \delta t \; \Sigma(\delta A^p) / \Sigma(\delta A^p)$$

A^p: area of the pore wall (m^2)

Column [13], $\delta v^k = \delta V - \delta v^f$ = [11] – [12]

v^k: core volume associated with the mean core radius r^k (mm^3).

V : liquid volume (experimental data)

Column [14], $\delta v^p = \delta v^k \times Q$ = [13]×[9]

Column [15], $\delta A^p = 20(\delta v^p / r^p)$ = 20× [14]/[6]

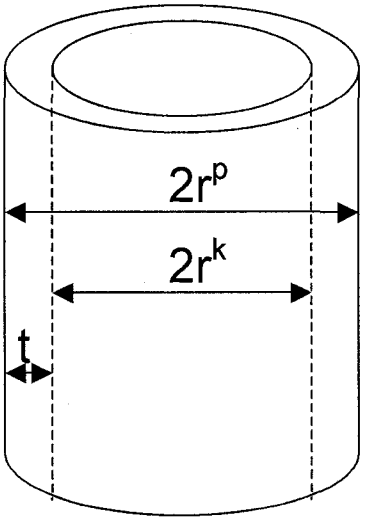

Figure A2: Cylindrical pore with monolayer adsorbed N_2.

Table A2: Calculated pore size distribution.

1 p/p^0	2 r^k (Å)	3 r^k_{avg} (Å)	4 r^p (Å)	5 δr^p (Å)	6 r^p_{avg} (Å)	7 t (Å)	8 δt (Å)
0.90	89.1		101.9			12.8	
0.85	57.8	73.4	67.5		84.7	9.9	2.1
0.80	42.1	50.0	50.7	16.8	58.7	8.6	1.1
0.75	32.7	37.4	40.5	10.2	45.6	7.8	0.8
0.70	26.4	29.5	33.7	6.5	37.1	7.3	0.5
0.65	21.8	24.1	28.7	5.0	31.2	6.9	0.4

9 Q	10 V (mm^3)	11 δV (mm^3)	12 δv^f (mm^3)	13 δv^k (mm^3)	14 δv^p (mm^3)	15 δA^p (m^2)	16 $\Sigma \delta A^p$ (m^2)	17 $\delta v^p / \delta r^p$
1.28	709							
1.37	707	2	0	2	3	1	1	0.2
1.45	705	2	0.1	1.9	2.8	1.2	2.2	0.3
1.55	694	11	0.1	10.9	16.2	9.1	11.3	2.6
1.65	635	59	0.6	58.4	96.4	61.8	73.1	19.3

Table A3: values of r^p, and t at different values of p/p^0 for nitrogen at 77.4 K.

p/p^0	r^p (Å)	t (Å)	p/p^0	r^p (Å)	t (Å)
0.40	15.60	5.35	0.70	33.7	7.35
0.45	17.40	5.60	0.75	40.5	7.85
0.50	19.45	5.80	0.80	50.7	8.60
0.55	21.85	6.15	0.85	67.5	9.65
0.60	24.9	6.5	0.90	101.9	12.75
0.65	28.7	6.85	0.95	199	16

Table A4: Standard data for adsorption of N_2 at 77 K on nonporous hydroxylated silica.

p/p^0	mol/m^2	n/n_m	p/p^0	mol/m^2	n/n_m
0.001	4.0	0.26	0.26	13.3	0.86
0.005	5.4	0.35	0.28	13.6	0.88
0.01	6.2	0.40	0.30	13.9	0.90
0.02	7.7	0.50	0.32	14.2	0.92
0.03	8.5	0.55	0.34	14.5	0.94
0.04	9.0	0.58	0.36	14.8	0.96
0.05	9.3	0.60	0.38	15.1	0.98
0.06	9.4	0.61	0.40	15.5	1.00
0.07	9.7	0.63	0.42	15.6	1.01
0.08	10.0	0.65	0.44	16.1	1.04
0.09	10.2	0.66	0.46	16.4	1.06
0.10	10.5	0.68	0.50	17.0	1.14
0.12	10.8	0.70	0.55	17.8	1.22
0.14	11.3	0.73	0.60	18.9	1.29
0.16	11.6	0.75	0.65	19.9	1.38
0.18	11.9	0.77	0.70	21.3	1.47
0.20	12.4	0.80	0.75	22.7	1.62
0.22	12.7	0.82	0.80	25.0	1.81
0.24	13.0	0.84	0.85	28.0	2.40